Temporal and Thermal Effects on Fluvial Erosion of Cohesive Streambank Soils

Akinrotimi Idowu Akinola

Dissertation submitted to the faculty of the Virginia Polytechnic Institute and State University in partial fulfillment of the requirements for the degree of

Doctor of Philosophy

In

Biological Systems Engineering

Theresa Wynn-Thompson, Co-Chair

Saied Mostaghimi, Co-Chair

Clinton L. Dancey

Matthew J. Eick

June 27, 2018

Blacksburg, Virginia

Keywords: fluvial erosion, soil aging, remolded soils, flume tests, erosion models, streambank erosion, stream temperature

TEMPORAL AND THERMAL EFFECTS ON FLUVIAL EROSION OF COHESIVE STREAMBANK SOILS

Akinrotimi I. Akinola

ACADEMIC ABSTRACT

The problem of controlling and predicting cohesive streambank erosion continues to persist although the immense environmental and economic impact of uncontrolled cohesive soil erosion is well documented. To explore this problem and offer insights into the fluvial erosion of cohesive soil, as well as improvements in modelling cohesive soil erosion, it is necessary to perform experiments exploring some of the peculiar behavior of cohesive soils. Therefore, the goal of this study was to evaluate the effects of soil age (or soil holding time), soil temperature, and eroding water temperature on the fluvial erosion of remolded cohesive soils.

To perform the studies in this work, laboratory tests were conducted rather than in-situ tests because these allow the examination of the general behavior of cohesive soils devoid of the characteristic variabilities, in addition to mineralogical differences, which these soils exhibit in the natural environment. Two natural streambank soils and one from a floodplain, all sourced from Montgomery County, VA, were used for the experiments. These soils were prepared in 5-cm by 5-cm cylindrical molds at their optimum moisture content and maximum dry density according to the standard proctor compaction test and mounted in a vertical flume wall, simulating the soil-water orientation of a vertical streambank. Three studies are presented.

The first study examined the sample preparation process, specifically investigating how time since sample preparation, termed “soil holding time”, influences the erosion behavior of remolded cohesive soils. Results of this study showed that, at a constant soil moisture content, fluvial resistance increased with holding time at rates which were significantly different by soil

type. Results further showed that the increase in fluvial erosion resistance with time was a function of the time since sample wetting rather than time since sample compaction.

In the second study, the effect of soil and water temperatures on the erosion of cohesive soils was investigated. Erosion tests were performed, at a constant soil holding time, at water temperatures of 15^0C and 25^0C. At 15^0C water temperature, erosion tests were performed at soil temperatures of 0^0C, 15^0C, and 25^0C; at 25^0C water temperature, erosion tests were performed at soil temperatures of 15^0C, 25^0C and 40^0C. Results showed that, irrespective of cohesive soil type, water temperature increase resulted in an increase in erosion rate. Conversely, irrespective of the cohesive soil type, soil temperature increase led to a decrease in erosion rate. Furthermore, for all soil types, when soil and water temperatures were equal, the effect of temperature change on erosion rate was negligible. Regression analyses showed that the observed erosion rate changes with temperature were a function of the temperature difference between soil and water rather than either temperature considered separately.

In the third study, two common erosion models – the linear excess shear stress model and the nonlinear Wilson erosion model – were evaluated using experimental data to determine which model better predicted erosion rates using the leave-one-out-cross-validation approach. Additionally, the two erosion models were modified through the addition of a linear expression, based on the relationship between the difference of soil and water temperatures and erosion rate (indicated by the second study), to account for thermal effects on erosion rate. These modified equations were compared to each other and to their original forms using the normalized objective function - an index which represents the percentage deviation of predictions from measured data. Study results show that the Wilson model generally performed better than the excess shear stress model in predicting erosion rates. Also the modified erosion models performed better in predicting

erosion rates compared to the original models. The normalized objective function showed that, over the range of test conditions, the original excess shear stress and Wilson erosion model predictions deviated from the experimental data by 80% to 334% and 79% to 156%, respectively, while the modified excess shear stress and the modified Wilson erosion model predictions deviated from the experimental data by 55% to 227% and 51% to 150% respectively. These results show that modifying the excess shear stress and the Wilson erosion models to account for temperature effects on erosion rate by adding a linear expression to the original models improved the predictive powers of the models.

Overall, the results of these studies address some of the problems pertaining to cohesive soil erosion research. The erosion resistance of remolded cohesive soils was shown to increase exponentially with time, showing the importance of this factor in the design of cohesive erosion experiments. Furthermore, this study cautions the direct comparison of cohesive soil erosion studies without accounting for soil holding time, and reveals the need for standardized soil preparation and testing protocols in cohesive soil erosion research. Also, the erosion of cohesive soils was shown to be affected by the amount of heat added to soils. This factor is important in fluvial system, where the addition heat to cohesive streambanks by flowing water will result in increased erosion. This suggests that the use of BMPs to control stream temperatures may be necessary to address the typical problem of streambank degradaion in urbanized watersheds. Additionally, the results obtained when cohesive soil erosion models were evaluated, modified, and compared, suggests that the current methods of erosion predictions for streambank stability analyses, such as the use of the excess shear stress erosion model to predict cohesive streambank erosion in the CONCEPTS computer model, could be improved using the modified models in place of the original excess shear stress model.

TEMPORAL AND THERMAL EFFECTS ON FLUVIAL EROSION OF COHESIVE STREAMBANK SOILS

Akinrotimi I. Akinola

GENERAL AUDIENCE ABSTRACT

In the United States, the annual cost of on-site soil erosion problems such as soil and nutrient losses, and off-site soil erosion problems such as sedimentation of lakes and river, loss of navigable waterways, flooding and water quality impairment, has been estimated at 44 billion USD (Pimentel, 1995; Telles, 2011). While eroding sediment sources can either be from land or from stream/river systems, the erosion from streambanks can be quite significant, reaching up to 80% of sediment leaving a watershed (Simon et al 2002; Simon and Rinaldi 2006). Despite many decades of research one the erosion of cohesive soils by flowing water (fluvial erosion), this significant aspect of environmental sustainability and engineering is still poorly understood. While past studies have given invaluable insight into fluvial erosion, this process is still poorly understood. Therefore, the objective of this dissertation was to examine the relationship between time and erosion resistance of remolded cohesive soils, and to quantify and model the effects soil and water temperature on the fluvial erosion of cohesive soils

First, erosion tests were performed to investigate how soil erosion resistance develops over time using three natural soils and testing in a laboratory water channel. Results showed that the erosion rate of the soils decreased significantly over the time since the soils were wetted. This study indicates researchers need to report their sample preparation methods in detail, including the time between sample wetting and sample testing.

Second, erosion tests were performed at multiple soil and water temperatures. Results showed that increases in water temperature led to increased erosion rates while increases in soil

temperature resulted in decreased erosion rate. When soil and water temperatures were equal, erosion results were not significantly different. Results also showed a linear relationship between erosion rate and the difference between soil and water temperatures, indicating erosion resistance decreased as heat energy was added to the soil.

Lastly, two common erosion models (the excess shear stress and the Wilson models) were evaluated, and were modified to account for soil and water temperature effects. Results showed that, compared to the original models, the modified models were better in predicting erosion rates. However, significant error between model predictions and measured erosion rates still existed.

Overall, these results improve the current state of knowledge of how erosion resistance of remolded cohesive soils evolves with time, showing the importance of this factor in the design of cohesive erosion experiments. Also, the results show that by accounting for thermal effects on erosion rate, the usability of erosion models can be improved in their use for erosion predictions in soil and water conservation and engineering practice.

ACKNOWLEDGEMENTS

I would like to express my sincere gratitude to everyone who helped me with this degree. First, I would like to thank my advisors for all their time and effort in ensuring that this research was seen to conclusion. I would specifically like to thank Dr. Thompson for her guidance and direction during every step of my study. Her genuine interest in my academic development and selfless support is much appreciated. Special thanks to Dr. Mostaghimi for being a constant source of encouragement. I want to thank Dr. Dancey and Dr. Eick for their assistance and unique insight. I would also like to thank Dr. Olgun for the time and effort he gave as a member of my committee for the greater part of my study.

I am grateful to Laura Lehmann and Dumitru Branisteanu for going over and beyond in helping with constructions, installations and equipment servicing. Their assistance was invaluable, and is much appreciated.

Lastly, I would like to thank my friends and family for their support. Special thanks to my wife, Aquisi, for being the best companion I could ever wish to have. Her ever smiling face and pleasant demeanor was a daily source of encouragement. Thanks also to my Dad and Mom, Asiwaju Michael Olawumi and Asiwaju-Obinrin Dorcas Oluwawemimo Akinola, for their innumerable sacrifices through the years and for raising me to always have faith in God for guidance in all things.

TABLE OF CONTENTS

LIST OF FIGURES

LIST OF TABLES

CHAPTER 1

INTRODUCTION

Introduction

According to the United States Environmental and Protection Agency (USEPA), sediment is a leading cause of water quality impairment in assessed streams and rivers (USEPA, 2016). Increased stream temperatures due to urbanization further aggravate this situation as stream temperature, which, in an urbanized watershed, can rise almost 10^0C during summer storms, has been shown to be positively correlated with fluvial entrainment of cohesive soils (Hester and Bauman, 2013; Nelson and Palmer, 2007, Parks 2012). Furthermore, hydropower operations, as well as other anthropogenic influences, such as reservoir discharges and industrial cooling water, change the natural hydrologic and thermal characteristics of stream channels, resulting in elevated stream temperatures.

Extensive research has been conducted to understand soil detachment and transport by overland flow in agricultural and urban lands (Knapen et. al, 2007) but little is currently known on the mechanics of cohesive streambank erosion. Although previous research has shown the importance of the physicochemical properties of soil and water on cohesive soil erosion (Grisssinger, 1966; Partheniades and Paaswell, 1970; Sargunam et al., 1973; Arulanandan et al., 1975), the effects of water and/or soil temperature on cohesive soil erosion are still poorly understood. Also, the effects of soil temperature on cohesive soil erosion is practically unknown although it is not unusual for stream and bank temperatures to differ. Therefore, there exists a

knowledge gap on how water and soil temperature affects cohesive soil erosion. This lack of knowledge exists in part as a result of the complexity of the process of cohesive soil erosion, which is affected by multiple factors such as mineralogy, particle size, cation exchange capacity, pore water pressure, pH, salinity, sodium adsorption ratio, aggregate size, bulk density, organic content, and compaction methods, as well as biological factors (Sharif, A.R. 2003; Grabowski et al. 2011).

Because streambank erosion results in channel instability, land and habitat loss, excess sediment supply, as well as the loss of functionality of urban structures like dams, dykes, levees and bridges, research is needed on the many factors that affect cohesive erosion.

Goals and Objectives

The overarching goal of this research was to determine the effects of soil and water temperatures on the erosion of cohesive soils, and to incorporate such in existing cohesive erosion models. An additional goal was to investigate the effect of remolded cohesive soil age on erosion rate. To achieve these goals, the following studies were performed in the order listed:

1. Determine if soil sample age (holding time) has a significant effect on the erosion rates of remolded cohesive soils;
2. Determine if soil and water temperature influence the erosion rates of cohesive soils;
3. Evaluate two erosion models using experimental data, and modify these models to capture the soil and water temperature effects on cohesive soil erosion.

CHAPTER 2

LITERATURE REVIEW

Streambank Erosion

Generally, streambank erosion occurs through the combination of three distinct processes namely – subaerial process, fluvial entrainment and mass wasting with each mechanism dominating over different temporal and spatial scales (Lawler, 1992; Cooper and Maddock, 2001).

Subaerial processes

Subaerial (under-air) processes are land based processes that shape the earth crust. With respect to streambank erosion, subaerial processes are the mechanisms that loosen streambank sediment materials prior to and in conjunction with fluvial erosion. Subaerial processes that directly weaken streambanks include needle-ice processes, wetting and drying processes and freeze thaw cycling. Subaerial processes are seasonal in nature and are affected by the amount and state of soil moisture (Thorne, 1982); an increase in soil moisture will decrease cohesion within the streambank matrix (Cooper and Maddock, 2001, Craig, 1992) while a decrease in soil moisture content has the potential of weakening soil strength due to the formation of desiccation cracks in response to the shrinking soil mass (Thorne and Lewin, 1979; Dietrich and Gallinatti, 1991; Cooper, 2001). Therefore, subaerial processes are closely related to and influenced by soil moisture which also affects the swelling behavior of cohesive soils, and the degree to which cohesive soils swell depends on the types and proportion of clay minerals it contains. Since subaerial processes are influenced by factors closely linked with climate, streambank erodibility

varies seasonally in response to varying subaerial forcings. In studying the seasonal variation of streambank erosion, Wolman (1959), and Hooke (1979) found that erosion due to subaerial processes is highest during winter. During winter, streambanks experience cycles of freezing and thawing may initially lead to more stable banks during the first 0-4 cycles (Lehrsch, 1998). However, higher freeze/thaw cycles will reduce aggregate stability (Mostaghimi et al, 1988; Edwards, 1991; Lehrsch, 1998) and thus increase cohesive streambank erosion (Wynn et al, 2008). Although the main subaerial processes with respect to streambank erosion are the freeze-thaw and wet-dry cyclings, erosion through the release of soil directly from melting ice crystals has also been observed (Wolman, 1959).

Fluvial erosion

Fluvial erosion is the detachment and entrainment of soil by moving water. With respect to non-cohesive soils, fluvial erosion occurs when eroding forces are greater than resisting forces with the resisting forces being a combination of individual particle weight and the degree of packing. For cohesive soils, the forces resisting erosion depends on the physicochemical properties of the soil and the interaction soil and water chemistry (Raudviki, 1998; Partheniades, 2009). Water flowing over a surface exerts hydraulic shear stress over that surface. When water flows over cohesive soils, the soil surface/bulk responds chemically (through ion exchange and adjusting to maintain electroneutrality) (Winterwerp and van Kesteren, 2004) and physically (by absorbing water and swelling) (Mitchell and Soga, 2005). Unlike non-cohesive soils where erosion occurs particle by particle, the fluvial erosion of cohesive soils is by flocs and aggregates (Mirtskhulava, 1966; Droppo, 2001) when the hydraulic forces are large enough to overcome the interparticle forces of attraction between the clay minerals (Raudviki, 1998). However, the degree of interparticle attraction in cohesive soils is affected by soil parameters such as grain size, clay type, water content, salt content, temperature and ion exchange capacity (Mehta, 1991; Grabowski,

2011). Interparticle attraction at the surface of cohesive soils is also affected by the chemical properties of the eroding fluid such as dissolved ions, temperature and pH (Mehta, 1991; Grabowski, 2011). A measure of the cohesive soils to erosion is often called soil erodibility, and the factors which affect this soil property are summarized in Figure 1.1. Although soil strength is often quantified using soil bulk parameters such as vane shear strength, compressive strength and dry unit weight, these do not quantify fluvial erodibility well since fluvial erosion is surface process (Arulanandan et al., 1980)

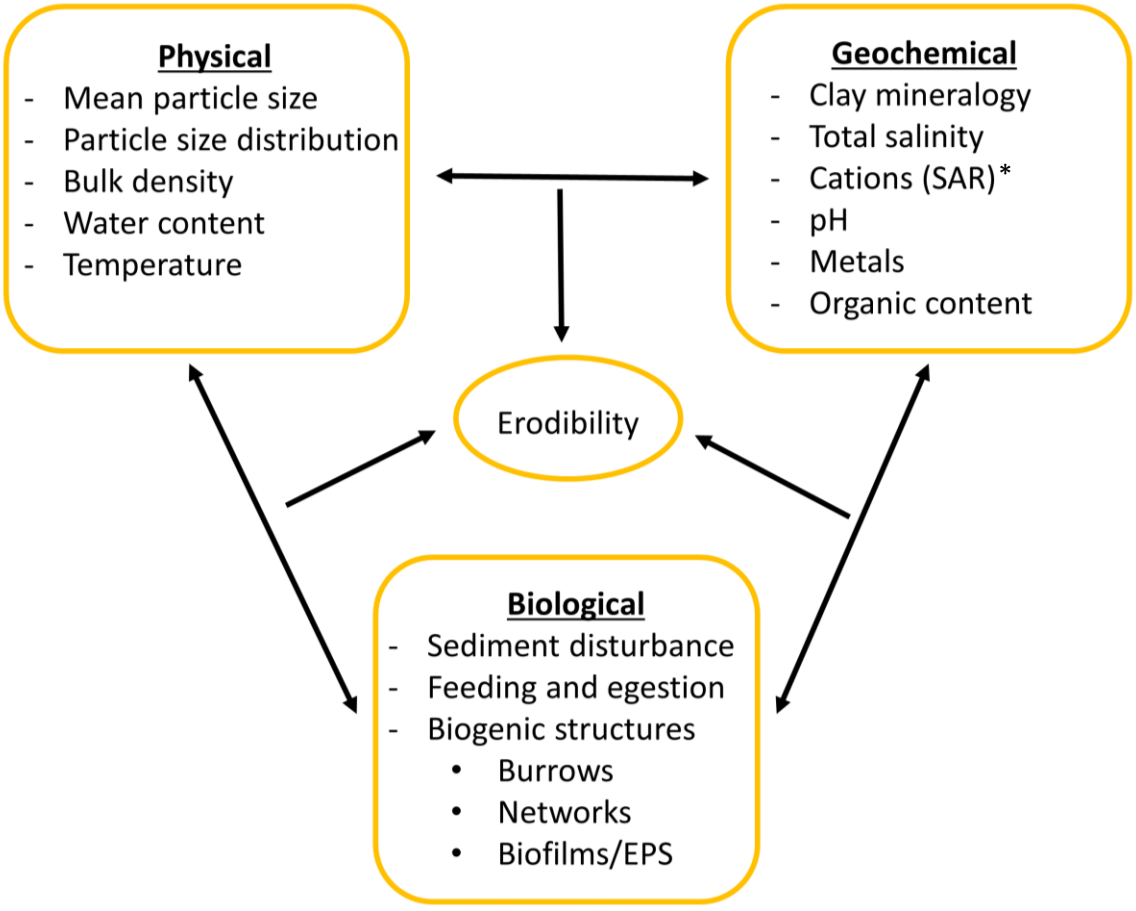

Figure 1.1 Processes and sediment properties influencing the erodibility of cohesive soils (adapted from Grabowski et al., 2011; * SAR – sodium adsorption ratio)

Mass wasting

Mass wasting (or geotechnical failure) of streambanks usually occurs when a failure plane develops as a result of excess hydrostatic pressure within the streambank. It occurs when the weight of the bank becomes greater than the bank shear strength, and the streambank slides suddenly into the channel. This sudden bank failure often follows high flow events when the weight of the streambank is increased due to absorbed water. Mass wasting can also be caused by the fluvial erosion of a bank toe over time (especially in stratified banks) with the bank failing by a rolling action in a process called cantilever failure (Simon and Collison, 2002).

Changes in Streambank Temperature

Over the past 100 years there has been an increasing awareness of climatic changes in the environment as improved measurement techniques have shown that, although random climatic variation is natural, a component of this variation is not due to nature but a direct result of human activities (Shine and Forster, 1999). A sharp increase in greenhouse gases (especially CO_2) attributed to the start of the industrial revolution has been accompanied by an increase in the global average surface temperature (IPCC, 2007) as surface temperature readings dating back to 1880 indicate a global surface temperature rise of about 1.4 ^{0}C (Smith et al., 2008). According to the Intergovernmental Panel on Climate Change (IPCC), *"observational evidence from all continents and oceans show that many natural systems are being affected by regional climate changes, particularly temperature increases"* and that *"eleven of the twelve warmest years since 1850 were among the last 12 years"* (IPCC, 2007). One of the impacts of increasing surface and air temperatures is a corresponding increase in stream temperature (Webb and Nobilis, 2007; Nelson and Palmer, 2007) since stream temperatures are partly controlled by heat fluxes at the air/water interface (Webb and Zhang, 1997; Mohseni and Stefan, 1999). Numerous studies have been

conducted to explore the relationship between air and water temperatures at different spatial scales, and the general consensus is that air temperature drives heat exchange at the air-water interface (Nelson and Palmer, 2007; Ducharne, 2008).

Also, urbanization affects stream temperatures as urbanization alters the heat retention, transport and dissipation properties landscapes. The urbanization of a catchment is typically accompanied by increased imperviousness and destruction of riparian vegetation which directly affect stream temperatures (Nelson and Palmer, 2007; Kaushal et al., 2010). Urbanization of a catchment reduces its infiltration capacity leading to increased runoffs and decreased times of concentration. This reduction in infiltration translates to reduced subsurface contribution to stream flows leading to lower stream thermal capacities which results in higher stream temperatures. Furthermore, a consequence of reduced time of concentration and increased runoff in urban watersheds is an increase in the ease of heat transfer from heated surfaces (such as paved roads, roofs and other structures) to stream channels. This form of heat transfer, most noticeable during summer convective storms, has been reported to lead to stream temperature surges of almost 10^0C (Pluhowski, 1970; Nelson and Palmer, 2007; Hester and Bauman, 2013).

Cohesive Soil Mineralogy

Cohesive soils as found in the natural environment are made up of clay, silt, fine sand, organic material, water, and sometimes gas components (Winterwerp & van Kesteren, 2004) in various fractions with at least 10% of the total soil mass composed of clay (Sparks, 1998). At a clay fraction greater than 10%, the overall erosive behavior of the soil mass is determined by the characteristics of the clay fraction due to the high specific surface area and surface charge distribution of clay minerals (Sparks, 1998). Therefore, understanding the mineralogy and

physicochemical properties of clays is invaluable in studying the erosion of cohesive soils. Clays are secondary minerals formed from the chemical weathering of primary minerals in the presence of water. Mechanical weathering of rocks produce sand, gravel and other crystalline structures which can also be eroded chemically to form clays. The overall process of rock decomposition (mechanical and chemical), erosion, transport, deposition and resuspension is known as the rock cycle. Although many clay types originate from similar parent rock, the effect of many varying factors such as temperatures, pressures and ionic solutions to which the degrading rock material has been subjected results in clay minerals which have little physical and chemical similarity to each other and to the parent rock material. Clay minerals are mainly composed of two dimensional silica tetrahedra and aluminum-hydroxide or magnesium-hydroxide octahedra in various combinations, and with different cationic substitutions. Four of the most common types of clay minerals include kaolinite, illite, vermiculite and smectite (Grabowski et al, 2011; Zhu et al, 2008; Parks, 2012).

Kaolinite

Kaolinites are phyllosilicates typically formed from the weathering of feldspars, and they have a silicon to aluminum ratio of 1. These clay minerals few or no isomorphic substitutions (i.e. the replacement of an atom by another of similar size without disrupting the structure of the crystal lattice), low cation exchange capacity (1-15 meq/100g) and are considered non-expanding.

Illite

Illites are 2:1 layer silicates in which negative charges due to isomorphic substitutions in the tetrahedral layers are balanced ionically by potassium cations. These ionic bonds prevent water molecules from entering the basal layers, and makes the exchange of potassium ions with other cations difficult, resulting in a non-expanding clay type.

Vermiculite

Vermiculites are 2:1 layer silicates in which charge deficiencies within the clay sheet are balanced by magnesium and calcium ions in the presence of a two layers of water molecules. As a result of the basal spacing resulting from this configuration, the interlayer cations are exchangeable and the clay type is considered semi-expanding.

Smectite

Smectites are 2:1 layer silicates, and the predominant smectite clay is montmorillonite in which the octahedral layer is dioctahedral gibbsite with aluminum as the cation. Montmorillonites have variable CEC due to isomorphic substitutions, especially Mg for Al, in the gibbsite layer, and they exhibit high shrink/swell properties due to low interlayer bonding strength-which easily allows water molecules between the clay sheets.

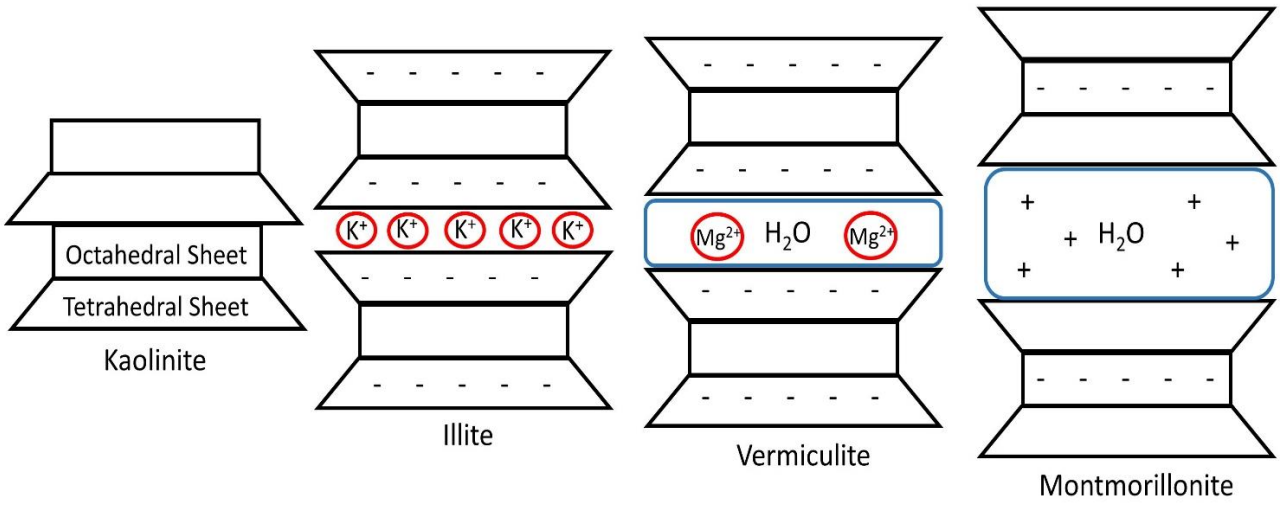

Figure 1.2 Schematic of common clays (McBride, 1994; Brady and Weil, 2008; Parks, 2012)

Surface Charges and the Electric Double Layer Theory

Origin of surface charges

The incidence of surface charges on cohesive soils is due to the following two processes:

(1) Permanent charge: where ions of similar sizes but different charges are substituted in the soil crystal lattice creating a net positive or negative change on the soil surface (isomorphic substitution). This usually occurs during the crystallization of the clay mineral resulting in permanent charges which are independent of environmental conditions.

(2) pH dependent or variable charge: adsorption of water, H^+, and OH^-, cations and anions from the soil solution creating a charged surface. Also surface charges result from the ionization of organic functional groups such as the dissociation of hydrogen ions from or onto the present organic functional group. These charges depend on environmental conditions, especially pH.

Electric double layer theory

The electric double layer can be defined as the structure of attracted counter ions and repelled co-ions in the vicinity of a charged colloidal surface in a manner different from the distribution of ions in the bulk solution. The electric double layer theory explains the electrostatic properties of a colloidal system composed of charged surfaces and an ionic solution (Singh and Uehara, 1999). With respect to cohesive soils, it is assumed that exchangeable ions reside directly on the surface of the soils (Bohn et al., 1985). Therefore, the cohesive soil mass is seen as a negatively charged soil bulk with a positively charged surface. However in rare cases such as highly acidic soils dominated by sesquioxides, allophanes or imogolites, clay surfaces may have a net positive charge. Cohesive soils form colloids in solution thus the electric double layer theory helps in understanding the dispersion of surface charges of such soils in solution.

The main forces at play in clay/water systems are electrostatic forces and Van der Waals forces. Other forces present in colloidal systems include solvation forces, hydrophobic/hydrophilic forces, thermal fluctuations and steric forces. In the long spatial range, the electrostatic behavior of coions and counter-ions is the most important mechanism affecting the diffusion of ions while in the short spatial range (of the order of a few nanometers from the solid/fluid interface) the Van der Waals forces become important (Li et al., 2007). Three of the major theories that have been proposed in the study of the dispersion of surface charges in ionic solutions include:

a) *Helmholtz theory (1879):* This is the simplest theory of the electric double layer. In this theory, it is assumed that there is a monolayer of charge satisfying counter-ions on the charged surface which bear no effect on the distribution of ions in the solution or in the vicinity of the charged surface. In this theory, the electric double layer is thought to act like a parallel plate capacitor, with the electrical potential linearly dissipated from the charged surface to the charge-satisfying counter ions;
b) *Gouy-Chapman theory (1913):* In this theory, it is assumed that charges at the surface are balanced by a diffuse layer of counter-ions in the solution. In this theory, ions are distributed in the electrolyte in the form of point charges, with the electrochemical potential and ion concentration following Poisson's electrostatics equation and Fick's diffusion equation, respectively;
c) *Stern theory (1924):* This theory is a combination of the Helmholtz theory and the Gouy-Chapman theory. In this theory, there is an inner layer of adsorbed counter-ions called the Helmholtz compact layer (Stern layer) at the surface, in addition to a diffuse double layer (Gouy-Chapman diffuse layer) outside the Stern layer. The surface separating the Stern layer and the Gouy-Chapman layer is called the shear or slipping plane where the zeta

potential is measured. This zeta potential, a function of surface charge, adsorbed ions and the type of bulk medium, reflects the electrokinetic properties of particles, and has been used to determine flocculation and dispersion properties of soil particles (Baumgarten et al., 2012). Unlike the Gouy-Chapman theory where ions are assumed to be point charges, the Stern theory accounts for the finite sizes and the specific adsorption/solvation of ions.

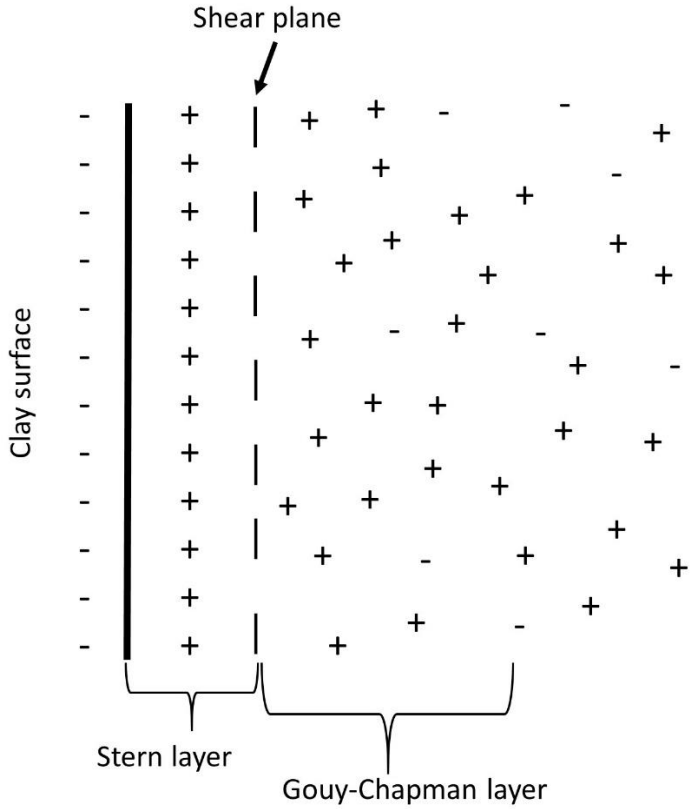

Figure 1.3 The electric double layer (adapted from Shang et al., 1994)

Brief History of Cohesive Soil Erosion Research (after Partheniades, 2009)

According to Partheniades (2009), the evolution of research in cohesive soil erosion can be separated into three distinct phases which, although they overlap and collectively continue to

influence current approaches to cohesive erosion research, are distinct in time and purpose. The first and earliest phase of cohesive soil erosion studies was as a result of a need to establish rational guidelines in stable channel design using empirical formulas and/or tables of allowable velocity. In this period, an understanding of the myriad of soil properties that affect erosion was not known therefore soil properties were given simply in terms of density or some measure of compaction. The use of regime theories logically developed in this early phase.

These theories, introduced by British engineers in the late nineteenth century for designing irrigation systems in India, are basically regression equations used to calculate channel width, depth, and gradient as functions of dominant channel hydraulic parameters such as effective/bankfull discharge and average bed size (Blench, 1952). An example of this is the work by Kennedy (1895) in which mean allowable velocity in a stable channel is given as a singular function of depth. Since these theories were developed from canals with sand beds and slightly cohesive to cohesive banks and contained empirical coefficients that must be estimated using 'judgement and experience' (Partheniades, 2009) their limitations were apparent when used in designing stable cohesive channels. The need to scientifically address these limitations as well as advances in fundamental fluid mechanics in early to mid-20th century led to the second phase of cohesive erosion research.

The knowledge of the importance of soil composition, compaction, and flow induced near bed shear stresses (rather than a bulk velocity index) as predictors of soil erosion led to the second phase of cohesive soil erosion research. Although the first mention of the term 'shear resistance' was by Du Baat in 1816, this soil parameter did not become an important parameter around which soil resistance to erosion would be oriented until around the 1950s when the limitations of the regime equations became apparent (Singh, 2003; Partheniades, 2009). The objectives of research

in this phase were to relate the critical bed shear stress (τ_c - also called the critical tractive force) to soil properties indicative of soil mechanical strength and/or aggregation. One of the most important and pervasive findings of this phase was that critical bed shear stress decreases with decreasing particle size up to the silt range (50 μm) but then increases again as particle size decreases further.

Smeardon and Beasley (1959, 1961) supported the validity of the tractive force theory by showing that soil cohesion can be measured by some physical soil tests and can predict the critical tractive force (τ_c). Additionally, plasticity index (PI), rather than clay content, is a better indicator of critical tractive force since percent clay is not a good measure of cohesion. Using a submerged vertical jet impinging on a horizontal soil surface, Moore and Masch (1962) determined the rate of scour of different cohesive soils as a function of Reynolds number, jet diameter, and height of the jet nozzle above the surface of the soil sample. The most important finding in this work was the existence of a point of "incipient scour" beyond which scour rate (change in the weight of the sample per time) increased linearly with Reynolds number. Espey (1963) obtained a range of shear stresses (8.6 – 96 Pa) at which failure occurred (using a rotating cylinder type apparatus) but did not relate the shear stresses to soil properties. Berghager and Ladd (1964) measured the cohesion and undrained strength characteristics of Boston blue clay (PI of 12.5%) using a direct shear apparatus. They found that saturated samples showed considerably more stability (no scouring at shear stresses up to 34 Pa) than unsaturated soil samples (which failed at the lowest possible shear stresses) compacted under the same consolidation pressure.

Comparison of the results in this second phase are highly suspect due to a number of factors, such as dissimilar flow and boundary conditions, different equipment and methodologies, lack of discrimination between fluvial erosion and mass wasting, and soil/water chemistry not

systematically specified or controlled (Berghager and Ladd, 1964). Nonetheless, significant findings include the following (after Partheniades, 2009):

- Critical shear stress can vary for soils of comparable bulk shear strength and comparable Atterberg limits; therefore, measures of macroscopic shear strength (such as the vane shear strength and plasticity index) are perhaps not correlated with erosion resistance.
- Bulk shear strength and Atterberg limits which control failure through the soil mass are not representative of soil physiochemical properties controlling fluvial erosion.
- Surface erosion resistance is dynamic and may change with time, water chemistry and temperature.
- Sample preparation (in terms of moisture content and compaction methods) affect the resistance of cohesive soils.

The third and latest phase of cohesive soil erosion research involved the study of erosion and deposition of cohesive soils with respect to flow structure and the dynamics of soil detachment as a function of soil physicochemical properties. Cristensen and Das (1974) studied the effects of critical tractive stress on the rate of erosion of remolded cohesive soils (Kaolinite/Illite and Ottawa sand mixtures) under steady flow conditions and found that rate of erosion increased significantly with increase in water temperature. Taylor and Vanoni (1972) showed an increase in near bed high intensity turbulent fluctuations with increasing fluid temperatures but Gularte et al. (1980) supposed that a higher fluid temperature should lead to lower bed shear stress (and consequently lower erosion) due to a lower viscosity and hence a lower turbulent shear coefficient. Mitchell (1993) theorized that the double layer interaction at the soil and water interface has a direct effect on the inter-particle forces of attraction on the soil surface and deduced that fluid properties (such

as temperature, salinity) can directly interfere with the stability of the double layer thus affecting cohesive soil erodibility. Christensen and Das (1973), Raudkivi and Hutchinson (1974), and Gularte et al., (1980) investigated cohesive soil erosion in terms of activation energies (using a process rate theory) and concluded that physicochemical properties of the soil/water module rather than the soil bulk mechanical properties are the prevailing "forces" in predicting soil erosion. Additionally, recent works such as those by Couper and Maddock (2001) and Wynn and Mostaghimi (2006) show that increasing stream temperatures can greatly amplify the rate of streambank retreat.

Representative Studies of Cohesive Soil Erosion Research

To fully appreciate the disparateness of cohesive erosion studies and how the current state of knowledge has been obtained through these studies, it is necessary to consider each study somewhat independently. Therefore, the following studies, presented as summaries, have been chosen as representative of the evolution of cohesive soil research through time.

Experiments on the Scour Resistance of Cohesive Sediments

W. L. Moore and F.D. Masch (1962)

The first part of this study presents scour inception and scour rate from the action of a vertical jet impinging on the surface of remolded and natural cohesive soils (5in diameter by 4 in length). The chemical compositions of the soil samples and of the eroding fluid (pH, temperature etc.) were not presented in the study but it was found that the different soil types (remolded/natural) had different points of scour inception. The depth of scour was calculated from the mass of soil eroded by relating depth to volume. Beyond the point of incipient scour, the scour rate for the different soil types increased with Reynolds number. The effect of nozzle sizes on scour rate was

also investigated and it was found that asides the change in slope of the plot of scour rate vs Reynolds number, the relationship between scour rate and impinging flow velocity remained valid. Additionally, for the range of nozzle distances used in this study (6-10 nozzle diameters) and for all soil types maximum scour rate beyond the point of incipient scour occurred near a distance of 8 nozzle diameters.

In the second part of the study, the authors presented a cylindrical rotating device similar to the Couette erosion device and used a glycerin/water mixture as their entraining fluid. This mixture reacted with the soil and formed an erosion resistant layer on the soil surface thus indicating that water chemistry can alter cohesive soil resistance to erosion by changing the soil chemistry.

Tractive Resistance of Cohesive Soils

I.S. Dunn (1959)

Dunn was one of the first to investigate the relationship between cohesive soil strength and a type of critical shear stress termed 'critical tractive force'. The goal of this work was to present a way of estimating the erosion resistance of cohesive soils from a measure of soil bulk strength which in this case was the 'vane shear strength'. Soil samples were taken from the top 0-5 inches of a number of channels in Colorado, Wyoming and Nebraska. The soil samples were prepared for reconsolidation by oven drying and sieving with a 2-mm diameter sieve to remove the macrostructure. The soil was then consolidated at water contents above saturation and liquid limits, between porous plates in a 6.25 diameter metal container for a duration of 3 days. After consolidation, the top of the soil was exposed to a column of water for two days before testing using an impinging jet device. Multiple soils were tested at different consolidation pressures and a vane device used to obtain the vane shear strength of the soil at the depth where scour ceased

after subjection to the action of the impinging jet. The authors found that erosion resistance increased with vane shear strength, and claimed that, for soils with a plasticity index between 5 and 16, plasticity index can be used to estimate the critical tractive force.

Erosion and Deposition of Cohesive Soils

E. Partheniades (1965)

Experiments were conducted in a straight rectangular flume (60ft x 1ft x 15in) to determine how applied boundary shear stress, suspended sediment concentration and cohesion strength of bed (measured with a device similar to a penetrometer) affect erosion rate of the San Francisco bay mud. The San Francisco mud is composed of roughly equal parts of clay and silt with the clay fraction primarily Montmorillonite with some Illite. The flume bed was either made of the San Francisco bay mud at field moisture content or of settled solids after the flume water had been mixed with the soil. The eroding water was maintained at ocean salinity to represent saline conditions at estuaries. The pH and temperature of the soil and eroding water were not measured.

It was found that suspended sediment concentration had no effect on the erosion rate of the mud. Also, the erosion rate was not affected by the cohesion strength of the bed as long as flow does not induce stresses, through the bulk of the soil, large enough to cause mass failure. It was found that for the bed conditions considered, a point of incipient scour existed above which erosion rate increased rapidly with increased boundary shear stress. The chemistry of the system was altered, albeit inadvertently, by the introduction of Iron oxides in the soil and eroding water during the course of the experiments which resulted in increased erosion resistance. This increased erosion resistance was believed to be caused by the increased electrochemical forces of attraction between the clay particles.

Resistance of Selected Clay Systems to Erosion by Water

E. H. Grissinger (1966)

The erosion rates of cohesive soils were investigated by subjecting four soil types to constant shear flow in a small flume. Four different soil combinations were used to represent a range of conditions commonly encountered in natural systems. These soil types were created by mixing weighted amounts of kaolinite, sodium montmorillonite, calcium montmorillonite and illite with Grenada silt loam (20% clay, 74% silt, 6% sand). The liquid limit and plastic limit moisture contents of the Grenada silt loam were 31% and 20% respectively, while the plasticity index was 11. The different soil combinations were poured into molds 5cm by 12.5cm. The orientation of the clay minerals was controlled by compacting the soil samples at moisture contents close to saturation or by increasing compaction efforts at constant moisture content. Another method used to control the orientation of the clay minerals was by subjecting saturated soil samples to elevated suction pressures ranging from 45 cmH_2O to 60 cmHg till the sample returned to its original volume. The mold containing a sample was placed in the outside bend of a flume wall immediately after a 5^0 change in flume direction and erosion rate determined by loss in weight after each experiment.

It was found that cohesive soil erosion was influenced by the type and percentage of clay minerals, bulk density at compaction and antecedent moisture content. Although the researcher didn't test for the effect of water temperature and sample aging time on the erosion rates, it was found that increasing these parameters reduces soil stability.

Fundamental Aspects of Erosion of Cohesive Soils

K. Arulanandan (1974)

Erosion tests were carried in a rotating cylinder apparatus developed earlier by Moore and Masch (1962). Remolded soil samples used were prepared by mixing Kaolinite, Illite and Montmorillonite with 60% silica flour. The dispersive properties of the different clay types and fractions were quantified by measuring the magnitude of the dielectric constant which is the difference in dielectric constant measured at 3e6 Hz and 75e6 Hz. CEC is known to be proportional to the magnitude of the dielectric constant. Critical shear stresses were measured using the methods described by Riley and Arulanandan (1972) and the test results showed that erosion rate decreased with increasing salt concentration of the eroding fluid. The researchers also found out that osmotic swelling of soil samples was accompanied by a reduction in the critical shear stress.

Erosion Resistance of Cohesive Soils

W. E. Kelly & R. C. Gularte (1981)

Rate process theory as applied to soil strength described by Mitchell (1964) was used to quantify the erosion of cohesive soils. A water tunnel (5.5m x 2m x 1.5m) with a cooling mechanism to maintain water temperatures within ± 0.2 ^{0}K was specifically designed for this experiment. Remolded Grundite (illite) was subjected to conditions in which either flow velocity was varied and water temperature held constant or flow velocity held constant while water temperature was varied. The soil sample was created at four different salinities (2.5-10 ppt NaCl) and 5 different moisture contents (40% - 80%). In all cases, the salinities of both soil sample and eroding water were the same and the pH of the system 8.5. The shear velocity was obtained from the average shearing force which was measured by using an instrumented shear plate. The researchers found out that erosion increased with increasing water temperatures. Also, increasing

salinity reduced the amount of soil eroded which was explained, within the parameters of the double layer theory, to be the result of increased net forces of attraction between clay particles.

Cohesive Material Erosion by Unidirectional Current

J.W. Kamphuis & K.R. Hall (1983)

Experiments were performed in a flume to determine the effects of consolidation, clay content, vane shear strength and plasticity index on critical shear stress and velocity. Testing were done on cohesive river bed materials from Mackenzie River (Normal Wells, Northwestern Canada) and surface samples around the same location. An additional sample types was created by adding uniformly graded silica sand to the land based soil to get cohesive soils at 15%, 30% and 45% clay content. Soil samples were consolidated with pressures ranging from 48 kPa to 350 kPa. The only parameters measured were the boundary shear stress and critical velocity at the point when erosion began. X-ray diffraction showed that soil samples from both the river bed and adjacent land were composed of 50-60% quartz, 15-20% Fe-chlorite, 20-25% illite and 1-10% montmorillonite. Each sample was prepared as soil blocks (150mm x 600mm x 100mm) by consolidating the parent soil in cubic press for 2-4 days till the soil reached 95% consolidation. The soil was then left to adjust for a day in the mold before being cured in a wet cloth for one day. During the experiments, soil/water pH and temperature were maintained at 18 ^{0}C ± 2 ^{0}C and 7.4 ± 0.2 respectively. The results of this experiment showed that shear stress and shear velocity at the point of incipient scour increased with increased compressive strength, consolidation pressure, plasticity index, vane shear strength and clay content.

Effect of Temperature on the Interfacial Properties of Silicates

R. Ramachandran & P. Somasundaran (1986)

The zeta potential of quartz (a primary silicate) and Na-kaolinite (a secondary silicate) was measured as a function of temperature under different pH conditions. Brazilian quartz was soaked in concentrated nitric acid to remove iron and washed in distilled water until the pH became constant to remove nitrate ions. The purified quartz was then stored at a pH of 2. Georgia kaolinites sourced from the University of Missouri were washed in NaCl (after Hollander et al., 1981) to obtain homoionic Na-kaolinite. Using the streaming potential technique previously used by Somasundaran and Kulkarni (1973), zeta potentials of these silicates were measured as a function of temperature. At all experimental pHs, the zeta potential of quartz reduced with increasing temperatures (10 ^{0}C, 35 ^{0}C and 75 ^{0}C). A hysteresis effect was observed as the zeta potential of quartz did not return to its initial value when the heated quartz was cooled. For Na-kaolinite, the zeta potential increased with increasing temperatures in the acidic pH range but decreased with increasing temperature in the alkaline pH range.

Conclusion

Based on the brief summaries of some of the representative erosion studies, the diversity of methods and aims in cohesive erosion studies can be inferred. Although the results of these studies are difficult to generalize, these studies nevertheless shed important light on the many factors that need to be considered in designing cohesive erosion experiments. In all, the nascent field of cohesive soil erosion will benefit immensely from studies that can further reveal the erosive behavior of cohesive sediments in fluvial systems. With many such studies over time, the

difficulties of predicting cohesive erosion occurrence and rates in the preservation of the natural environment and in the engineering of fluvial systems will be surmounted.

References

Arulanandan, K., Gillogley, E., and Tully, R. (1980). "Development of a Quantitative Method to Predict Critical Shear Stress and Rate of Erosion of Natural Undisturbed Cohesive Soils." Rep. No. GL-80-5, U.S. Army Engineer Waterways Experiment Station, Vicksburg, MS.

Arulanandan, K., Loganthan, P., and Krone, R. B. (1975). "Pore and eroding fluid influences on surface erosion of soil." *J. Geotech. Engrg. Div.*, ASCE, 101(1), 51–66.

Baumgarten, W., Neugebauer, T., Fuchs, E., and Horn, R. (2012). "Structural stability of marshland soils of the riparian zone of the Tidal Elbe River." *Soil Till. Res.*, 125, 80-88.

Berghager, D., and Ladd, C. C. (1964). Erosion of Cohesive Soils. Department of Civil Engineering Research Report R64–1, Massachusetts Institute of Technology, Boston, MA.

Blench, T. (1952). "Regime theory for self-formed sediment-bearing channels." *Trans. ASCE*, 117, 383–400.

Bohn. H. L., McNeal, B. L., and O'Connor, G. A. (1985). Soil Chemistry. Wiley & Sons, NY.

Christensen, R. W., and Das, B. M. (1973). "Hydraulic erosion of remolded cohesive soils." Soil erosion: Causes and mechanisms; prevention and control, Special Rep. 135, Highway Research Board, Washington, D.C., 8–19.

Couper, P. R., and Maddock, I. P. (2001). "Subaerial river bank erosion processes and their interaction with other bank erosion mechanisms on the River Arrow, Warwickshire, UK." *Earth Surf. Proc. Land.*, 26(6), 631–646.

Craig, R. F. (1992). Soil Mechanics, 5th edition. Chapman and Hall, London.

Dietrich W. E., and Gallinatti J. D. (1991). Fluvial geomorphology. In Field Experiments and Measurement Programs in Geomorphology, Slaymaker O (ed.). Balkema: Rotterdam.

Droppo, I. G. (2001). "Rethinking what constitutes suspended sediment." *Hydrol. Process*, 15, 1551–1564.

Ducharne, A. (2008). "Importance of stream temperature to climate change impact on water quality." *Hydrol. Earth Syst. Sc.*, 12, 797–810.

Dunn, I. S. (1959). "Tractive resistance to cohesive channels." *J. Soil Mech. and Found. Div.*, ASCE, 85(3), 1–24.

Edwards, L. M. (1991). "The effect of alternate freezing and thawing on aggregate stability and aggregate size distribution of some Prince Edward Island soils." *J. Soil Sci.*, 42, 193–204.

Espey, W. H. (1963). A new test to measure the scour of cohesive sediment. Department of Civil Engineering Technical Report UYD01-6301, The University of Texas, Austin, TX.

Grabowski, R. C., Droppo, I. G., and Wharton, G. (2011). "Erodibility of cohesive sediment: The importance of sediment properties." *Earth-Sci. Rev.*, 105(3), 101-120.

Grissinger, E. H. (1966). "Resistance of selected clay systems to erosion by water." *Water Resour. Res.*, Wiley, 2(1), 131–138.

Gularte, R. C., Kelly, W. E., and Nacci, V. A. (1980). "Erosion of cohesive sediments as a rate process." *Ocean Engng.*, 7, 539-551.

Hester, E. T., and Bauman, K. S. (2013). "Stream and retention pond thermal response to heated summer runoff from urban impervious surfaces." *J. Am. Water Resour. As.*, 49(2), 328–342.

Hollander, A. F., Somasundaran, P., and Gryte, C. C. (1981). Adsorption from Aqueous Solution. Plenum, New York.

Hooke J. M. (1979). "An analysis of the processes of river bank erosion." *J. Hydrol.*, 42, 39–62.

IPCC. (2007). The physical science basis. In: Solomon, S., Qin, D., Manning, M., Chen, Z., Marquis, M., Averyt, K. B., Tignor, M., Miler, H. L., eds. *Contribution of Working Group I to the Fourth Assessment Report of the International Panel on Climate Change Program*. Cambridge, UK/New York, USA: Cambridge University Press, 996.

Kamphuis, J. W., and Hall, K. R. (1983). "Cohesive material erosion by unidirectional current." *J. Hydraul. Eng*., 109(1), 49-61.

Kaushal, S. S., Likens, G. E., Jaworski, N. A., Pace, M. L., Sides, A. M., Seekell, D., Belt, K. T., Secor, D. H., and Wingate, R. L. (2010). "Rising stream and river temperatures in the United States." *Frontiers Ecol. Environ*., 8(9), 461–466.

Kelly, E. K., and Gularte, R. C. (1981). "Erosion resistance of cohesive soils." *J. Hydr. Div.,* ASCE, 107(10), 1211–1224.

Kennedy, R. G. (1895). "The prevention of silting in irrigation canals." Proc., Inst. of Civ. Engrs., London, England, Vol. CXIX.

Knapen A, Poesen J, Govers G, Gyssels G, Nachtergaele J. (2007). "Resistance of soils to concentrated flow erosion: a review." *Earth Sci. Rev.,* 80(1–2), 75–109.

Lawler, D. M. (1992). "Process dominance in bank erosion systems." *Lowland floodplain rivers: Geomorphological perspectives*, P. A. Carling and G. E. Petts, eds., Wiley, NY 117–143.

Lehrsch, G. A. (1998). "Freeze-thaw cycles increase near-surface aggregate stability." *Soil Sci.*, 163(1), 63–70.

Mitchell, J. K., and Soga, K. (2005). *Fundamentals of soil behavior,* 3rd Ed., Wiley, London.

Mirtskhulava, T. E. (1966). "Erosional stability of cohesive soils." *J. Hydraul. Res.*, 4(1), 37-50.

Mehta, A. J. (1991). "Review notes on cohesive sediment erosion." *Proc. Coastal Sediments,* Seattle, WA, 1(1), 40– 53.

Mohseni, O., and Stefan, H. G. (1999). "Stream temperature/air temperature relationship: a physical interpretation." *J. Hydrol.*, 218, 128–141.

Moore, W. L., and Masch, F. D. (1962). "Experiments on the scour resistance of cohesive sediments." *J. Geophys. Res.*, 67(4), 1437–1449.

Mostaghimi S., Young, R. A., Wilts, A. R, Kenimer, A. L. (1988). "Effects of frost action on soil aggregate stability." *Trans. ASAE*, 31, 435–439.

Nelson, K. C., and Palmer, M. A. (2007). Stream temperature surges under urbanization and climate change: Data, models, and responses. *J. Am. Water Resour. As.*, 43(2), 440-452.

Parks, O. W. (2012). "Effect of Water Temperature on Cohesive Soil Erosion". M.Sc. Thesis, Dept. of Biological Systems Engineering, Virginia Polytechnic Institute and State University, Blacksburg, VA.

Partheniades, E. (1965). "Erosion and Deposition of Cohesive Soils." *J. Hydr. Div.*, ASCE, 91, 105–139.

Partheniades, E. (2009). Cohesive Sediments in Open Channels, Butterworth-Heinemann, Burlington, MA.

Partheniades, E., and Paaswell, R. E. (1970). "Erodibility of channels with cohesive boundary." *J. Hydr. Div.*, ASCE, 96(3), 755–771.

Pluhowski, E. J. (1970). "Urbanization and its Effect on the Temperature of Streams on Long Island, New York." Geological Survey Professional Paper, 627-D.

Ramachandran, R., and Somasundaran, P. (1986). "Effect of temperature on the interfacial properties of silicates." *Colloids Surf.*, 21, 355–369.

Raudkivi, A. J. (1998). Loose boundary hydraulics, 4th Ed., Balkema, Rotterdam, The Netherlands.

Raudkivi, A. J., and Hutchison, D. L. (1974). “Erosion of kaolinite clay by flowing water.” Proc. Roy. Soc. London, 337, 537–544.

Riley, J. P., and Arulanandan, K. (1972) "A Method for Measuring the Erodibility of Soils." Technical Note 72-2, Department of Civil Engineering, University of California, Davis, CA.

Sargunam, A., Riley, P., Arulanandan, K., and Krone, R. B. (1973). “Physico-chemical factors in erosion of cohesive soils.” *J. Hydr. Div.*, ASCE, 99(3), 555–558.

Shang, J. Q., Lo, K. Y., and Quigley, R. M. (1994). “Quantitative-determination of potential distribution in Stern-Gouy double-layer model.” *Can. Geotech. J.*, 31(5), 624-636.

Sharif, A. R. (2003). “Critical shear stress and erosion of cohesive soils.” Ph.D. thesis, Dept. of Civil, Structural, and Environmental Engineering, State Univ. of New York at Buffalo, Buffalo, NY.

Shine, K. P., and Forster, P. M. (1999). “The effect of human activity on the radiative forcing of climate change: a review of recent developments.” *Global Planet. Change*, 20, 205–225.

Simon, A., and Collison, A. J. C. (2002). “Quantifying the mechanical and hydrologic effects of riparian vegetation on streambank stability.” *Earth Surf. Proc. Land.*, 27, 527-546.

Singh, U., and Uehara, G. (1986). Electrochemistry of the double layer: Principles and applications to soils. In “Soil Physical Chemistry” (D. L. Sparks, Ed.), 1–38. CRC Press, Boca Raton, FL.

Singh, V. P. (2003). “On the theories of hydraulic geometry.” *Int. J. Sediment Res.*, 18(3), 196–218.

Smerdon, E. T., and Beasley, R. P. (1959). ‘‘Tractive force theory applied to stability of open channels in cohesive soils.’’ Res. Bull. No. 715, Agricultural Experiment Station, University of Missouri, Columbia.

Smerdon, E. T., and Beasley, R. P. (1961). "Critical tractive forces in cohesive soils." *Agr. Eng.*, 42(1), 26-29.

Smith, T. M., Reynolds, R. W., and Lawrimore, J. (2008). “Improvements to NOAA's historical merged land-ocean surface temperature analysis (1880–2006).” *J. Clim.*, 21, 2283–2296.

Somansundaran, P., and Kulkarni, R. D. (1973) “A new streaming potential apparatus and study of temperature effects using it.” *J. Colloid. Interface Sci.*, 45(3), 591-600.

Sparks, D. L. (2003). *Environmental Soil Chemistry,* Academic Press, London, UK.

Taylor, B. D., and Vanoni, V. A. (1972). “Temperature Effects in High-Transport Flat-Bed Flows.” *J. Hydr. Div*, ASCE, 98(12), 2191–2206.

Thorne, C. R. (1982). Processes and mechanisms of river bank erosion. In Gravel-bed Rivers: Fluvial Processes, Engineering and Management. Hey, R. D., Bathurst, J. C., Thorne, C. R. (eds). John Wiley, NY, 227–271.

Thorne C. R., and Lewin J. (1979). “Bank processes, bed material movement and planform development in a meandering river”. In Adjustments of the Fluvial System. D. D. Rhodes and G. P. Williams (eds). Kendall/Hunt, Dubuque, IA, 117-137.

USEPA. (2016). National summary of impaired waters and TMDL information. Washington, DC.

Winterwerp, J. C., and van Kesteren, W. M. (2004). Introduction to the Physics of Cohesive Sediment in the Marine Environment, Dev. Sedimentol., vol. 56, Elsevier, Amsterdam, The Netherlands.

Webb, B. W., and Nobilis, F. (2007). “Long-term changes in river temperature and the influence of climatic and hydrologic factors.” *Hydrol. Sci.*, 52, 74–85.

Webb, B. W., and Zhang, Y. (1997). “Spatial and seasonal variability in the components of the river heat budget.” *Hydrol. Process.*, 11, 79–101.

Wolman M. G. (1959). “Factors influencing erosion of a cohesive river bank.” *Am. J. Sci.*, 257, 204–216.

Wynn, T. M., and Mostaghimi, S. (2006). “Effects of riparian vegetation on stream bank subaerial processes in southwestern Virginia, USA.” *Earth Surf. Proc. Land.*, 31(4), 399–413.

Zhu, Y. H., Lu, J. Y., Liao, H. Z., Wang, J. S., Fan, B. L., and Yao, S. M. (2008). “Research on cohesive sediment erosion by flow: An overview.” *Sci. China Ser. E.*, 51(11), 2001-2012.

CHAPTER 3

INFLUENCE OF SAMPLE HOLDING TIME ON THE FLUVIAL EROSION OF REMOLDED COHESIVE SOILS

Citation: Akinola, A. I., T., Wynn-Thompson, C. G. Olgun, F. Cuceoglu, S. Mostaghimi. 2018. "Influence of Sample Holding Time on the Fluvial Erosion of Remolded Cohesive Soils". Journal of Hydraulic Engineering, ASCE. 144(8). https://doi.org/10.1061/(ASCE)HY.1943-7900.0001504.

Abstract

Despite extensive research on bridge scour and channel erosion, predicting the occurrence and rate of cohesive soil erosion remains problematic. The lack of standard procedures for sample preparation and testing has resulted in wide variations in testing conditions, devices, and soil properties across erosion studies, ultimately preventing the synthesis of cohesive erosion studies and progress in understanding the fundamental processes of cohesive soil erosion. Therefore, the objective of this study was to evaluate the effects of sample holding time on the fluvial erosion of remolded cohesive soils to inform the development of standard testing procedures.

Three different soils (fat clay, lean clay and silty sand) were tested in a flume following multiple different sample holding times. Results show that erosion rate can decrease 85-95% within 72 hours of soil wetting, depending on clay mineralogy. These results highlight the importance of maintaining a consistent soil preparation protocol in cohesive soil erosion

experiments and reporting soil sample holding durations when conducting cohesive erosion research using remolded samples.

Author keywords: Cohesive soil; Fluvial erosion; Streambank erosion; Flume

Introduction

The importance of cohesive soil erosion research cannot be overemphasized. In the US alone, the annual total on-site and off-site costs of damages due to soil erosion, as well as the cost of erosion prevention, is estimated at 44 billion US dollars (Pimentel et al. 1995; Telles et al. 2011). Prior research summaries showed that streambank retreat can account for up to 80% of watershed sediment yield (Simon et al 2002; Simon and Rinaldi 2006). Willett et al. (2012) documented streambank sediment contributions of up to 96% of total sediment yield in two watersheds of the Central Claypan Region of Missouri, United States. While river or stream migration is a natural dynamic process, excessive bank erosion leads to land and habitat loss, as well as the loss of functionality of urban structures like dams, dykes, levees and bridges through excessive sediment supply or direct scour.

Streambank retreat

Generally, streambank retreat occurs through the combination of three distinct processes – subaerial weakening, fluvial entrainment and mass wasting - with each mechanism dominating over a different temporal and/or spatial scale (Lawler 1992; Couper and Maddock 2001). Typically considered a precursor of fluvial erosion and mass wasting (Prosser et al. 2000), subaerial weakening includes 'land-based' processes that disrupt the soil surface, such as needle-ice formation and wetting-drying and freeze-thaw cycling. Fluvial erosion is the detachment and entrainment of soil by moving water. This dominates at the bank toe, leading to increased bank angles and mass wasting. Mass wasting is a geotechnical failure of the streambank frequently occurring when the weight of the saturated bank becomes greater than the bank shear strength. The focus of this research is on fluvial erosion, therefore this process will be presented in detail.

Fluvial erosion

Fluvial erosion is the mobilization of soil at the soil/water interface by moving water. With respect to non-cohesive soils, detachment and transport of individual particles occur when eroding forces are greater than resisting forces, with the resisting forces being a function of individual particle weight, packing, and exposure. For cohesive soils, the forces resisting erosion depend on the physicochemical properties of the soil and the interaction between soil and water chemistry (Raudkivi and Tan 1984; Raudviki 1998; Partheniades 2009). Physically, water flowing over a surface exerts shear stress on that surface. When water flows over cohesive soils, the soil surface and structure respond chemically through ion exchange and adjustments to maintain electroneutrality (Winterwerp and van Kesteren 2004) and physically by absorbing water and swelling (Mitchell and Soga, 2005). Unlike non-cohesive soils where erosion occurs particle by particle, the erosion of cohesive soils is usually in aggregates (Mirtskhulava 1966; Utley and Wynn 2008) when the hydraulic forces are large enough to overcome the interparticle forces of attraction between the aggregates (Raudviki 1998). The degree of interparticle attraction in cohesive soils is affected by soil parameters such as grain size, clay content and type, water content, salt content, temperature, and ion exchange capacity (Arulanandan et al. 1980; Mehta 1991; Grabowski et al. 2011). Interparticle attraction at the surface of cohesive soils is also affected by the chemical properties of the eroding fluid such as dissolved ions, temperature, pH, (Mehta 1991; Grabowski et al. 2011), as well as the biological properties of the soil matrix (Sgro et al. 2005; Wynn and Mostaghimi 2006).

A measure of the erosive resistance of cohesive soils is known as soil erodibility and the factors which affect this parameter can be classified as physical, geochemical or biological factors (after Grabowski et al. 2011). Physical factors affecting soil erodibility include mean particle size,

particle size distribution (Young 1980; Thomsen and Gust 2000; Gerbersdorf et al. 2007; Debnath et al. 2007), bulk density and consolidation (Grissinger 1966; Kamphuis and Hall 1983; Jepsen et al. 1997; Amos et al. 2004; Bale et al. 2007), water content (van Ledden et al. 2004), pore-water pressure (Simon and Collison 2001) and temperature (Zreik et al. 1998; Mehta and Parchure 2000; Parks 2012). Geochemical factors include clay mineralogy (Kandiah 1974), total salinity, sodium adsorption ratio, pH (Kandiah 1974; Parchure and Mehta 1985; Winterwerp and van Kesteren 2004; Debnath et al. 2007), metals (Winterwerp and van Kesteren 2004) and organic content (Lick and McNeil 2001; Morgan 2006; Gerbersdorf et al. 2007). Biological factors include processes which promote biostabilization or bioturbation of cohesive sediments, such as feeding and egestion (Graf and Rosenberg 1997), and the presence of biogenic structure (Morgan and Rickson 1995; Wynn and Mostaghimi 2006; Widdows et al. 2009; Fernandes et al. 2009) or secretions.

Cohesive soil mineralogy

Simply determining which soils are cohesive is difficult: repulsive and attractive forces exist in soils and the net force is often a function of the combined physical, biological, and chemical properties of the soil. However, cohesive soils can be defined as soils composed of clay, silt, fine sand, organic material, water, and gas components, with the clay content high enough to influence the erosive behavior of the soil through the action of the electrochemical and atomic forces of the clay fraction (Winterwerp & van Kesteren 2004; Partheniades 2009). Soils with a plasticity index less than 10 are also commonly classified as cohesionless, although this criterion is frequently inadequate in describing soil behavior (Hanson, 1991).

Since the erodibility of a cohesive soil is largely influenced by its clay mineralogy, an understanding the mineralogy and physicochemical properties of clays is invaluable in studying the erosion of cohesive soils. Clays are secondary minerals or phyllosilicates formed from the

chemical weathering of rock in the presence of water and are mainly composed of two dimensional silica tetrahedra and aluminum-hydroxide or magnesium-hydroxide octahedra in various combinations and with different cationic substitutions. Three major clay minerals are kaolinites, micas (e.g illites and vermuculites), smectites (e.g. montmorillonite), with kaolinites being the least reactive and smectites the most reactive (Partheniades 2009). Kaolinites are 1:1 layer clay minerals with a single tetrahedral silica and octahedral alumina sheet forming the fundamental structure. Kaolinites are stable, possess very low isomorphic substitution, resist movement of water into the lattices and are therefore non-expansive. Vermiculites and illites are two of the major types of micacious clays with a basal 2:1 layer phyllosilicate structure having a single octahedral layer between two tetrahedral sheets. In illites, structured interlayer cations (K, Mg or Ca) within the clay sheets prevent the entrance of water molecules into the structure making this clay type non-expanding. Vermiculites are weathered micas in which interlayer K ions have been replaced by hydrated cations (such as Mg and Fe) making this clay type slightly expandable. In contrast, montmorillonites are highly expandable clays with low interlayer bonding strength due to weak oxygen and cation/oxygen bonds which allows relatively easy movement of water and hydrated cations into the interlayer space.

Measurement and modeling of cohesive soil erosion

Cohesive erosion testing is typically conducted to either characterize local site conditions or to better understand and model cohesive erosion, and a number of devices, based on different operating principles, have been developed to perform these tests. Some of these devices include the circular couette flow erosion device (Moore and Masch 1961; Raudkivi and Tan 1984), the jet erosion test device (Dunn 1959; Hanson 1991; Hanson and Cook 2004), the hole erosion test device (Wan and Fell 2002; 2004), traditional laboratory flumes - straight and annular

(Partheniades 1965; Arulanandan et al. 1980), and the erosion function apparatus (Briaud et al. 1999; 2001). In-situ devices are used to characterize local field conditions, with little control of soil and environmental variabilities, while ex-situ devices are used to test soil erosion in a carefully managed process by reducing natural site variability as much as possible. Therefore the appropriate test device and type of soil sample are selected based on the objectives of the study - to characterize a specific site or to test for specific influences on cohesive soil erosion.

The erosion of cohesive soils is often modeled using the excess shear stress equation (Partheniades 1965; Hanson 1990; Hanson and Cook 1997). This equation is expressed as:

$$E_r = k_d(\tau - \tau_c)^a \quad for\ \tau > \tau_c \tag{3.1}$$

where E_r = erosion rate (m/s), k_d = erodibility coefficient ($m^3/N{\cdot}s$), τ = applied hydraulic shear stress (Pa), τ_c = critical shear stress (Pa), and a= an empirical exponent usually assumed to be unity. Using an erosion test device, cohesive soil is subjected to a range of hydraulic shear stresses and the erosion rates are measured. The data are then fit to the excess shear stress equation to determine model parameters (the critical shear stress and the erodibility coefficient). While the model parameters are frequently considered constant for a given soil, research has shown these parameters can vary seasonally by up to a factor of 3 (Wynn et al. 2008) and with properties of the entraining fluid, such as salt content and temperature (Partheniades 1965; Grissinger 1966; Passwell 1973; Sargunam et al. 1973; Ariathurai and Arulanandan 1978; Arulanandan et al. 1980; Mehta 1986; Grabowski et al. 2012). Therefore, for experimental cohesive soil erosion research to

be comparable, the major factors that affect the erosion process must be accounted for and carefully moderated during testing.

One of the factors that must be carefully controlled during cohesive soil erosion experiments that use remolded samples is the soil holding time. In this context the soil holding time is defined as the time interval between the time the sample is brought to the initial testing moisture content and when erosion testing is performed. The strengthening of a soil mass with time after reconstruction is a beneficial soil process that increases aggregate stability (Kemper and Rosenau 1984; Shainberg et al. 1996); however, it can lead to significant test variability if not carefully controlled during erosion tests utilizing remolded cohesive soils. For laboratory erosion tests where in-situ conditions are desired, it is important to carefully preserve field conditions of density and moisture content, and to minimize disturbances during handling and transporting (Tohurst et al. 2000). Utomo and Dexter (1980) measured the compression resistance and water stability of disturbed soils over time, keeping moisture content and temperature constant, and found that these two soil properties increased with time. Kemper and Rosenau (1984) studied the rate of cohesion development in two different soils using aggregate stability and modulus of rupture as surrogates of cohesion and found that both properties increased with time (methods described in Kemper and Rosenau 1986). However, to the best knowledge of the authors, no researchers have specifically investigated the impact of sample holding time on the susceptibility of cohesive soils to fluvial entrainment. In fluvial erosion studies, researchers, by default, have a set soil holding time based on the researcher's soil preparation methodology. Since these methods vary as widely as there are researchers, sample holding times for prior research likely also varied among researchers and possibly within individual studies. Additionally, lack of documentation of experimental methodology suggests that strict sample preparation and testing protocols may not

have been followed by prior researchers. Therefore, the objective of this research is to quantify the effects of remolded soil sample age on the fluvial erosion of cohesive soils for the purpose of informing the development of standard cohesive soil preparation and erosion testing procedures. And, although this study pertains to laboratory experiments involving remolded cohesive soils simulating streambank erosion, the results are also applicable to erosion research in the marine environment where, for laboratory or in-situ tests, cohesive test beds are formed through sediment flocculation and self-weight consolidation.

Methodology

Soil preparation

For this research, three different natural soils were chosen to represent a range of riparian soil types. The first soil is a montmorillonite/kaolinite-dominated soil obtained along the banks of Stroubles Creek in Blacksburg, Virginia, at a depth of 45-60 cm from the top of the bank. Taking sand, silt and clay fractions as having particle size ranges of 2 mm to 75 μm, 75 to 2 μm, and < 2 μm respectively, grain size distribution tests using sieve analysis and hydrometer tests [ASTM D422-63 (ASTM 2007); ASTM C136 (ASTM 2006)] showed that this soil contains 27% sand, 65% silt and 8% clay. The clay fraction (particle size < 2 μm) was previously determined to contain 35% kaolinite, 25% montmorillonite, 20% illite, 15% H-I vermiculite, 3% chlorite and 2% quartz using x-ray diffraction and thermogravimetric analysis (Karathanasis and Harris 1994; Wynn et al. 2008). For this soil, pretreatment procedures before clay fractionalization included organic matter removal with 30% H_2O_2 at pH 5 (after Kunze 1965), sand removal by wet sieving with a 50-μm sieve and clay dispersion using 1 M Na_2CO_3 (after Gee and Or 2002). The second soil is a vermiculite-dominated soil obtained from the top 8-38 cm of the lowest terrace along the New River near Whitethorne, Virginia. Similar to the preceding soil, grain size distribution tests showed

that this soil contains 44% sand, 43% silt and 13% clay. The clay fraction (particle size < 2 μm) was previously determined to contain of 35% H-I vermiculite, 10% vermiculite, 10% mica, 15% kaolinite, 13% quartz, 10% chlorite and 6% smectite using pipette, x-ray diffraction and thermal analyses (Harris et al. 1980). The third soil is a kaolinite/illite dominated soil obtained along the banks of Tom's Creek near Whitethorne, Virginia, at a depth of 45-80 cm. Grain size distribution tests showed that this soil contains 66% sand, 28% silt and 6% clay. X-ray diffraction tests showed that the clay fraction (particle size < 2 μm) is 30-70% kaolinite and illite, 10-30% H-I vermiculite and less than 10% goethite, smectite and feldspar.

These soils were air dried, homogenized using an electric soil grinder (HM-375, Houghton Manufacturing Co., Vicksburg, MI), and passed through a 2-mm sieve to ensure a consistent soil gradation when the soils were remolded. The first, second and third soils were classified as fat clay (CH), lean clay (CL), and silty sand (SM) respectively, based on grain size distribution and Atterberg limit tests [ASTM D422-63 (ASTM 2007); ASTM C136 (ASTM 2006); ASTM D4318 (2003); Cuceoglu 2016]. Standard Proctor compaction tests [ASTM D698 (ASTM 2003)] were conducted on the sieved soils to evaluate the maximum dry density and the corresponding optimum moisture content. The maximum dry density is the highest dry density possible under a particular compactive effort and the moisture content at which this dry density is obtained is called the optimum moisture content. During preliminary tests, cores prepared at their respective maximum dry densities and optimum moisture contents did not visibly swell for the duration of the tests, therefore each soil core was prepared and tested at these values to minimize the effect of soil swelling on erosion measurements. The properties of the soils as tested, post-sieving, are given in Table 3.1.

Table 3.1 Soil specifications

USCS soil classification[a]	Liquid limit[a] (%)	Plastic limit[a] (%)	Max. dry density (g/cm^3)	Optimum moisture content (%)	Major minerals (15% and above)	Minor minerals (less than 15%)
Fat Clay (CH)	51.2	24.5	1.6	22.6	Montmorillonite Kaolinite Illite H-I vermiculite	Chlorite Quartz
Lean Clay (CL)	44.2	31.6	1.4	29.9	H-I vermiculite Kaolinite	Vermiculite Mica Quartz Chlorite Smectite
Silty Sand (SM)	30.7	20.5	1.7	18.2	Kaolinite Illite H-I vermiculite Quartz	Goethite Smectite Feldspar

Note: These specifications apply to the soils after sieving
[a] Data from Cuceoglu 2016

To prepare each soil at its optimum moisture content, the initial moisture content of the soil was measured [ASTM D2216 (ASTM, 2010)] and the amount of tap water required to bring the total moisture content of the soil mass to the optimum moisture content was added. The soil mass was then mixed and compacted into a 5-cm by 5-cm cylindrical mold in three lifts using a 4.64 kg-slide hammer lifted to a height of 50 cm. The soil surface was scarified before adding the next layer. Once created, each soil core not tested immediately was stored above a layer of water in a 100% humidity glass chamber to maintain a constant moisture content during the soil core holding period. All soil types were tested immediately and at 6, 24, 48 and 72 hours after sample preparation. The silty sand was further tested at 96 and 120 hours after preparation. Ten replicates of each soil at each holding time were tested for a total of 170 flume runs. This number of replicates was informed by preliminary erosion tests 0 hr holding time which indicated that, for the lean clay and the silty sand, 10 replicates would be sufficient for estimating the mean within a 95% confidence interval and a 20% margin of error. Since the number of replicates required for erosion

tests on the fat clay at these statistical conditions was prohibitive, the number of replicates were kept at ten.

Flume description

The erosion experiments were performed in a 8 m by 1 m by 0.4 m recirculating flume (Figure 1; Engineering Laboratory Design Inc., Lake City, MN). The flume has a maximum capacity of 5000 L and is equipped with a 500 Hp pump which can drive flows of up to 70 L/s in the flume channel. Since the goal of these experiments was to simulate streambank erosion, where detachment is the only requisite for erosion, an artificial wall was built to give this bank and flow configuration; a curved wall was created at the upstream end of the channel to gradually transition the width of the flume from 1.0 m to 0.4 m. The artificial wall was constructed of 1.25-cm thick PVC sheets supported with a wooden structure running the entire length of the flume channel. The face of the wall was roughened over the entire length of the insert by gluing sand (Premium Play Sand No. 1113, Quickrete, Atlanta, GA; D_{50} = 0.15 mm, D_{84} = 0.3 mm) to the surface of the PVC sheets. The upstream end of the channel was equipped with a flow straightener to dissipate turbulence and develop one dimensional flow.

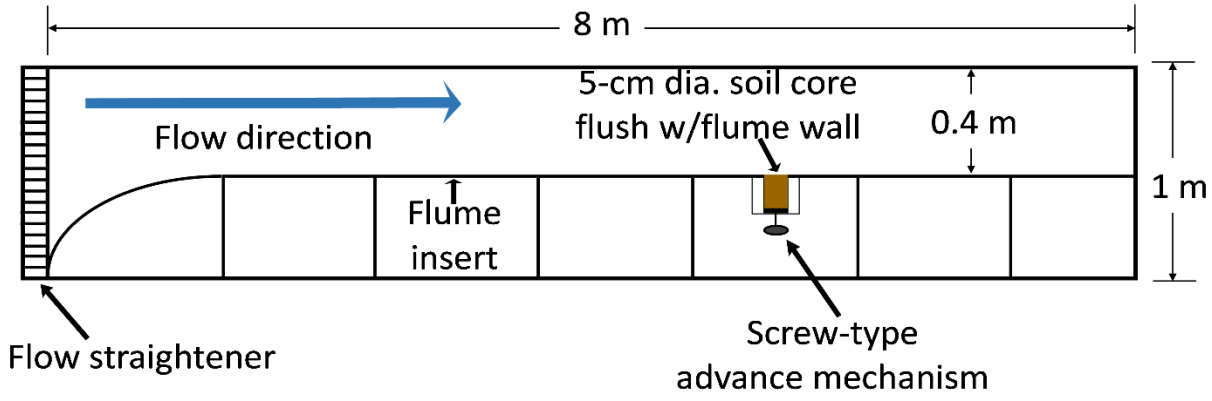

Figure 3.1 Flume setup (top view; not drawn to scale)

To simulate the geometry of soil-water interaction along a streambank, the soil core was introduced into the flume channel through a circular hole in the vertical PVC wall. The sample distance from the channel inlet was selected where the boundary layer was fully developed and secondary flows were minimized. Flow development was confirmed by measuring 3D velocity profiles down the center of the flume channel for the flow rate used in the study. Velocity profiles were measured using a Vectrino II acoustic Doppler profiling velocimeter (ADV; Nortek AS, Vangkroken, Norway) at a frequency of 50 Hz with a bin size of 1 mm. To measure these velocities, the flume was set to the highest flow rate and the ADV was oriented perpendicular to the flow direction at a distance where the centerline velocity of the channel could be measured. The sample placement point, 6 m from the channel inlet, was the point along the channel length where flow was fully developed without any tailgate effects, and was determined by comparing the streamwise and crosswise velocities along the flume channel. The height of the center of the sample placement point (5 cm from the bottom of the flume channel) was determined in a similar manner, by inspecting velocity profiles at different heights from the channel floor adjacent to the wall. The lowest point with no discernable bed effects on the flow structure was chosen for the sample placement. A screw-type core advancer was used to maintain the sample flush with the flume wall.

Testing procedure

Prior to testing, the flume tank was filled with tap water from the Blacksburg-Christiansburg VPI Water Authority, and the water was heated to 25°C using four 1000-W aquarium heaters (True Temp T-1000, Transworld Aquatic Ent., Inglewood, CA). However, water temperature varied slightly during testing resulting in an overall mean flow temperature of 26.9°C with a standard deviation of 1.1°C. Testing began by setting the flume to the predetermined setting

(0.5% channel slope and 0.055 m^3/s flow rate) to produce a wall shear stress of approximately 5 Pa. Then a sample core was advanced by hand using the core advancer until approximately 3 mm of the soil core protruded beyond the ring. This protrusion was shaved off and the core was inserted into the sample-support bracket built in the flume wall. The core was then advanced using a screw-type mechanism until the surface of the soil core was flush with the flume wall. The core advancer was marked (initial point), the surface of the sample was covered with a plastic tray and the flume was started. Covering the sample with a plastic tray before running the flume prevented the application of hydraulic shear on the core surface as the flow developed in the channel. A new soil core was used for each experiment. Testing started once the flow became fully developed (about 2 minutes). The ADV was set to a recording frequency of 50 Hz. The distance to the wall was monitored via the ADV readout and the sample was advanced back to the initial distance after every 1 mm of erosion to keep the sample flush with the flume wall. Previous work (Parks 2012) showed that the precision of the ADV distance measurements is affected by the flow and varies from the mean distance measured by an average of 0.01 to 0.27 mm, with a maximum deviation of 0.64 mm. Therefore, choosing to advance the core after 1 mm erosion ensured that erosion had progressed sufficiently beyond the error bounds of the ADV distance-to-boundary reading. At the end of the experiment, the sample advancer was marked as the final point and the distance eroded, from the initial point to the final point, was measured using a ruler to provide a secondary erosion measurement. Due to the relatively higher erosion rate of the silty sand, this soil was eroded for 10 minutes while the lean clay and fat clay were eroded for 15 minutes. These durations were chosen to minimize changes to the moisture content of each core since testing at higher durations resulted in a significant change in the moisture content (and hence erodibility) of the core.

Data analysis

The average erosion rate for each test was calculated as the total distance advanced to keep the soil core flush with the flume wall, divided by the testing time. Although the flume was maintained at a single setting to produce a wall shear stress of 5 Pa, the measured wall shear stresses varied from one test to another due to random error. The average shear stress for the tests was 4.89 Pa with a standard deviation of 1.37 Pa. To account for the effects of variations in the applied shear stress, erosion rates were non-dimensionalized by dividing each erosion rate by the shear velocity for that test.

Shear velocity measurements for each run was obtained by fitting velocity measurement from the ADV to the rough law of the wall:

$$\frac{U}{u_*} = \frac{1}{k}\ln\frac{y}{y_0} \qquad (3.2)$$

where U is the streamwise velocity at a distance y from the soil surface; u_* is the shear velocity; k is the von Karman constant (0.4); and y_o is the roughness height. From the law of the wall, the slope of the regression of the downstream velocity profile in the log-law region against the natural logarithm of distance measurements gives the shear velocity divided by the von Karman constant.

The dimensional and non-dimensionalized erosion rates were tested for normality using the Shapiro-Wilk W test (Shapiro and Wilk 1965) within the JMP statistical software (version 13.0, JMP Software, Cary, NC, USA). The results of these tests indicated that half of the data

were not from a normal distribution; therefore, both parametric (Student's t) and non-parametric (Wilcoxon rank-sum test) methods were used to analyze the data. The parametric test was used when the data sets to be compared are both normally distributed, while the nonparametric test was used when either or both datasets were not normally distributed. Log-linear regression models, which gave improved R^2 values over linear regression models, were fit to the plot of the mean erosion rate by holding time for each soil type. Statistical tests for differences in slopes were performed using the analysis of covariance (ANCOVA) procedure with soil type used as a categorical predictor. This was followed with pairwise tests of slopes, using the same test, to determine if differences in the regression slopes were statistically significant.

Results

Overall, 170 erosion tests were conducted (fat clay – 50, lean clay – 50, silty sand - 70) at multiple sample holding times. During testing, it was observed that all soil types generally had some initial period of one to four minutes when there was no erosion. This initial period of zero erosion was much longer for the lean clay and the fat clay, as compared to the silty sand. After this initial period, the lean clay and fat clay generally eroded in a more discrete manner compared to the silty sand; that is, the interval between subsequent 1-mm erosion depths was much longer for the lean clay and fat clay compared to the silty sand. Because erosion rates of the silty sand had not reached a constant erosion rate compared to the other two soil types after 72 hours of sample holding, this soil was further tested at holding times of 96 and 120 hours. As stated previously, sample holding time is defined for these experiments as the time since sample compaction and wetting; i.e., wetting and compaction were done at the same time.

Dimensionless erosion rates, initially high for the lean clay and the silty sand, dropped exponentially with time since sample wetting. In these experiments there was a clear trend of decreasing erosion rates with increasing sample holding time across the three soil types (Figures 2 and 3) until a near zero erosion rate was reached. This trend is more clearly seen in the lean clay and the silty sand because of their much higher erosion rates at the shorter holding durations. The interquartile range of the erosion rates generally decreased with time for all soil types. However, for the silty sand, there was an increase in the spread of the erosion rates observed at a holding time of 48 hours. These observations were the same with the non-dimensional erosion rates. Although the erosion rates of the silty sand generally reduced with time, the mean erosion rates for this soil at 24-hour and 48-hour holding times, 53.4 and 53.7 mm/hr respectively, were not statistically different, as determined using the Wilcoxon rank-sum test. The cause of this increase in erosion rate variability was not discernable and could have been the result of minor differences in soil texture or compaction. For each soil type, the logarithmic regression of dimensionless erosion rate with time is given in Figure 3.

Non-dimensionalized erosion rates with time since sample preparation were fit (by soil type) to linear equations and differences in the slopes were determined with the ANCOVA statistical procedure using the JMP statistical software. Results of these tests indicated that all pairs of slopes of the regression of the non-dimensionalized erosion rates (Er/u_*) with time since sample preparation were significantly different (all $p < 0.001$). This test also indicated that each intercept of the linear regression of $Er/u_*$by soil holding time was significantly different from the others (all $p < 0.001$). For the fat clay, the linear regression of Er/u_* by soil holding time showed a slightly improved fit relative to the log regression and is given below:

$$\frac{Er}{u_*} = 2.9e^{-5} - 4.3e^{-7} \times soil\ age; R^2 = 0.22\ \ (Fat\ Clay) \qquad (3.3)$$

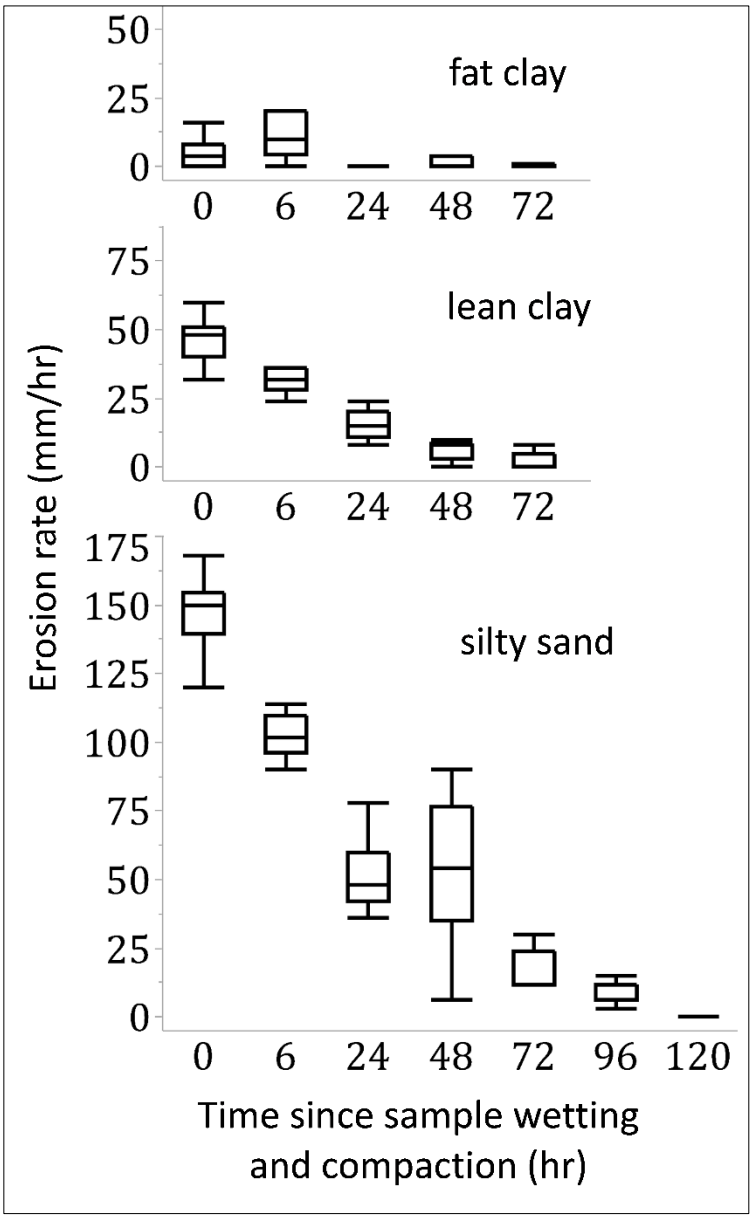

Figure 3.2 Box-plots of erosion rate with time since sample wetting and compaction.

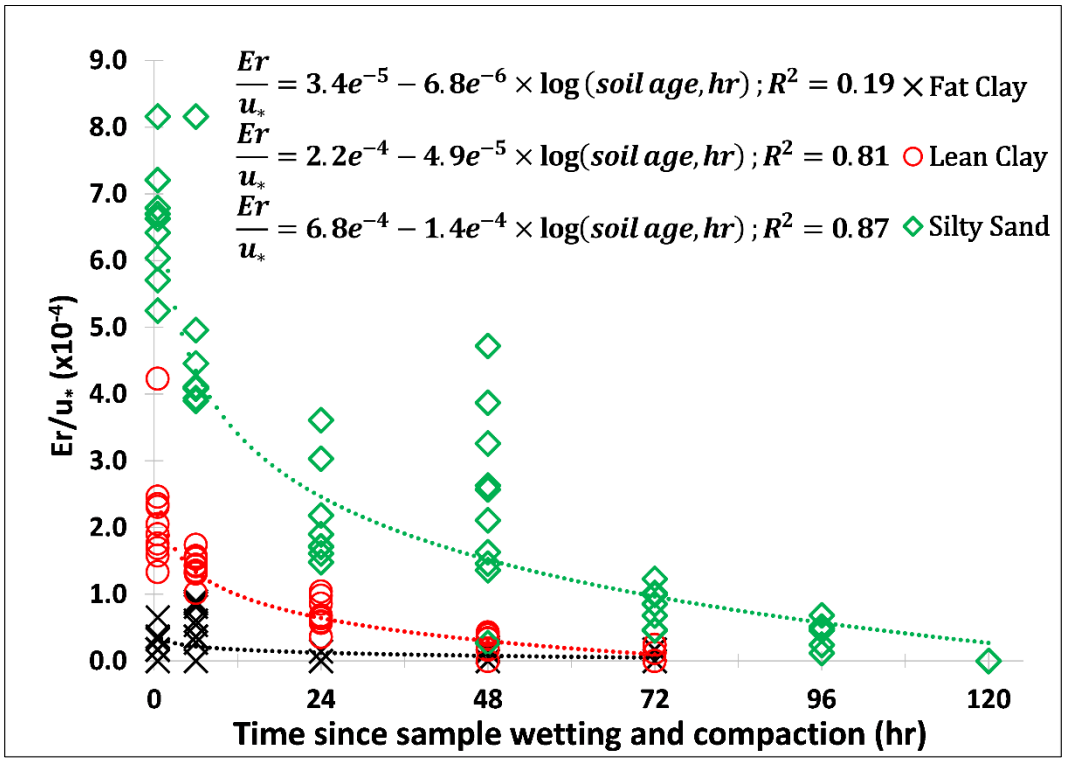

Figure 3.3 Change in dimensionless erosion rate with time since sample wetting and compaction.

Since neither the groups of erosion rates nor that of the non-dimensionalized erosion rates were all normally distributed, non-parametric comparisons of each group of erosion tests within each soil type were performed using the Wilcoxon rank-sum test ($\alpha = 0.05$). The Wilcoxon rank-sum test showed that, for the lean clay and the silty sand, all pairs (pairs with respect to soil holding time) of non-dimensionalized erosion rates were statistically different ($p < 0.05$). However for the silty sand, the pair of non-dimensionalized erosion rates at holding times of 24 and 48 hours were not different ($p = 0.85$), likely due to the large variance at 48 hours, mentioned previously. For the fat clay, there were no statistical differences in non-dimensionalized erosion rates at 0/6 hours ($p = 0.087$), 24/48 hours ($P = 0.15$), 24/72 hours ($P = 0.50$), and 48 and 72 hours ($P = 0.46$); all other pairs were statistically different ($P < 0.05$).

Discussion

Erosion testing of cohesive soils is conducted primarily for two different reasons, namely: 1) to characterize the behavior of a particular field site for engineering design or channel modelling; or, 2) to better understand the process of soil erosion or cohesion at a more fundamental level. The choice of which test to perform therefore depends on the objectives of the researcher. In the latter case, under which this study falls, testing is typically conducted using laboratory tests performed with carefully preserved field samples or remolded samples to minimize variability and ensure consistent and reproducible results.

Generally, a significant increase in soil erosion resistance as a function of time since sample preparation was observed for all soil types. It can be observed from the box plots of Er/u_* vs sample holding time (Figure 2) that the greatest decrease in erosion rates occurred within the first 24 hours since sample preparation. Decreases in mean erosion rates over the first 24 hours since soil wetting were 92%, 70%, and 64% for the fat clay, lean clay, and silty sand, respectively. This rapid increase in soil erosion resistance within the first 24 hours of sample preparation is likely due to an initial higher cohesive bond development in the soil as soil water rapidly actuated the formation of new interparticle bonds. These dramatic changes in erosion resistance may partly explain differences in critical shear when multiple studies are compared. For example, Julian and Torres (2006) using data from Dunn (1959) presented an equation for predicting cohesive bank critical shear stress from percent silt and clay. However, the study by Dunn was performed with remolded samples which would have experienced holding effects unrepresentative of field conditions. A comparison of the studies by Dunn and Smerdon and Beasley (1959) shows that, for similar plasticity indices and sample strengths, the critical tractive stress predicted by Dunn is 10-15 times

that predicted by Smerdon and Beasley (Kamphuis and Hall 1983; Partheniades 2009). Since the soil samples utilized by Dunn were held for 5 days while those used by Smerdon and Beasley were held for 20 hours, it is possible that this difference in critical shear is partly as a result of different holding times, in addition to differences in test devices and sample preparation methods.

Temporal changes in soil cohesion or strength is not a recently discovered phenomenon. In previous studies, increase in soil strength with time has been attributed to consolidation (Mehta and Partheniades 1982; Athanasopoulos 1993; Zreik et al. 1998), formation of new particle bonds, accretion of existing particle-particle bonds, and interlocking of clay platelets (Kemper and Rosenau 1984; Dexter et al. 1988), as well as thixotrophy (Mitchell 1960; Nalezny and Li 1967; Mitchell and Solymar 1984; Schmertmann 1991; Baxter and Mitchell 2004). Grissinger (1966) studied the effect of the percentage of clay minerals, bulk density, and antecedent moisture content on the erosion of clay mixtures and found, in addition to the main test results, that there was a negative relationship between the rate of erosion and the amount of time between sample preparation and erosion tests. Zreik et al. (1998) performed seven experiments on cohesive sediment bed deposits (aged between 1.8 and 18.9 days) and found that bed erosion resistance increased with increasing bed age. Zreik and his colleagues argued that the observed increase in bed erosion resistance with age was due to 'thixotropy' which they defined as "a structural change at constant composition whereby the sediment structure moves toward a more stable configuration than the one it acquired during deposition and self-weight consolidation". More recently, Nouwakpo et al. (2015), using a special apparatus and a flume, tested for the ease of fluidization and bed erosion of three different types of reconstructed natural cohesive soils under saturation and under drained conditions at different holding times, up to 72 hours. Their experiments showed an increase in apparent cohesion within the first 24-hour post-wetting period followed by a gentle

decrease in apparent cohesion beyond 24 hours. The increase in cohesion was attributed to the development of inter-particle bonds within 24 hours of soil wetting followed by increasing soil aggregation which compromised soil cohesion. However, their methodology was designed to measure bulk cohesion rather than surface/fluvial erodibility.

To investigate the mechanism responsible for the observed increase in fluvial erosion resistance with time, additional tests were conducted on the silty sand by wetting the soil for 24 hours before compacting and testing. Erosion tests (three replicates per time since sample wetting) were conducted at 24, 48, and 96 hours after wetting (0, 24, and 72 hours after soil compaction). The results obtained showed that, although these samples were wetted 24 hours before compaction, erosion rates still decreased with time in a manner comparable to that of experiments where samples were compacted immediately after wetting (Figure 4). The slopes and the intercepts of both regression lines (Figure 4) were not statistically different indicating that the observed effect was due to wetting not compaction. This indicates that the increase in erosion resistance is related to the redistribution of water in the soil. Following soil wetting, there is an overall increase in the number of individual physical and chemical bonds within the soil matrix as well as a strengthening of these bonds as attracting and repelling ions settle into a more stable configuration with time. Therefore erosion tests conducted with vague or no indication of the time of testing in relation to sample wetting are difficult if not impossible to compare across studies.

The slopes of the regression of Er/u_* against time since sample preparation were significantly different for all soil types. This result shows that, although an increase in erosion resistance with time was observed for all soil types, the rate at which erosion resistance increased differed, with the silty sand having the highest slope and the fat clay having the lowest slope. The statistically significant differences in slopes therefore indicate that the holding effect observed, in

terms of the degree to which soil erosion resistance increases with time, is soil-specific. This is the first time, in the authors' opinion, that this has been shown. Furthermore, Er/u_* values, initially different for each soil, decreased to near zero over time. This means that over time, the shear stress at which erosion began increased, suggesting that the critical shear stress for each soil, τc, became greater than 5 Pa. Therefore a common assumption that τc is an invariable soil property, parameterized as a constant in the excess shear stress equation, should be questioned.

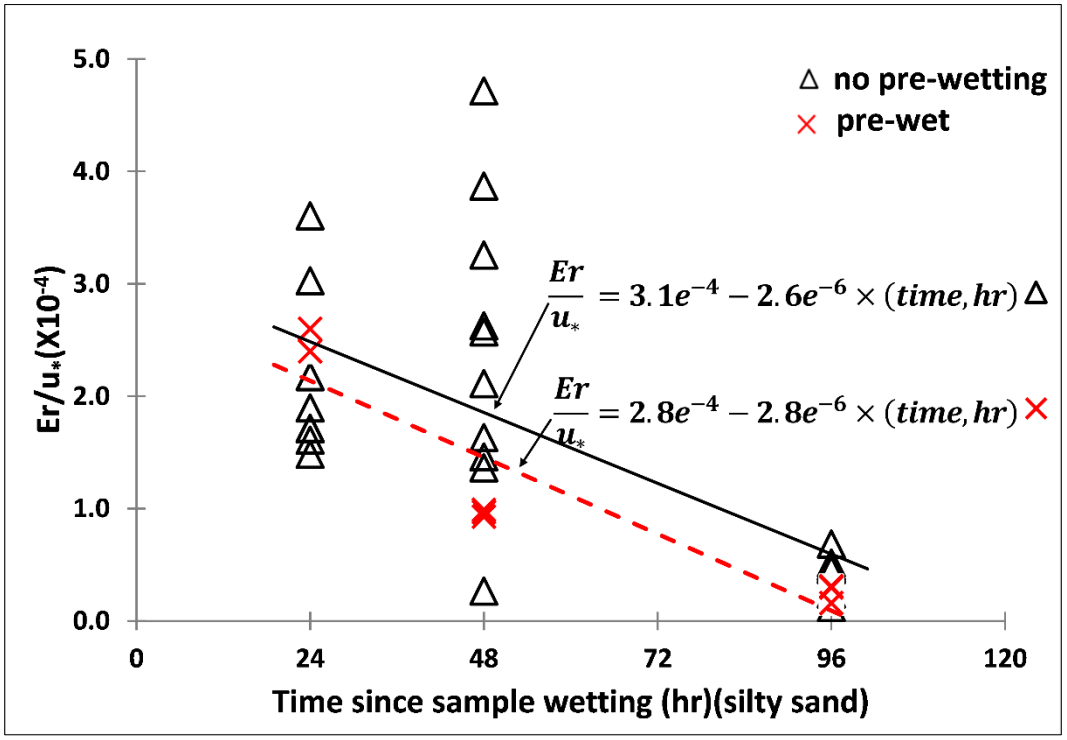

Figure 3.4 Erosion rates of prewetted and non-prewetted silty sand as a function of time since sample wetting

While there was a mixture of clay minerals in each soil, the dominant clay types in the three soils tested were kaolinite/illite (silty sand), H-I vermiculite (lean clay) and

kaolinite/montmorillonite (fat clay). These clay types exhibit very different physical and chemical characteristics that affect their instantaneous fluvial erodibility as well as cohesion development with time. Although the lean clay had twice 1.65 times the amount of clay, by weight, as the fat clay, the fat clay contained montmorillonite, which is the most electrochemically active of the clay minerals listed above, having the highest specific surface area. It is therefore possible that the fat clay more readily reacted with water after wetting to generate a relatively higher number of bonds between clay sheets resulting in a high cohesion and low erodibility. However, erosion rates of the fat clay were close to the measurement limits of the profiler, so these values may not be entirely representative of the behavior of the soil. Also, the silty sand contained less clay than the lean clay and therefore stabilized less rapidly. Based on the foregoing, we theorize that the differences in the rate of change in erosion rates observed is a direct function of the soil mineralogy and the attending array of physical bonds within each structure. Additionally, increasing erosion resistance with time is due to the gradual movement of water molecules into the interstitial spaces of the phyllosilicate sheets, increasing the number of bonds between clay sheets, as well as increased bond strength with the hydration of peripheral and interstitial cations. Future work include testing to see if differences in erosion rates exists still exist at higher applied shear stresses.

Figure 2 shows the range of values obtained at each sample holding time. Even with consistent sample preparation and testing methodology in a controlled laboratory environment, the individual results varied, underscoring the importance of replicates in cohesive soil erosion research. Table 2 shows a summary of the erosion results as well as calculations of the sample size required to estimate the mean with a confidence interval of 95%, allowing for a 20% margin of error. The required sample sizes ranged from 1 to nearly 1000 as a function of the sample variance. It can be observed from this table that the number of replicates required increased as the

erosion rates neared the measurement limits of the ADV. This number can therefore be improved with the use of a more sensitive instrument or by testing at a higher applied shear stress.

Table 3.2 Erosion results and required replicates

Holding Time (hr)	Fat Clay			Lean Clay			Silty Sand		
	Er[a] (mm/hr)	StDev[b] (mm/hr)	N[c]	Er (mm/hr)	StDev (mm/hr)	N	Er (mm/hr)	StDev (mm/hr)	N
0	5.2	5.0	89	49.6	15.3	9	147.0	15.3	1
6	10.6	7.7	50	31.8	4.0	2	108.6	22.0	4
24	0.4	1.3	960	15.0	5.3	12	53.4	17.3	10
48	1.6	2.1	160	6.0	3.8	38	53.7	26.3	23
72	0.8	1.6	427	2.4	3.4	190	20.4	6.4	10
96	--	--	--	--	--	--	10.2	3.8	13
120	--	--	--	--	--	--	0	0	--

[a] Er: Average erosion rate
[b]StDev: Standard deviation
[c] N: Number of replicates required to determine the mean with an alpha level = 0.05 and margin of error = 20%

In the bulk of previous cohesive soil erosion research, the number of test replicates appeared to have been chosen without evaluating the adequacy of such. For in-situ tests, differences in erosion rates are usually attributed to natural variabilities in field sites (Hanson and Simon 2001; Clark and Wynn 2007). However, variations in erosion rates were observed in this research, although strict sample preparation and testing procedures were followed. Therefore, it is apparent that natural cohesive soils exhibit an intrinsic natural stochastic attribute beyond the control of the experimenter. To account for this source of variability, experiments must be replicated. Daly et al. (2015) evaluated the number of samples required to estimate erodibility parameters (of the excess shear equation) using the JET device and found that three JET tests per soil, which was the norm, was expressly inadequate in estimating the erodibility parameters with 95% confidence in the mean. Therefore there is a high probability of erroneous conclusions from

experiments with insufficient replications. In the research presented here, ten replicates, informed by preliminary tests, were run for each soil type/holding time combination. Although a strict soil preparation protocol was maintained for every soil core tested and the test was done in a controlled environment, variations of up to a magnitude were observed in the measured erosion rates further underscoring the importance of replicates in cohesive soil erosion research. Therefore it is vital that preliminary experiments be conducted to determine the required number of replicates to have a measure of confidence in the results.

Conclusions

The results of this research showed that, for cohesive soils remolded at optimum moisture content, erosion resistance increased with time since sample preparation. This effect may not be observable if soils were prepared at lower than optimum moisture contents, or if erosion testing were for much longer durations since swelling and moisture content changes would then influence soil erosion behavior. Comparisons between the soil types showed that the rates of increase in fluvial erosion resistance with time were significantly different between all pairs of soils, indicating that this effect varies by soil (clay) type (alpha=0.05). Further tests indicated that the temporal increase in fluvial erosion resistance observed is a function of time since sample wetting rather than time since sample compaction. Due to the inherent variability in cohesive soils, experiments should be replicated based on information from preliminary studies to have valid results.

In view of these findings, the importance of maintaining and documenting a consistent time since sample wetting is apparent - indicating that results of prior research should be viewed cautiously, especially when sample holding times were not reported or carefully controlled.

Holding effects may partly explain the difficulty of combining erosion results from different prior studies into a single coherent whole since these studies were conducted using different experimental procedures. Therefore it is recommended for future studies, that test conditions (sample preparation, time since sample wetting, etc.) be carefully controlled during experiments and reported in detail. Overall, there is an acute need for a standard method of preparing and testing cohesive soil samples, and for reporting these findings, to ensure comparability of future studies.

Acknowledgements

Funding was provided for this study by the Virginia Tech Institute for Critical Technology and Applied Science (ICTAS) and the 4-VA Competitive Research Grants. The authors would also like to thank SGS Minerals Services and Dr. Martin C. Rabenhorst at the University of Maryland for clay mineral testing.

References

Amos, C. L., Bergamasco, A., Umgiesser, G., Cappucci, S., Cloutier, D., Denat, L., Flindt, M., Bonardi, M., and Cristante, S. (2004). "The stability of tidal flats in Venice Lagoon - The results of in-situ measurements using two benthic, annular flumes." *J. Marine Syst.*, 51(1– 4), 211–241.

Ariathurai, R., and Arulanandan, K. (1978). "Erosion Rates of Cohesive Soils." *J. Hydr. Div.*, 104(2), 279–283.

Arulanandan, K., Gillogley, E., and Tully, R. (1980). "Development of a Quantitative Method to Predict Critical Shear Stress and Rate of Erosion of Natural Undisturbed Cohesive Soils." *Rep. No. GL-80-5*, U.S. Army Engineer Waterways Experiment Station, Vicksburg, MS.

ASTM. (2007). "Standard test method for particle-size analysis of soils." *ASTM 422-63*, West Conshohocken, PA.

ASTM. (2010). "Standard test methods for laboratory determination of water (moisture) content of soil and rock by mass." *ASTM D2216*, West Conshohocken, PA.

ASTM. (2011). "Standard practice for classification of soil for engineering purpose (unified soil classification system)." *ASTM D2487*, West Conshohocken, PA.

ASTM. (2012). "Standard test methods for laboratory compaction characteristics of soil using standard effort (12400 ft-lbf/ft^3 (600 kN-m/m^3))." *ASTM D698*, West Conshohocken, PA.

Athanasopoulos, G. A. (1993). "Preconsolidation versus aging behavior of kaolinite clay." *J. Geotech. Engrg.*, 10.1061/(ASCE)0733-9410(1993)119:6(1060).

Bale, A. J., Stephens, J. A., and Harris, C. B. (2007). "Critical erosion profiles in macro-tidal estuary sediments: Implications for the stability of intertidal mud and the slope of mud banks." *Cont. Shelf Res.*, 27(18), 2303–2312.

Baxter, C. D. P., and Mitchell, J. K. (2004). "Experimental study on the aging of sands." *J. Geotech. Geoenviron. Eng*., 10.1061/(ASCE)1090-0241(2004)130:10(1051).

Briaud, J.-L., Ting, F. C. K., Chen, H. C., Cao, Y., Han, S. W., and Kwak, K. W. (2001). "Erosion function apparatus for scour rate predictions." *J. Geotech. Geoenviron. Eng*., 10.1061/(ASCE)1090-0241(2001)127:2(105).

Briaud, J.-L., Ting, F. C. K., Chen, H. C., Guadavalli, R., Perugu, S., and Wei, G. (1999). "SRICOS: Prediction of scour rate in cohesive soils at bridge piers." J. *Geotech. Geoenviron. Eng*., 10.1061/(ASCE)1090-0241(1999)125:4(237).

Clark, L. A., and Wynn, T. M. (2007). "Methods for determining streambank critical shear stress and soil erodibility: Implications for erosion rate predictions." *Trans. ASABE*, 50(1), 95–106.

Couper, P. R., and Maddock, I. P. (2001). "Subaerial river bank erosion processes and their interaction with other bank erosion mechanisms on the River Arrow, Warwickshire, UK." *Earth Surf. Proc. Land.*, 26(6), 631–646.

Cuceoglu, F. (2016). "An Experimental Study on Soil Water Characteristics and Hydraulic Conductivity of Compacted Soils", M.Sc. Thesis, Virginia Polytechnic Institute and State University, Blacksburg, VA.

Daly, E. R., Fox, G. A., Al-Madhhachi, A. S. T., and Storm, D. E. (2015). "Variability of fluvial erodibility parameters for streambanks on a watershed scale." *Geomorphology*, 231, 281–291.

Debnath, K., Nikora, V., Aberle, J., Westrich, B., and Muste, M. (2007). "Erosion of cohesive sediments: Resuspension, bed load, and erosion patterns from field experiments." *J. Hydraul. Eng.*, 10.1061/(ASCE)0733-9429(2007)133:5(508).

Dexter, A. R., Horn, R., & Kemper, W. D. (1988). “Two mechanisms for age-hardening of soil.” *Eur. J. Soil Sci., 39*(2), 163-175.

Dunn, I. S. (1959). ‘‘Tractive resistance to cohesive channels.*’’ J. Soil Mech. Found. Div*., 85(3), 1–24.

Fernandes, S., Sobral, P., and Alcântara, F. (2009). “Nereis diversicolor and copper contamination effect on the erosion of cohesive sediments: A flume experiment.” *Estuar. Coast. Shelf S.*, 82(3), 443–451.

Gee G.W. and Or D. (2002). “Particle-size analysis”. *Methods of Soil Analysis Part 4 - Physical Methods*, edited by J. H. Dane and G. C. Topp, American Society of Agronomy, Madison, WI, 255–289.

Grabowski, R. C., Droppo, I. G., and Wharton, G. (2011). “Erodibility of cohesive sediment: The importance of sediment properties.” *Earth-Sci. Rev.*, 105(3), 101-120.

Gerbersdorf, S. U., Jancke, T., and Westrich, B. (2007). “Sediment Properties for Assessing the Erosion Risk of Contaminated Riverine Sites.” *J Soils Sediments*, 7(1), 25–35.

Grabowski, R. C., Wharton, G., Davies, G. R., and Droppo, I. G. (2012). “Spatial and temporal variations in the erosion threshold of fine riverbed sediments.” *J. Soils Sediments*, 12(7), 1174–1188.

Graf, G., and Rosenberg, R. (1997). “Bioresuspension and biodeposition: a review.” *J. Marine Syst.*, 11(3–4), 269–278.

Grissinger, E. H. (1966). “Resistance of selected clay systems to erosion by water.” *Water Resour. Res.*, Wiley, 2(1), 131–138.

Hanson, G. J. (1990). “Surface erodibility of earthen channels at high stresses. Part II-Developing an in situ testing device.” *Trans ASAE*, 33(1), 132–137.

Hanson, G. J. (1991). "Development of a jet index to characterize erosion resistance of soils in earthen spillways." *Trans. ASAE,* 34(5), 2015–2020.

Hanson, G., and Cook, K. (1997). "Development of excess shear stress parameters for circular jet testing." *Paper No.972227,* American Society of Agricultural Engineers, St. Joseph, MI.

Hanson, G. J., and Simon, A. (2001). "Erodibility of cohesive streambeds in the loess area of the midwestern USA." *Hydrolog. Process.,* 15(1), 23–38.

Harris, W. G., Iyengar, S. S., Zelazny, L. W., Parker, J. C., Lietzke, D. A., and Edmonds, W. J. (1980). "Mineralogy of a chronosequence formed in New River alluvium." *Soil Sci. Soc. Am. J.*, 44(4), 862–868.

Jepsen, R., Roberts, J., and Lick, W. (1997). "Effects of bulk density on sediment erosion rates." *Water Air Soil Poll.*, 99, 21–31.

Julian, J. P., and Torres, R. (2006). "Hydraulic erosion of cohesive riverbanks." *Geomorphol.*, 76(1–2), 193–206.

Kandiah, A. (1974). "Fundamental aspects of surface erosion of cohesive soils." Ph.D. Thesis, University of California., Davis.

Kamphuis, J. W., and Hall, K. R. (1983). "Cohesive material erosion by unidirectional current." J. Hydraul. Eng., 10.1061/(ASCE)0733-9429(1983)109:1(49).

Karathanasis, A. D., and Harris, W.G. (1994). "Quantitative thermal analysis of soil materials." *Quantitative Methods in Soil Mineralogy*, edited by J. E. Amonette and L. W. Zelazny, Soil Science Society of America Inc., Madison, WI., 360–411.

Kemper, W. D., and Rosenau, R. C. (1984). "Soil cohesion as affected by time and water content." *Soil Sci. Soc. Am. J.*, 48(5), 1001-1006.

Kemper, W. D., and Rosenau, R. C. (1986). "Aggregate stability and size distribution." Methods of soil analyses, A. Klute, ed., 2d Ed., American Society of Agronomy, Madison, WI., 425-552.

Kunze, G.W., 1965. “Pretreatments for mineralogical analysis.” *Methods of Soil Analysis*, edited by C. A. Black, American Society of Agronomy, Madison, WI, 568–577.

Lawler, D. M. (1992). “Process dominance in bank erosion systems.” *Lowland floodplain rivers: Geomorphological perspectives*, P. A. Carling and G. E. Petts, eds., Wiley, NY 117–143.

Lick, W., and McNeil, J. (2001). “Effects of sediment bulk properties on erosion rates.” *Sci. Total Environ.*, 266, 41–48.

Mehta, A. J. (1986). “Characterization of cohesive sediment properties and transport processes in estuaries.” *Estuarine cohesive sediment dynamics*, A. J. Mehta, ed., Lecture Notes on Coastal Studies, Springer-Verlag, Berlin, Germany, 290–325.

Mehta, A. J. (1991). “Review notes on cohesive sediment erosion.” *Proc. Coastal Sediments*, Seattle, WA, 1(1), 40– 53.

Mehta, A. J., and Parchure, T. M. (2000). “Surface erosion of fine-grained sediment revisited.” *Muddy coast dynamics and resource management*, B. W. Flemming, M. T. Delafontaine and G. Liebezeit, eds., Elsevier, NY, 55–74.

Mehta, A. J., and Partheniades, E. (1982). “Resuspension of deposited cohesive sediment beds.” *Proc., 18th Coast. Eng. Conf.*, Cape Town, South Africa, 1569–1588.

Mirtskhulava, T. E. (1966). "Erosional stability of cohesive soils." *J. Hydraul. Res.*, 4(1), 37-50.

Mitchell, J. K., and Soga, K. (2005). *Fundamentals of soil behavior*, 3rd Ed., Wiley, London.

Mitchell, J. M. (1960). “Fundamental aspects of thixotropy in soils.” *J. Soil Mech. Found. Engrg.*, 86(3), 19-52.

Mitchell, J. K., and Solymar, Z. V. (1984). "Time-dependent strength gain in freshly deposited or densified sand." *J. Geotech. Engrg.,* 10.1061/(ASCE)0733-9410(1984)110:11(1559).

Moore, W. L., and Masch, Jr., F. D.(1962). "Experiments on the scour resistance of cohesive sediments." *J. Geophys. Res.,* 67(4), 1437–1449

Morgan, R. P. (2006). *Soil Erosion and Conservation*, 3rd ed. Blackwell, Oxford, England.

Morgan, R. P., and Rickson, R. J. (1995). *Slope stabilization and erosion control: A bioengineering approach*, Chapman and Hall, New York.

Nalezny, C. L., and Li, M. C. (1967). "Effect of soil structure and thixotropic hardening on the swell behavior of compacted clay soils." *Highway Research Record, No. 209,* Washington, D.C.

Nouwakpo, S. K., Huang, C., Weltz, M. A., Pimenta, F., Chagas, I., and Lima, L. (2014). "Using fluidized bed and flume experiments to quantify cohesion development from aging and drainage." *Earth Surf. Proc. Land.,* 39(6), 749–757.

Paaswell, R. E. (1973). "Causes and mechanisms of cohesive soil erosion: The state of the art." *Highway Research Board Special Rep. No. 135,* National Research Council, Washington, D.C., 52-74.

Parchure, T. M., and A. J. Mehta. (1985). "Erosion of soft cohesive sediment deposits." *J. Hydraul. Eng.*, 10.1061/(ASCE)0733-9429(1985)111:10(1308).

Parks, O. W. (2013). "Effect of Water Temperature on Cohesive Soil Erosion", M.Sc. Thesis, Virginia Polytechnic Institute and State University, Blacksburg, VA.

Partheniades, E. (1965). "Erosion and Deposition of Cohesive Soils." *J. Hydr. Div.,* HY1(91), 105–139.

Partheniades, E. (2009). *Cohesive Sediments in Open Channels*, Butterworth-Heinemann, Burlington, MA.

Pimentel, D., Harvey, C., Resosudarmo, P., Sinclair, K., Kurz, D., McNair, M., Crist, S., Shpritz, L., Fitton, L., Saffouri, R., and Blair, R. (1995). "Environmental and economic costs of soil erosion and conservation benefits." *Science*, 267(5201), 1117–23.

Prosser, I. P., Hughes, A. O., and Rutherfurd, I. D. (2000). "Bank erosion of an incised upland channel by subaerial processes: Tasmania, Australia." *Earth Surf. Proc. Land.*, 25(10), 1085–1101.

Raudkivi, A. J. (1998). *Loose boundary hydraulics*, 4th Ed., Balkema, Rotterdam, The Netherlands.

Raudkivi, A. J., and Tan, S. K. (1984). "Erosion of Cohesive Soils." *J. Hydraul. Res.*, 22(4), 217–233.

Sargunam, A., Riley, P., Arulanandan, K., and Krone, R. B. (1973). "Physico-chemical factors in erosion of cohesive soils." *J. Hydr. Div.*, 99(3), 555–558.

Schmertmann, J. H. (1991). "The mechanical aging of soils." *J. Geotech. Engrg.*, 10.1061/(ASCE)0733-9410(1991)117:9(1288).

Sgro, L., Mistri, M., and Widdows, J. (2005). "Impact of the infaunal Manila clam, Ruditapes philippinarum, on sediment stability." *Hydrobiologia*, 550(1), 175–182.

Shainberg, I., Goldstein, D., and Levy, G. J. (1996). "Rill erosion dependence on soil water content, aging, and temperature." *Soil Sci. Soc. Am. J.*, 60(3), 916–922.

Shapiro, S. S., and Wilk, M. B. (1965). "An analysis of variance test for normality (complete samples)." *Biometrika*, 52(3–4), 591–611.

Simon, A., and Collinson, A. J. C. (2001). "Pore-water pressure effects on the detachment of cohesive streambeds: Seepage forces and matric suction." *Earth Surf. Processes* Landforms, 26(1), 1421–1442.

Simon, A., and Rinaldi, M. (2006). "Disturbance, stream incision, and channel evolution: The roles of excess transport capacity and boundary materials in controlling channel response." *Geomorphology*, 79 (3–4), 361–383.

Simon, A., Thomas, R. E., Collison, A. J. C., and Dickerson, W. (2002). "Erodibility of cohesive streambeds in the Yalobusha River System." *Res. Rep. No. 26*, U.S. Dept. of Agriculture, Agricultural Research Service, National Sedimentation Laboratory, Oxford, MS.

Smerdon, E. T., and Beasley, R. P. (1959). ''Tractive force theory applied to stability of open channels in cohesive soils.'' *Res. Bull. No. 715,* Agricultural Experiment Station, University of Missouri, Columbia.

Soil Survey Staff. (1975). *Soil Taxonomy: A Basic System of Soil Classification for Making and Interpreting Soil Surveys,* Soil Conserv. Serv., U.S. Dept. Agric. Handbook, vol. 436, U.S. Govt. Printing Office, Washington, D.C.

Statzner, B., Fievet, E., Champagne, J., Morel, R., and Herouin, E. (2000). "Crayfish as geomorphic agents and ecosystem engineers: biological behavior affects sand and gravel erosion in experimental streams." *Limnol. Oceanogr.*, 45(5), 1030–1040.

Telles, T. S., Guimarães, M. de F., and Dechen, S. C. F. (2011). "The costs of soil erosion." *R. Bras. Ci. Solo*, 35(2), 287–298.

Thomsen, L., and Gust, G. (2000). "Sediment erosion thresholds and characteristics of resuspended aggregates on the western European continental margin". *Deep-Sea Res. I,* 47(10), 1881–1897.

Utley, B. C., and Wynn, T. M. (2008). "Cohesive soil erosion: Theory and Practice." *Proc., ASCE World Environmental and Water Resources Congress*, Honolulu, HI.

Utomo, W. H., and Dexter, A. R. (1980). "Effect of ageing on compression resistance and water stability of soil aggregates disturbed by tillage." *Soil Till. Res.*, 1, 127–137.

van Ledden, M., van Kesteren, W. M., and Winterwerp, J. C. (2004). "A conceptual framework for the erosion behaviour of sand–mud mixtures." *Cont. Shelf Res.*, 24(1), 1–11.

Wan, C. F., and Fell, R. (2002). "Investigation of internal erosion and piping of soils in embankment dams by the slot erosion test and the hole erosion test." *UNICIV Rep. R-412*, July 2002, The Univ. of New South Wales, Sydney, Australia.

Wan, C. F., and Fell, R. (2004). "Investigation of rate of erosion of soils in embankment dams." *J. Geotech. Geoenviron. Eng.*, 10.1061/(ASCE)1090-0241(2004)130:4(373).

Widdows, J., Brinsley, M. D., and Pope, N. D. (2009). "Effect of Nereis diversicolor density on the erodability of estuarine sediment." *Mar. Ecol. Prog. Ser.*, 378, 135–143.

Willett, C. D., Lerch, R. N., Schultz, R. C., Berges, S. a., Peacher, R. D., and Isenhart, T. M. (2012). "Streambank erosion in two watersheds of the Central Claypan Region of Missouri, United States." *J. Soil Water Conserv.*, 67(4), 249–263.

Winterwerp, J. C., and van Kesteren, W. M. (2004). *Introduction to the Physics of Cohesive Sediment in the Marine Environment*, Dev. Sedimentol., vol. 56, Elsevier, Amsterdam, The Netherlands.

Wynn, T. M. (2004). "The Effects of Vegetation on Streambank Erosion." Ph.D. Dissertation, Virginia Polytechnic Institute and State University, Blacksburg, VA.

Wynn, T. M., Henderson, M. B., and Vaughan, D. H. (2008). "Changes in streambank erodibility and critical shear stress due to subaerial processes along a headwater stream, southwestern Virginia, USA." *Geomorphology*, 97(3), 260–273.

Wynn, T. M., and Mostaghimi, S. (2006). "Effects of riparian vegetation on stream bank subaerial processes in southwestern Virginia, USA." *Earth Surf. Proc. Land.*, 31(4), 399–413.

Young, R. A. (1980). "Characteristics of eroded sediment". *Trans. ASAE*, 23(5), 1139-1146.

Zreik, D. A., Krishnappan, B. G., Germaine, J. T., Madsen, O. S., and Ladd, C. C. (1998). "Erosional and Mechanical Strengths of Deposited Cohesive Sediments." *J. Hydraul. Eng.*, 10.1061/(ASCE)0733-9429(1998)124:11(1076).

CHAPTER 4

SOIL AND WATER TEMPERATURE EFFECTS ON THE FLUVIAL EROSION OF REMOLDED COHESIVE SOILS

Abstract

One of the major challenges in water resource engineering is an understanding of the fundamental processes governing the erosion of cohesive streambank soils. Despite decades of research in the field of cohesive soil scour and transport, models which can be used to accurately predict the occurrence and rate of cohesive scour remains elusive (Grabowski, 2011). Given that the erodibility of cohesive soils is affected by factors such as soil and water temperature, salinity, pH, and other physical, geochemical and biological factors (Huang et al., 2006; Partheniades, 2009; Grabowski et al., 2011), it is necessary to investigate the erosion response of cohesive soils to pertinent flow and environmental conditions to clearly understand the cohesive soil erosion process. Therefore, the objective of this study was to evaluate the effects of water and soil temperatures on the fluvial erosion of remolded cohesive soils.

Three natural soils with different dominant clay types were chosen for this study: montmorillonite- dominated fat clay, vermiculite-dominated lean clay and kaolinte/illite-dominate silty sand. These soils were remolded at maximum dry densities and corresponding optimum moisture contents in a 5-cm by 5-cm cylindrical ring. Fifteen minute erosion tests were performed at water temperatures of 15^0C and 25^0C and soil temperatures of 0^0C, 15^0C and 25^0C, and 15^0C, 25^0C and 40^0C, respectively, and erosion rates were taken as the total distance of soil eroded per erosion testing time.

Test results show that, irrespective of soil type, erosion rate increased with an increase in water temperature but decreased with an increase in soil temperature. The results also show that when soil and water temperatures were equal, there was no significant change in the erosion rate (alpha=0.05). Further analysis showed that, irrespective of cohesive soil type, erosion rate was a function of the difference in water and soil temperatures and not either temperatures alone, indicating that the important thermal factor in the erosion process is the change in the enthalpy of the soil. These results show the importance of accounting for soil and water temperatures in cohesive soil tests and suggest that, in addition to discharge, the control of stormwater temperature using specially designed BMPs may be necessary to combat the degradation of streambanks which generally accompanies the urbanization of watersheds.

Introduction

According to the United States Environmental Protection Agency (USEPA), sediment is currently the second leading cause of water quality impairment in assessed streams and rivers (USEPA, 2016). It is estimated that the annual cost associated with sediment pollution in the United States is in excess of 20 billion USD (Pimentel et al. 1995; Telles et al. 2011) since high suspended sediment concentrations negatively impact recreation and water use by municipal and industrial users, while excessive sedimentation interferes with navigation. To address these problems, the possible sources of sediment have to be known and the amount of sediment contribution from each source recognized. In watersheds experiencing channel degradation, stream banks have been determined to be major sources of instream sediment, contributing as much as 90% (Simon and Thomas, 2002), 81% (Simon and Hupp, 1992), 82% (Simon et al., 2004) and 78% (Simon et al., 2002) of the total sediment load to the channels (Simon and Rinaldi, 2006).

Many single thread headwater channels have non-cohesive beds and cohesive streambanks and in places, such as southeast US, where legacy sediments are ubiquitous and there is extensive urbanization, streambank retreat is a common watershed management challenge. Streambank retreat occurs primarily through the combination of three distinct processes of erosion: subaerial weakening, fluvial erosion and mass wasting (or geotechnical failure). Subaerial weakening is the action of 'land-based' processes such as freezing, thawing and needle ice effects on the cohesion of streambanks; this process renders streambanks more susceptible to erosion by the action of flowing water and gravity. Fluvial erosion is the erosion of streambanks by the action of hydraulic shear imposed on the bank surface by flowing water whereas mass wasting occurs when the weight of the bank exceeds the cohesive forces holding the bank together, resulting in the sudden collapse of the bank. Since the physicochemical properties of cohesive soils greatly influence their erosive

behavior (Winterwerp and van Kesteren, 2004; Partheiades, 2009), cohesive streambank retreat is dependent, not only on hydrodynamic characteristics of the flow, but also on the physical, geochemical and biological characteristics of the cohesive soils or clays that constitute the streambank (Grabowski, 2011).

In the last half century, remarkable progress has been made in the study of non-cohesive sediment transport with advances in fluid mechanics, aided by numerical and computational methods, directly impacting this field. However, the closely related field of cohesive sediment erosion – the science of cohesive sediment detachment, entrainment and transport – has not experienced such progress, largely due to the complex behavior of cohesive soils as a result of their physicochemical properties. The force balance approach used in non-cohesive sediment transport research cannot be easily applied to cohesive sediments whose behavior is affected by physical, electrochemical and biological factors such as consolidation, density profile, particle size distribution, salt content, clay content and assemblage, pH, temperature, organic content and extracellular polymeric substances (Raudkivi, 1998; Huang et al., 2006; Partheniades, 2009; Grabowski et al., 2011). Furthermore, the mineralogical variability of the clay fraction of cohesive soils in the natural environment makes predicting the erosion behavior of such soils difficult, as indicated by the lack of standardized testing protocols for cohesive erosion studies.

Cohesive soils exist in the natural environment as a complex mixture of different mineral types, water, air, and organic and inorganic materials from various biotic and abiotic processes. The highly varied composition of natural cohesive soils means that in-situ tests are affected by temporal and spatial soil variability which further complicates research into the fundamental behavior of cohesive soils. Grabowski et al. (2011) classified properties of cohesive soils influencing erosion into physical, geochemical and biological properties (Table 1).

Table 4.1 Sediment properties and processes that affect soil erodibility (after Grabowski, 2011)

Classification	Process/Soil Property
Physical	Mean particle size
	Particle size distribution
	Bulk density
	Water content
	Temperature
Geochemical	Clay mineralogy
	Total salinity
	Sodium adsorption ratio
	pH
	Metals
	Organic content
Biological	Sediment disturbance
	Feeding and egestion
	Biogenic structures

One of the more important environmental variables affecting cohesive erosion that must be investigated is temperature, since one of the changes that is immediately experienced in fluvial systems as a result of urbanization is increased stream temperatures (Hester and Bauman, 2013; Xin and Kinouchi, 2013). Additionally, anthropogenic activities such as deforestation, hydropower operations, reservoir discharges and industrial cooling water change the natural hydrologic and thermal characteristics of fluvial systems, resulting in elevated stream temperatures (Kozarek,

2011; Nelson and Palmer, 2007; Van Buren et al., 2000). It is also possible to have elevated streambank temperatures relative to that of the stream flow since the loss of riparian shade and the presence of urban infrastructure such as pipelines and utility lines, as well as modern technologies such as bridge deck deicing systems using thermal energy sources, can result in localized elevated soil temperatures. Water temperature has been shown to be positively correlated with the fluvial entrainment of remolded cohesive soils (Hoomehr et al., 2018). Although previous research has shown the importance of the physicochemical properties of soil and water on cohesive soil erosion (Grisssinger, 1966; Partheniades and Paaswell, 1970; Sargunam et al., 1973; Arulanandan et al., 1975), the effect of water temperature on cohesive soil erosion has not been fully explored while the effect of soil temperature on the same is largely unknown.

Grissinger (1966) investigated the effects of clay composition, surface clay orientation, and moisture content on the erosion rates of mixtures of a natural clay and industrial clay minerals in a small 5-cm wide recirculating flume. The researcher observed that erosion rate increased with the temperature of the eroding water, but since water temperature effects on erosion rate were not the subject of this study, no explanations were given for this phenomenon. Raudkivi and Hutchinson (1974) studied the effects of water temperature and salinity on the erosion rates of industrial kaolinites with size fractions < 1μm, 2 to 5 μm and 5 to 8 μm. The clays were first prepared and tested with distilled deionized water. The clays, molded in a consolidometer as 51-mm by 38-mm wide samples, were introduced through the bottom of the channel into the eroding fluid and the erosion rate was measured as a change in weight of the sample. In the first series of tests using distilled deionized water as both eroding and soil preparation water, the change in erosion rate with water temperature converged to a U-shaped function. The authors explained this phenomenon using the Arrhenius rate equation as a similitude. They reasoned that the parabolic

shape of the erosion data was a combination of two separate exponential curves, one decreasing and one increasing. The authors suggested the decrease of erosion rate with temperature was caused by a decrease in hydraulic shear resulting from the reduction in flow viscosity as flow temperature increased, while the increase in erosion rate with temperature was thought to result from the weakening of interparticle attraction forces as these particles acquire energy and vibrate, disrupting antecedent cohesion. However, using 0.005, 0.010 and 0.100 molar solutions of $NaNO_3$ instead of deionized water as both soil preparation and eroding fluids resulted in an increase in clay cohesion and non-generalizable trends in erosion rate as temperature increased. Zreik et al. (1998) studied the influence of thixotropic effects on the erosion on deposited cohesive beds in an annular flume and found that at the top of the bed, where bed density was constant, erosion rate increased with temperature. Kemper et al. (1987) studied how clay content, organic matter and soil temperature influence the evolution of cohesion in cohesive admixtures having clay contents between 0 and 35%. The original three soils utilized had clay contents ranging from 21% to 51% and the dominant clay mineral in all three soils was illite with lesser fractions of smectite, kaolinite and vermiculite. To prepare the soil at multiple clay contents, the tested soils were fractionized into their sand, silt and clay fractions and then reconstituted into soil cores with predetermined percentages of sand, silt and clay. In their study, soil cohesion and its progression with time were assessed by evaluating the wet aggregate stability (Kemper and Rosenau, 1986) and modulus of rupture for each soil. Both of these soil properties increased with soil temperature. The authors investigated soil temperatures as high as 90°C, which is well beyond the temperature limit for optimum biological activities (30 - 40°C); therefore, the authors reasoned that the observed increase in cohesion recovery with temperature is ‘primarily physical-chemical in nature’

Since temperature is one of the major cyclic environmental variables, the effect of this variable on the erosion of cohesive soils is worth investigating in detail. In previous research where the effect of temperature on some measure of soil stability was studied, too many soil and water variables were investigated simultaneously which, coupled with the inherent stochasticity of the erosion process, made definitive insights into the effect of temperature on cohesive soil erosion difficult, if not impossible. Therefore, the goal of this research is to investigate the effects of water and soil temperatures on the erosion of remolded cohesive soils in a controlled laboratory environment.

Materials and Methods

Overview

The experiments were performed using soil and water temperatures commonly occurring in mid-latitudes. For the 15°C water temperature, experiments were performed at soil temperatures of 0°C, 15°C and 25°C; for the 25°C water temperature experiments, soil temperatures were 15°C, 25°C and 40°C. Two soil temperatures are therefore common to each of the water temperatures, and this design allowed for inferences under the following conditions: (1) constant water temperature with varied soil temperature across the two water temperatures and three cohesive soils; (2) constant soil temperature with varied water temperature across two soil temperatures and three cohesive soils; and, (3) the same soil and water temperatures for three cohesive soils. Overall, the combinations of soil type, eroding water temperature and soil temperature for this study is given in Figure 4.1.

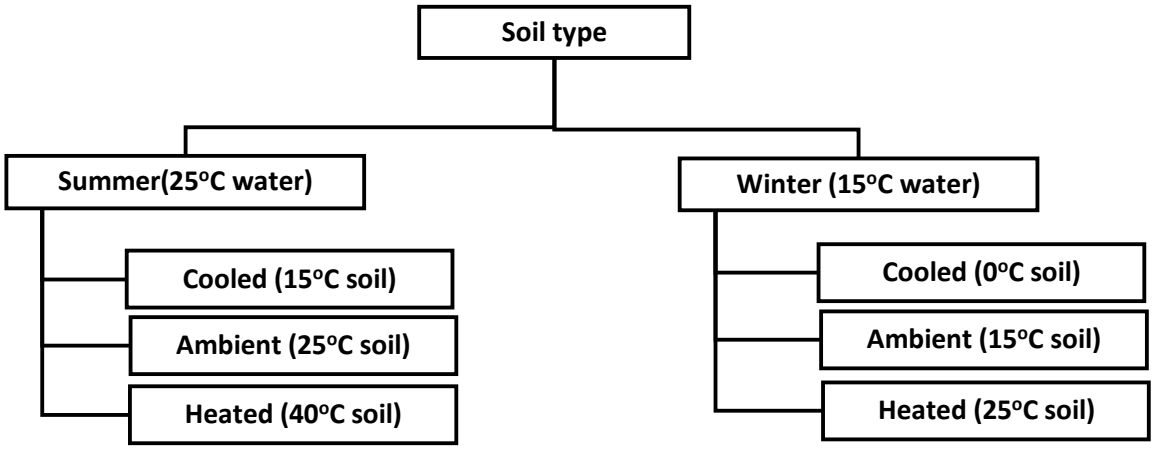

Figure 4.1 Experimental conditions

Soil preparation

Three different natural cohesive soils with different mixtures of clay minerals were chosen for these experiments. The mineralogy and physical properties of these soils are summarized in Table 2, and in Akinola et al. (2018). Once obtained from the field, the soils were air dried and pulverized with an electric grinder (HM-375, Houghton Manufacturing Co., Vicksburg, MI) to break up the soil clods. The soils were thereafter sieved with a #10 (2-mm) sieve to remove particles larger than sand. Standard Proctor tests [ASTM D698-12 (ASTM 2012)] were conducted to determine the maximum dry density and optimum moisture contents (Table 2).

Table 4.2 Soil characteristics after sieving with a 2-mm sieve

USCS soil classification[a]	Liquid limit[a] (%)	Plastic limit[a] (%)	Max. dry density[a] (g/cm^3)	Optimum moisture content[a] (%)	Major minerals (15% and above)	Minor minerals (less than 15%)
Fat Clay (CH)	51.2	24.5	1.6	22.6	Montmorillonite Kaolinite Illite H-I vermiculite[b]	Chlorite Quartz
Lean Clay (CL)	44.2	31.6	1.4	29.9	H-I vermiculite Kaolinite	Vermiculite Mica Quartz Chlorite Smectite
Silty Sand (SM)	30.7	20.5	1.7	18.2	Kaolinite Illite H-I vermiculite Quartz	Goethite Smectite Feldspar

[a] Data from Cuceoglu 2016; [b] Hydroxy-interlayered vermiculite

Each soil core was prepared in a 5-cm by 5-cm aluminum cylindrical ring. To prepare each soil core, the moisture content of the soil was determined [ASTM D2216 (ASTM, 2010)] and the amount of tap water (from the Blacksburg-Christiansburg VPI Water Authority) needed to bring the soil to optimum moisture content at the maximum dry density was added to the soil mass. The wet soil was mixed thoroughly and placed in an airtight 100% humidity glass jar at room temperature for 16 hours to allow for moisture equilibration through the soil mass. Sample preparation and holding times were kept strictly consistent to ensure uniform soil consistency between cores and so that aging effects did not introduce variations in erosion resistance between the soil cores (Akinola et al., 2018). The soil mass for each soil core was divided into three parts to prepare each core in three lifts. Next, each soil layer was compacted using a manual hydraulic press (Dake 10 Ton Floor Press, # 972210) retrofitted for this purpose. The soil core ring was

placed in the wooden base of the hydraulic press, a third of the prepared soil was poured into the ring and the layer compressed to a third of the ring length using the hydraulic press. The hydraulic press was equipped with a pressure gauge through which the compression pressure applied to each layer of soil was monitored as a secondary indicator of sample preparation consistency. Each layer of soil was scarified before adding the next lift. Each soil core was made at room temperature (1 hr), sealed in a water proof plastic bag, transferred to a water-bath equipped with a temperature sensor (Thermo Scientific Precision Digital Water Bath, # 2833), and brought to the test temperature over two hours. Preliminary studies showed the soil cores would achieve a uniform temperature within two hours. For soil temperatures 40°C and 25°C, the water-bath was simply set to these temperatures. To maintain the soil core at 15°C, the water-bath was set to 15°C and placed in a 4°C walk-in cooler. For soil cores at 0°C, the water-bath was placed in the 4°C walk-in cooler, set to 0°C and filled with ice cubes. Each soil core was tested immediately after reaching the testing temperature.

Flume setup

The experiments were conducted in an 8-m by 1-m by 1-m recirculating flume (Figure 4.2; Engineering Laboratory Design Inc., Lake City, MN). The flume has a tank capacity of 5000 L and is equipped with a 373 kW motor for a maximum flow rate of 0.07 m^3/s. Velocity measurements within the flume were made with a Vectrino II Acoustic Doppler Profiling velocimeter (ADP) (Nortek AS, Vangkroken, Norway). The temperature of the flume tank was controlled using four 1000-W aquarium heaters (True Temp T-1000, Transworld Aquatic Ent., Inglewood, CA). The width of the flume was narrowed to 0.4 m using an inset wall made with 1.25-cm thick PVC sheets. The surface of this wall was roughened by adhering sand to the surface (Premium Play Sand No. 1113, Quickrete, Atlanta, GA; D_{50} = 0.15 mm, D_{84} = 0.3 mm). The

entrance of the flume was equipped with a perforated metal flow straightener to dissipate flow turbulence as water entered the flume channel, as well as a convex structure to transition the flow from a 1-m wide flume to a 0.4-m wide channel. The sample location was 6 m from the channel entrance at a point where flow was uniform. This location was determined by analyzing 3-D velocities profiles taken with the ADP down the center of the flume, at frequency of 50 Hz and a bin size of 1 mm. The center of the sample inlet was placed 5 cm from the channel bed, where bed effects were not discernable, as determined by evaluating 3-D velocity profiles at different heights above the flume bed normal to the constructed wall. The sample was introduced into the flow through an orifice in the wall to simulate soil orientation along a vertical stream bank. While prior researchers placed soil samples in the flume bottom, this orientation requires both detachment and entrainment for erosion. In reality, soil on a streambank is readily entrained once it is detached from the soil matrix. Therefore, the samples were placed in the vertical flume wall to negate the potential impact of the detachment process on erosion measurements. A screw-mechanism was used to advance the soil core and maintain it flush with the flume wall as testing progressed, and a temperature controller was built around the soil core holder behind the sample inlet point to maintain the soil core at the appropriate temperature during testing.

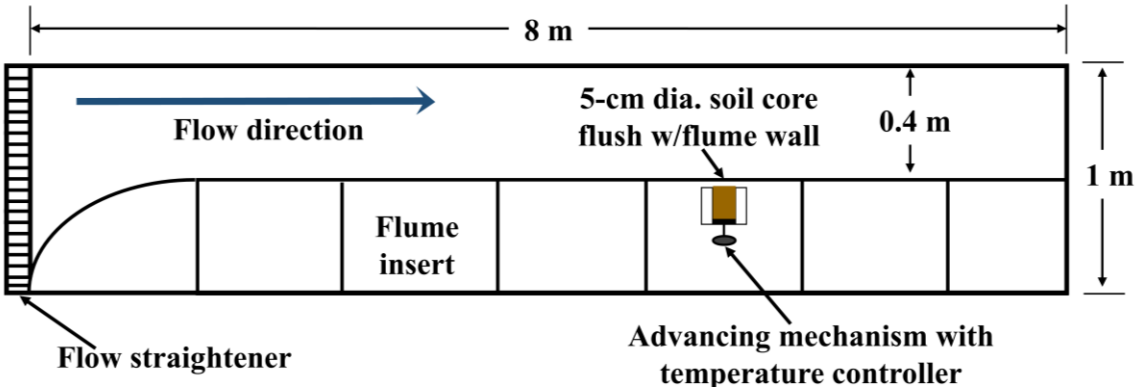

Figure 4.2 Plan view of flume schematic (not to scale)

Experimental procedure

The flume reservoir was filled with tap water (Blacksburg-Christiansburg VPI Water Authority) and brought to the test temperature using the tank heaters for 25°C flow temperature, or by cooling the laboratory space to 15°C for 15°C flow temperature. The soil core was prepared at the appropriate temperature (described previously) and advanced about 3 mm by hand using a metal cylindrical rod designed for this purpose. The exposed surface was shaved off and the soil core was inserted into the temperature-controlled sleeve. The core was then advanced until the surface of the eroding front was flush with the constructed wall. The soil surface was covered with a plastic tray and the flume turned on. Once the flow became fully developed, the surface of the soil was uncovered and the ADP was turned on in succession. Through the ADP, the distance between the ADP probe head and the soil surface was measured in real time, which enabled the distance of erosion to be tracked as testing proceeded. Flow velocity as well as distance to the soil surface were collected with the ADP at a frequency of 50 Hz. The distance of the ADP probe head to the soil surface was monitored; the eroding face was advanced back to the initial position, flush with the wall, after every millimeter of erosion. A millimeter of erosion was chosen as the benchmark for erosion based on two considerations. First, the ADP has a minimum bin size of 1 mm. Second, a preliminary study determined the average error in the distance to the wall measurements varied over a range of 0.01 to 0.27 mm under various flow conditions, with a maximum instantaneous deviation of 0.64 mm (Parks, 2012). Therefore 1 mm was chosen as the minimum justifiable distance for erosion detection. Each erosion test was run for 15 minutes using a new soil core. This 15-minute duration was chosen such that erosion did not exceed the core length and the soil water content did not change significantly over the testing period. Each soil type (fat clay, lean clay and silty sand), soil temperature and eroding water temperature condition was replicated five times for a total of 90 individual flume experiments.

Data analysis

Erosion rate was determined as the total depth of soil eroded during 15 minutes of testing. Although the flow rate and the flume bed slope were kept constant for all 15-minute experiments, producing a calculated wall shear stress of 5 Pa, the actual shear stresses varied due to slight differences in flow rate and soil surface roughness, as well as changes in water viscosity with temperature. Therefore, non-dimensional erosion rates were obtained by dividing each erosion rate by the corresponding shear velocity to eliminate variability caused by slight differences in the applied shear stress. Shear velocity (u^*) values were determined by fitting velocity profile data in the log-law region to the rough 'law of the wall' equation given below:

$$\frac{U}{u^*} = \frac{1}{k}\ln\frac{y}{y_0} \qquad (4.1)$$

where U is the streamwise velocity at a distance, y, from the soil surface; u^* is the shear velocity; k is the von Karman constant (0.4); and y_o is the roughness height.

Since normality tests on the data using the Shapiro-Wilk test (Shapiro and Wilk, 1965) showed that both the dimensional and nondimensionalized erosion data were not normally distributed, the results were analyzed using the nonparametric Wilcoxon rank-sum test to detect differences in erosion rates at the different experimental conditions. Also, for each soil type, the relationship between soil and flow temperatures and erosion rates was explored using least-squares regression analyses.

Results

Each combination of soil type (fat clay, lean clay and silty sand), water temperature (0˚C,15˚C, and 25˚C) and soil temperature (0˚C, 15˚C, and 25˚C or 15˚C, 25˚C, and 40˚C) was replicated five times, for a total of 90 erosion tests, i.e. 30 tests per soil type (Figure 4.3). All experiments were conducted under a single flume setting with the flow rate, channel slope, and tail gate height set to develop a wall shear stress of 5 Pa. At this shear stress, each soil eroded without the total erosion exceeding the soil core length during a 15-minute test. Altogether, the silty sand was the most erodible soil while the fat clay was the least erodible of the three soils used in this study (Figure 4.3). The mean erosion rates for each soil type at all soil and water temperatures are given in Table 3.

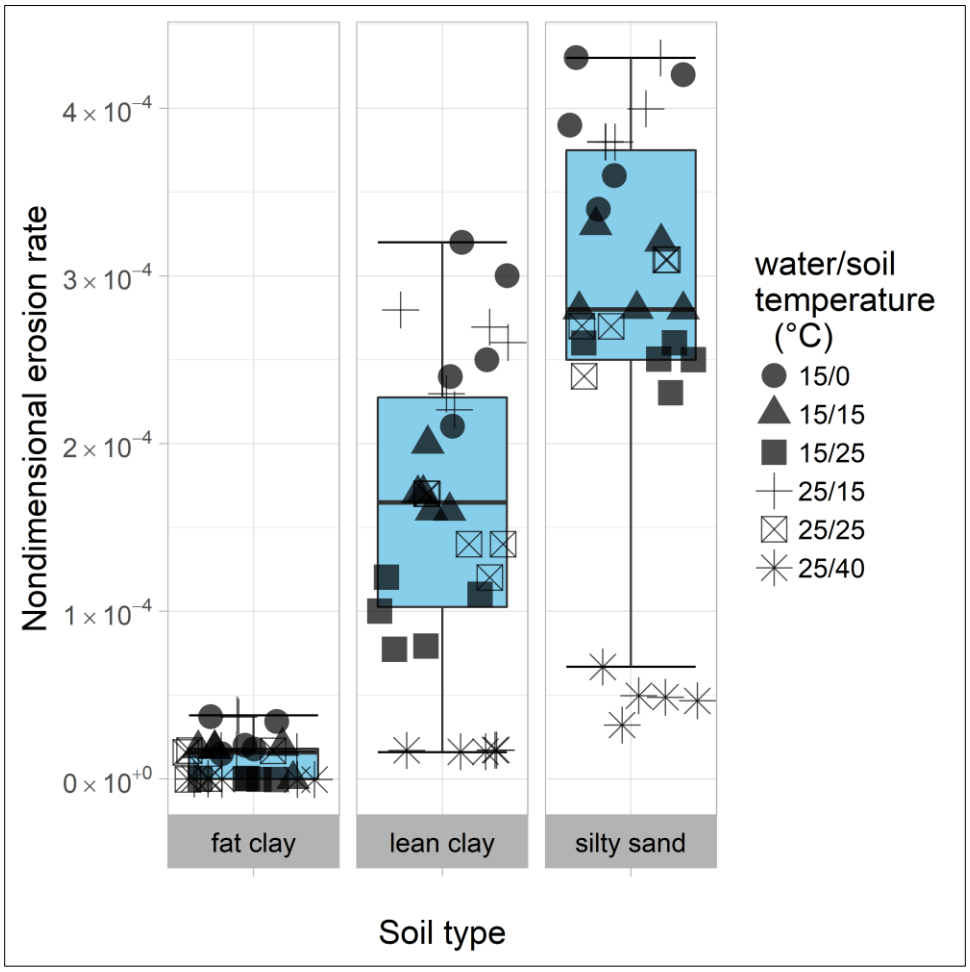

Figure 4.3 Nondimensional erosion rates for each soil type.

Table 4.3 Mean and median erosion rates for all experimental conditions

Water/Soil temperature (^{0}C)	Fat clay		Lean clay		Silty sand	
	Median Er[a] (mm/hr)	Mean Er[b] (mm/hr)	Median Er (mm/hr)	Mean Er (mm/hr)	Median Er (mm/hr)	Mean Er (mm/hr)
15/0	4	5.6	52	58.4	88	92.0
15/15	4	3.2	36	38.4	72	72.8
15/25	0	0.0	20	20.0	64	61.6
25/15	4	5.6	60	59.2	96	97.6
25/25	4	2.4	36	36.8	76	77.6
25/40	0	0.0	4	4.0	12	12.0

[a] Median Er – Median erosion rate; [b] Mean Er – Mean erosion rate

For each soil type and soil temperature, average dimensional and nondimensional erosion rates increased with water temperature. At 25˚C soil temperature, an increase in water temperature from 15˚C to 25˚C resulted in the median erosion rate increasing by 80% and 19% for the lean clay and the silty sand, respectively, and from 0 to 4 mm/hr for the fat clay. Pairwise comparisons of these results using the nonparametric Wilcoxon test showed that the median nondimensional erosion-rate increases with water temperature were statistically significant for the lean clay and the silty sand but not statistically significant for the fat clay (alpha=0.05). However, it should be noted that the relatively lower erosion rates of the fat clay and the closeness of its erosion rates to the detection limit of the ADP, at all experimental soil and eroding water temperatures (Figure 4.3), made detecting statistical difference less likely. At the 15˚C soil temperature, an increase in water temperature from 15˚C to 25˚C resulted in the median erosion rate of the lean clay and the silty sand increasing by 67% and 33% respectively. However, the median erosion rate of the fat clay did not change although the mean erosion rate increased. Pairwise comparisons of nondimensional erosion rates using the Wilcoxon test showed that the changes observed were statistically significant for the lean clay and the silty sand, but not for the fat clay (alpha=0.05).

At a water temperature of 15°C, increasing the soil temperature from 0°C to 15°C resulted in a 31% and 18% decrease in the median erosion rates of the lean clay and the silty sand respectively (Table 3). For the fat clay, the median erosion rates as soil temperature increased from 0^0C to 15^0C were the same, although the mean erosion rate decreased. Increasing the soil temperature from 15°C to 25°C (15°C water) resulted in a 100%, 44% and 11% decrease in the median erosion rate of the lean clay, fat clay and silty sand respectively (Table 3). Also, at this water temperature, a 25°C increase in soil temperature from 0°C to 25°C resulted in a 100%, 62% and 27% decrease in the median erosion rates of the fat clay, lean clay and silty sand, respectively (Table 3). Pairwise comparisons of nondimensional erosion rates using the Wilcoxon test showed that, for the lean clay and the silty sand, the median erosion rates at each soil temperature were significantly different from those at the other temperatures; for the fat clay, all erosion rates were significantly different from each other except the erosion rates at water temperatures of 0°C and 15°C (alpha=0.05).

At a water temperature of 25°C, soil temperature increase from 15°C to 25°C resulted in the median erosion rates of the lean clay and silty sand decreasing by 40% and 21% respectively. For the fat clay, this change in soil temperature did not result in any change in median erosion rate although the mean erosion rate decreased (Table 3). Also, increasing the soil temperature from 25°C to 40°C, at a water temperature of 25°C, resulted in the median erosion rates of the lean clay, fat clay and silty sand decreasing by 100%, 89%, and 84% respectively (Table 3). Additionally, a 25°C increase in soil temperature from 15°C to 40°C resulted in a 100%, 93% and 88% decrease in the median erosion rates of the fat clay, lean clay and silty sand, respectively. Pairwise comparisons of nondimensional erosion rates using the Wilcoxon test showed that, for the lean clay and the silty sand, the erosion rates at each soil temperature were significantly different from

that at the other temperatures (alpha=0.05). However, for the fat clay, only the erosion rates at the soil temperatures of 15°C and 40°C were significantly different (alpha=0.05).

Wilcoxon comparisons of nondimensional erosion rates (Er/u^*) between conditions of equal soil and water temperatures (i.e. between a condition where soil and water temperatures were both 25°C and the other condition where soil and water temperatures were both 15°C) showed that, irrespective of soil type, erosion rates were not significantly different (alpha=0.05).

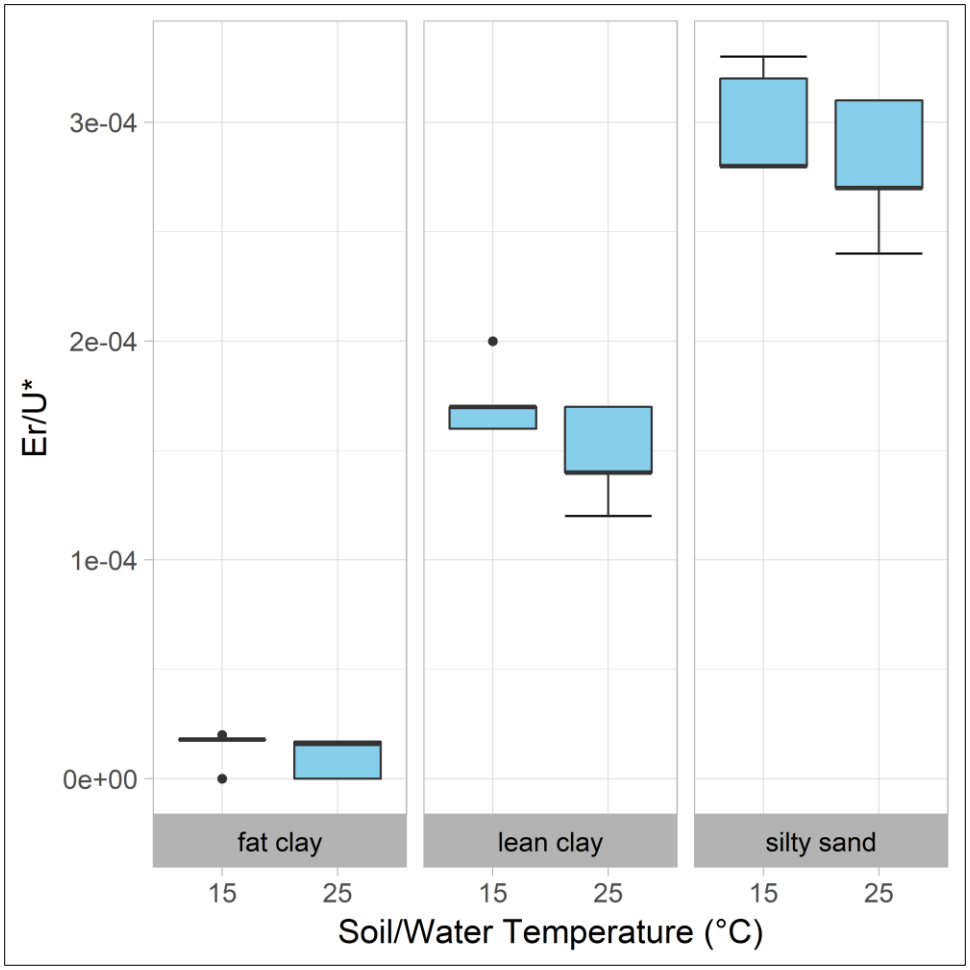

Figure 4.4 Nondimensional erosion rate vs. soil temperature when soil and water temperatures are equal.

Discussion

Cohesive erosion tests are typically performed to either characterize a specific stream reach for modeling and engineering design or to increase our understanding of the fundamental processes controlling cohesive soil erosion and to develop process-models. Although many significant advancements have been made in understanding the principles of cohesive erosion as a direct result of research efforts since the mid-1950s, there still exists a significant lack of understanding of the basic processes of cohesion development, and the detachment and transport of cohesive soils. The research needed to correct this problem will of necessity be multifaceted, some focused on spatially larger scale in-situ testing and other utilizing remolded soils or undisturbed soils, as well pure clays in various combinations.

In the research presented here, naturally occurring cohesive soils were utilized in a controlled laboratory setting to test the effects of water and soil temperatures on the fluvial erosion of cohesive soils. Although some prior studies noted an increase in the rate of erosion with water temperature (Grissinger, 1966; Raudkivi and Hutchinson, 1974; Kelly and Gularte, 1981; Zreik et al., 1998), none has focused, within the same study, on the interaction of soil and water temperatures on cohesive soil erosion. Therefore, this research fills a void by showing the combined importance of soil and water temperatures on cohesive soil erosion.

Water temperature effects on cohesive soil erosion

Study results clearly show an increase in erosion rate with water temperature, regardless of soil mineralogy. A few previous studies offer some insight into the observed phenomenon. Kelly and Gularte (1981) investigated the applicability of the double layer and rate process theories to cohesive soil erosion by conducting erosion tests using a remolded illitic soil adjusted to different

salt and water contents. Two types of experiments were conducted – one type with constant water temperature and varied flow velocity, and another type with constant velocity and varied temperature. The researchers observed an increase in erosion rate with eroding fluid temperature regardless of soil salinity. Zreik et al. (1998) performed erosion experiments using cohesive sediment beds subject to a range of shear stresses in an annular flume. The cohesive sediment bed was prepared by thoroughly agitating a mixture of Boston Blue Clay powder and water in the flume channel and allowing this to settle over predetermined time periods before testing commenced. The sediment age was taken as the time from the end of mixing to the start of the experiment. The testing procedure involved subjecting cohesive beds at a certain age, first to a constant shear stress and sampling the flow until a constant sediment concentration was reached, after which the shear stress, via the rotational velocity of the flume and the lid in contact with the water surface, was increased to the next value. Seven tests were performed with the bed age and applied shear stress ranging from 1.8 to 18.9 days and 0.1 to 1 Pa, respectively. Primarily, the results of this study showed that erosion resistance increased with bed age. Also, for some of the erosion runs, the erosion rate of the first 5 mm of the bed increased with temperature despite the negative effect of increased bed age on bed erodibility. This observation was attributed to a weakening of interparticle forces of attraction as water temperature increased.

Overall, under similar hydraulic conditions, it could be concluded that water at a higher temperature is more erosive than that at lower temperature. This could partly explain observed increase in streambank erosion with urbanization (May et al., 1997; Colosimo and Wilcox, 2007), since urbanization has been shown to result in increased stream temperatures (Hester and Bauman, 2013; Nelson and Palmer, 2007).

Soil temperature effects of cohesive soil erosion

To the best of the authors' knowledge, no previous study has investigated the direct effect of cohesive soil temperature on surface erosion. However, a number of studies have shown a correlation between soil temperature and indices of soil stability. Coote et al. (1988) monitored the seasonal changes of shear strength and aggregate stability of selected agricultural soils in southwestern and eastern Ontario, Canada. Shear strength was measured using a vane method (Liu and Thornburn, 1964) and aggregate stability was expressed as percent of dry aggregates, less than 0.5 mm, retained by wet sieving (method from Kemper and Chepil, 1965). Study results showed that shear strength and aggregate stability exhibit high variability with seasonal changes due to changes in soil moisture content. In addition to the main findings of their study, the authors also found that shear strength and aggregate stability increased when frozen soils were heated to 20°C under a constant soil moisture content. Bullock et al. (1988) evaluated the effects of freezing, water content, and aging on soil cohesion using three different soils from agricultural fields in Idaho, Utah and Oregon. The clay contents of these soils ranged from 20 to 25%. Test results showed that soil cohesion, measured as aggregate stability (methodology in Kemper and Rosenau, 1986), increased as ambient temperatures increased from the winter through the spring and summer seasons. Since soil moisture content, which also varies with season, is known to affect cohesion, the researchers also tested soils brought to different moisture contents over the course of a year. Their results showed an increase in aggregate stability with increasing temperature as well as with increasing moisture content. Therefore, when soil temperature increase leads to decreased moisture contents, the erosion rate will reduce with increased temperatures/decreased moisture contents. Wynn et al (2008) studied the monthly variation of soil erodibility coefficient and critical shear using a jet testing device. Erosion tests were performed monthly, from February 2005 to January 2006, at six test locations. The results of this study showed significant seasonal differences in

streambank critical shear and erodibility coefficient which were attributed to the effects of freezing, drying and cracking on soil rather than to the direct effect of soil temperature on soil erodibility.

Overall, there are no studies that specifically address the change in the fluvial erosion of cohesive soil with soil temperature. While there are several studies (Coote et al.,1988; Mutchler and Carter, 1983; Couper and Maddock, 2001; Wynn et al., 2008) that have shown seasonal effects on soil erosion, these effects are linked more to changes in soil moisture content or state with changes in soil temperature, rather than just changes in soil temperature at a constant moisture content.

Combined soil and water temperature effects on cohesive soil erosion

When both soil and water temperatures were equal, the effect of temperature changes on the erosion rates was negligible, suggesting that changes in erosion rate with either water or soil temperature depends on the temperature difference, and potentially on the direction of heat energy transfer. In general, when soil absorbs thermal energy, erosion rate increases and when it losses thermal energy, erosion rate decreases. Much of the previous research which noted a change in erodibility with temperature (i.e. water temperature) did not account for heat loses or gains by the soil, and although the results obtained in this study are compatible with trends observed in previous research, the potential for conflicting results exists if the temperatures at which the cohesive soils were tested were not controlled. Furthermore, this research may explain the relationship between stream temperature regimes and stream degradation in urbanized areas. As urbanization proceeds, the degree of imperviousness leads to quicker transport of water at higher temperatures due to heat exchange between impervious surfaces and surface runoff (Nelson and Palmer, 2007; Somers, 2012). Although the effects of urbanization on channel stability is usually attributed to, and rightly

so, changes in streamflow such as increased peak discharge and volume, as well as reduced time to peak (Baker et al., 2012), less is known about how changes in water temperatures as a result of urbanization affect the degradation rate of streambanks. In urbanized watersheds, which often experience streambank erosion, stream temperatures can increase by almost 10°C during summer storm events (Hester and Bauman, 2013; Nelson and Palmer, 2007). Additionally, during winter, increased erosion rates have been observed and attributed to freeze-thaw cycling of soils under higher moisture contents (Wynn and Mostaghimi, 2006). Under these conditions, a soil and water temperature differential will exist which, based on the results of this study, will accelerate the erosion rates.

It is therefore posited that thermal influences on the erosion rate of cohesive soil is related to the heat transfer between the water and the soil modules rather than to either soil or water temperature independent of the other (explained in the next section). The effects of both bank and water temperatures should thus be measured or controlled in future cohesive erosion studies. The implications of such studies are especially important in areas experiencing urbanization, since drastic changes in water temperatures due to the urban heat island effect are expected.

Heat transfer effects on cohesive soil erosion

When the results of this study are examined in detail, it is seen that the mechanism driving the soil and water temperature effects on the erosion rates is the temperature difference between the soil and the eroding flow. Figure 4.5 shows a plot of the temperature difference and the erosion rate for all experimental data. It is observed that as water temperature minus soil temperature increased, erosion rate increased for all three soil types. Considering the natural variation which cohesive soils exhibit, as indicated by the experimental results of most replicated studies, the relatively high R^2 values of the regression of nondimensional erosion rates and temperature

difference (Figure 4.5) suggest that a linear relationship between erosion rate and temperature difference can be assumed.

Overall, we theorize that heat transfer between water and the cohesive soil increases the propensity for erosion. At a given soil temperature, a cohesive soil mass settles into an equilibrium state and for erosion to take place, eroding water must supply energy to the eroding front to break cohesive bonds; this energy is in the forms of kinetic energy (hydraulic shear) and thermal energy. In other words, erosion rate can be increased either by increasing flow shear stress or the soil temperature. When a positive temperature differential exists between the water and the streambank, there is heat transfer from the water to the soil, supplying cohesive bonds energy, in addition to the kinetic energy of the water, to break free in the erosion process. As this temperature difference increases, so does the observed erosion rate. When a negative temperature differential exists, the direction of heat is from the soil to the water, and the soil erodes less than under a condition of equal soil and water temperatures due to the decreased thermal available energy for erosion.

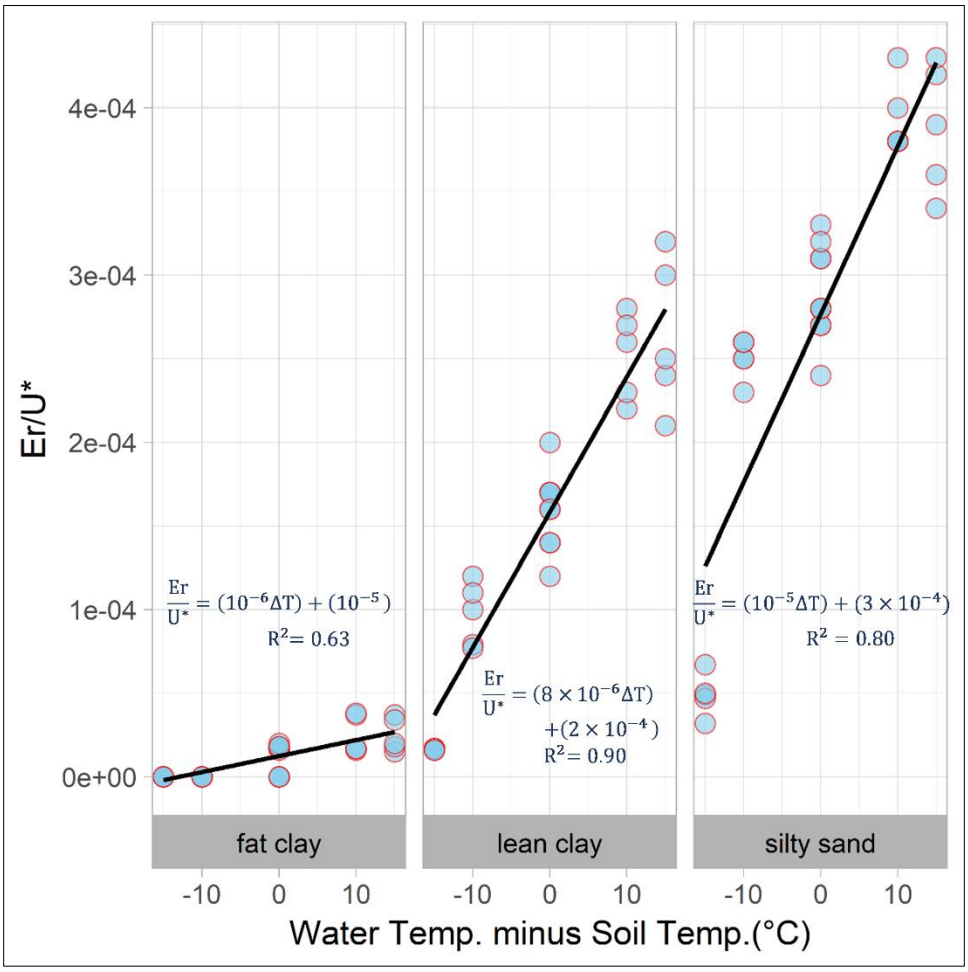

Figure 4.5. Nondimensional erosion rate vs temperature difference

The eroding system can be thus viewed as an interplay of soil and water modules responsible for erosion resistance and erosion actuation, respectively. At a constant moisture content, increasing the soil temperature leads to less erosion while increasing the eroding fluid temperature increases the amount of erosion. The results presented in this paper therefore reveal the importance of controlling for both soil and water temperatures in cohesive erosion research and practice, and offer suggestions of controlling soil and water temperatures to contain erosion susceptibility in the natural environment. For example, to prevent urban stream degradation temperature control should be a part of storm water management. In all, more experiments are

needed to confirm the findings of this study considering that only two water temperatures were utilized.

Conclusions

In this study, erosion tests were designed to reduce the sources of variation to a minimum to isolate the effects of soil and water temperatures. These experiments were performed under a strict protocol with temperature control for both the soil and eroding fluid. In this study, test results showed that at a constant soil moisture content, erosion rates decreased with increasing soil temperatures, irrespective of soil type or water temperature (15°C or 25°C) while erosion rates increased as water temperature increased irrespective of soil temperature (15°C or 25°C). However, when both the soil and water temperatures were equal, erosion rates did not vary with temperature, indicating the transfer of heat energy between the soil and the eroding fluid significantly affects soil erosion rates.

This study reveals the importance of carefully monitoring and controlling soil temperatures as well as eroding fluid temperatures in cohesive erosion experiments. Without controlling for these temperatures, erroneous results become unavoidable leading to spurious conclusions and generalizations. This study shows a critical and urgent need for cohesive soil erosion testing protocols to ensure that studies are performed with similar methods which will assure valid conclusions and an ability to compare results across studies. Furthermore, since stream temperature increases with the degree of urbanization of the drainage area, it can be inferred that stream degradation commonly observed in urbanizing watersheds is partly a result of increased stream temperatures. This suggests that, in addition to urban BMPs used to control stream flow rates, BMPs designed to control water temperatures may be desirable.

References

Arulanandan, K., Loganthan, P., and Krone, R. B. (1975). "Pore and eroding fluid influences on surface erosion of soil." *J. Geotech. Engrg. Div.*, ASCE, 101(1), 51–66.

ASTM. (2010). "Standard test methods for laboratory determination of water (moisture) content of soil and rock by mass." ASTM D2216, West Conshohocken, PA.

ASTM. (2012). "Standard test methods for laboratory compaction characteristics of soil using standard effort (12400 ft-lbf/ft^3 (600 kN-m/m^3))." *ASTM D698*, West Conshohocken, PA.

Baker, D., Pomeroy, C., Annable, W., MacBroom, J., Schwartz, J., and Gracie, J. (2008). "Evaluating the effects of urbanization on stream flow and channel stability—State of practice" World Environmental and Water Resources Congress, ASCE, Reston, VA, 1–10.

Bullock, M. S., Kemper, W. D., and Nelson S. D. (1988). Soil cohesion as affected by freezing, water content, time and tillage. *Soil Sci. Soc. Am. J.*, 52, 770-776.

Colosimo, M. F., and Wilcox, P. R. (2007). "Alluvial sedimentation and erosion in an urbanizing watershed, Gwynns Falls, Maryland." J. Amer. Water Resour. Assoc., 43, 499-521.

Coote, D.R., C.A. Malcolm-McGovern, G.J. Wall, W.T. Dickinson, and R.P. Rudra. (1988). Seasonal variation of irritability indices based on shear strength and aggregate stability in some Ontario soils. *Can. J. Soil Sci.,* 68, 405–416.

Couper, P. R., and Maddock, I. P. (2001). "Subaerial river bank erosion processes and their interaction with other bank erosion mechanisms on the River Arrow, Warwickshire, UK." *Earth Surf. Proc. Land.*, 26(6), 631–646.

Cuceoglu, F. (2016). "An Experimental Study on Soil Water Characteristics and Hydraulic Conductivity of Compacted Soils", M.Sc. Thesis, Virginia Polytechnic Institute and State University, Blacksburg, VA.

Grabowski, R. C., Droppo, I. G., and Wharton, G. (2011). "Erodibility of cohesive sediment: The importance of sediment properties." *Earth-Sci. Rev.*, 105(3), 101-120.

Grissinger, E. H. (1966). "Resistance of selected clay systems to erosion by water." *Water Resour. Res.*, Wiley, 2(1), 131–138.

Gularte, R. C., Kelly, W. E., and Nacci, V. A. (1980). "Erosion of cohesive sediments as a rate process." *Ocean Engng.*, 7, 539-551.

Hanson, G. J. (1990). "Surface erodibility of earthen channels at high stresses. Part II-Developing an in situ testing device." *Trans. ASAE*, 33(1), 132–137.

Hanson, G. J., and Cook, K. R. (1997). "Development of excess shear stress parameters for circular jet testing." ASAE Annual Int. Meeting, ASAE, St. Joseph, MI.

Hester, E. T., and Bauman, K.S. (2013). "Stream and retention pond thermal response to heated summer runoff from urban impervious surfaces." *J. Am. Water Resour. As.*, 49(2), 328–342.

Hoomehr, S., Akinola, A. I., Wynn-Thompson, T., Garnand, W., Eick, M. J. (2018). "Water Temperature, pH, and Road Salt Impacts on the Fluvial Erosion of Cohesive Streambanks." *Water*, 10(3):302.

Huang, J., Hilldale, R.C., and Greimann, B.P. (2006). Cohesive sediment transport. In: Yang, C.T. (ed.), Erosion and sedimentation manual. U.S. Bureau of Reclamation, Technical Service Center, Denver, CO., Ch.4.

Kelly, E. K., and Gularte, R. C. (1981). "Erosion resistance of cohesive soils." *J. Hydr. Div.*, ASCE, 107(10), 1211–1224.

Kemper, W. D., and Chepil, W. S. (1965). Size distribution of aggregates. In: C. A. Black (ed.). Methods of soil analysis, Part 1. Agronomy (9), 499-510.

Kemper, W. D., and Rosenau, R.C. (1986). Aggregate stability and size distribution. In: Methods of Soil Analysis, Part 1. Physical and Mineralogical Methods. Agronomy Monograph no. 9. Society of Agronomy/Soil Science Society of America, pp. 425–442.

Kemper, W. D., Rosenau, R. C., and Dexter, A. R. (1987). "Cohesion development in disrupted soil affected by clay and organic matter content and temperature." *Soil Sci. Soc. Am. J.*, 51, 860-867.

Kozarek, J. L. (2011). "Channel morphology and riparian vegetation influences on fluvial aquatic habitat". Ph.D. Dissertation, Virginia Polytechnic Institute and State University, Blacksburg, VA.

Liu, T. K. and Thornburn, D. H. (1964). "Investigations of surficial soils by field vane rest." ASTM Symposium on Soil Exploration. Spec. Tech. pub. no. 35, ASTM, Philadelphia, Pa. pp. 44-52.

May, C.W., Horner, R. R., Karr, J. R., Mar, B. W., and Welch, E. B. (1997) "Effects of urbanization on small streams in the Puget Sound Ecoregion" Watersh. Protect. Techn. 2:483-494.

Mutchler, C. K., and Carter, C. E. (1983). Soil erodibility variation during the year. *Trans. ASAE*, 26, 1102–1104, 1108.

Nelson, K. C., and Palmer, M. A. (2007). Stream temperature surges under urbanization and climate change: Data, models, and responses. *J. Am. Water Resour. As.*, 43(2):440-452.

Odgaard, A. J. (1987). Streambank erosion along two rivers in Iowa. *Water Resour. Res.*, 23(7), 1225-1236.

Parks, O. W. (2013). "Effect of Water Temperature on Cohesive Soil Erosion". M.Sc. Thesis, Virginia Polytechnic Institute and State University, Blacksburg, VA.

Partheniades, E. (1965). "Erosion and Deposition of Cohesive Soils." *J. Hydr. Div.*, ASCE, Vol. 91, 105–139.

Partheniades, E. (2009). *Cohesive Sediments in Open Channels*, Butterworth-Heinemann, Burlington, MA.

Partheniades, E., and Paaswell, R. E. (1970). "Erodibility of channels with cohesive boundary." *J. Hydr. Div., ASCE*, 96(3), 755–771.

Pimentel, D., Harvey, C., Resosudarmo, P., Sinclair, K., Kurz, D., McNair, M., Crist, S., Shpritz, L., Fitton, L., Saffouri, R., and Blair, R. (1995). "Environmental and economic costs of soil erosion and conservation benefits." *Science*, 267(5201), 1117–23.

Raudkivi, A. J. (1998). *Loose boundary hydraulics*, 4th Ed., Balkema, Rotterdam, The Netherlands.

Raudkivi, A. J., and Hutchison, D. L. (1974). Erosion of kaolinite clay by flowing water. *Proc. Roy. Soc. London* 337, 537–544. doi: 10.1098/rspa.1974.0066

Raudkivi, A. J., and Tan, S. K. (1984). "Erosion of cohesive soils." *J. Hydraul. Res.*, 22(4), 217–233.

Sargunam, A., Riley, P., Arulanandan, K., and Krone, R. B. (1973). "Physico-chemical factors in erosion of cohesive soils." *J. Hydr. Div.*, ASCE, 99(3), 555–558.

Shapiro, S.S., and Wilk, M.B. (1965). "An Analysis of Variance Test for Normality (Complete Samples)". *Biometrika*, 52(3/4), 591–611.

Simon, A., Bingner, R., Langendoen, E., and Alonso, C. (2002). Actual and reference sediment yields for the James Creek Watershed, Mississippi. National Sedimentation Laboratory Research Report, vol. 31. 185 pp.

Simon, A., and Hupp, C. R. (1992). Geomorphic and vegetative recovery processes along modified stream channels of West Tennessee. U.S. Geological Survey Open-File Report, vol. 91-502. 142 pp

Simon, A., Langendoen, E., Bingner, R., Wells, R. R., Yuan, Y., and Alonso, C. (2004). Suspended-sediment transport and bed-material characteristics of Shades Creek, Alabama and Ecoregion 67: developing water-quality criteria for suspended and bed-material sediment. National Sedimentation Laboratory Technical Report, vol. 43. 150 pp.

Simon, A., and Rinaldi, M. (2006). "Disturbance, stream incision, and channel evolution: The roles of excess transport capacity and boundary materials in controlling channel response." *Geomorphology*, 79 (3–4), 361–383.

Simon, A., and Thomas, R. E. (2002). "Processes and forms of an unstable alluvial stream with resistant, cohesive streambeds". *Earth Surf. Proc. Land.*, 27, 699–718

Sparks, D. L. (2003). *Environmental Soil Chemistry*, Academic Press, London, UK.

Telles, T. S., Guimarães, M. de F., and Dechen, S. C. F. (2011). "The costs of soil erosion." *R. Bras. Ci. Solo,* 35(2), 287–298.

[USACE] United States Army Corps of Engineers. (1981). The Streambank Erosion Control Evaluation and Demonstration Act of 974, Section 32, Public Law 93-25. Final Report to Congress, Main Report and Appendix A.

[USEPA]. United States Environmental Protection Agency. (2016). National summary of impaired waters and TMDL information. Washington, DC.

Van Buren, M. A., W. E. Watt, J. Marsalek, and B. C. Anderson. (2000). Thermal enhancement of stormwater runoff by paved surfaces. *Water Res.*, 34(4), 1359-1371.

Winterwerp, J. C., and van Kesteren, W. G. M. (2004). *Introduction to the physics of cohesive s ediment in the marine environment*, Elsevier, Amsterdam, The Netherlands.

Wynn, T. M., Henderson, M. B., and Vaughan, D. H. (2008). "Changes in streambank erodibility and critical shear stress due to subaerial processes along a headwater stream, southwestern Virginia, USA." *Geomorphology*, 97(3), 260–273.

Xin, Z, and Kinouchi, T. (2013). "Analysis of stream temperature and heat budget in an urban river under strong anthropogenic influences." *J. Hydrol.*, 489, 16–25.

Zreik, D. A., Krishnappan, B. G., Germaine, J. T., Madsen, O. S., and Ladd, C. C. (1998). "Erosional and Mechanical Strengths of Deposited Cohesive Sediments." *J. Hydraul. Eng.*, 10.1061/(ASCE)0733-9429(1998)124:11(1076).

CHAPTER 5

MODELLING TEMPERATURE EFFECTS ON COHESIVE SOIL EROSION

Abstract

In many urbanized watersheds, channels continue to experience degradation despite efforts to arrest the effects of altered flow regimes through stormwater management practices. While research has shown that the loss of forested riparian buffers, urbanization, and climate change can increase stream water temperatures by as much as 7˚C (Kozarek, 2011; LeBlanc et al., 1997; Nelson and Palmer, 2007; Stefan and Sinokrot, 1993; Van Buren et al., 2000), the role of temperature on cohesive channel erosion is not well established. And, despite decades of research to understand the mechanics of cohesive soil erosion, cohesive soil erosion models are limited in applicability since they do not account for changes in erosion rates due to factors other than the applied shear stress. For example, the excess shear stress model, which is the principal cohesive soil erosion model, is premised on a false assumption of constant soil properties - the erodibility coefficient and critical shear stress - in a thermally variable environment. Therefore, the objective of this study is to test and improve the excess shear stress model and the Wilson erosion model, to reflect the response of the fluvial erosion process to changes in both cohesive soil and eroding water temperatures.

Data from multiple erosion studies using remolded montmorillonite and vermiculite-dominated natural soils, tested in an 8 m x 1 m x 0.4 m recirculating flume at multiple hydraulic shear stresses and soil and water temperatures were used to parametrize and test the excess shear

stress and Wilson erosion models. Next, thermal effects on erosion rates were incorporated in these models, and the modified models were evaluated and compared to each other and to the original models using cross validation prediction indices.

The results of this research showed that, generally, the Wilson erosion model performed better in predicting erosion rates compared to the excess shear stress model. Also, the modified models, which account for soil and water temperatures, were overall better in predicting erosion rates compared with the original models. Overall, the long term aim of this study is incorporate the model changes suggested in this study in watershed and erosion models currently being used to predict cohesive streambank erosion.

Introduction

Background

Land use change through urbanization, industrial development and agriculture is a definitive precursor to channel degradation through the combined effects of altered channel hydraulic, hydrologic and thermal properties on the dynamic equilibrium of fluvial systems (Booth, 1990; Fan and Li, 2004; Bledsoe and Watson, 2007). However, despite many decades of research into the processes of sediment entrainment, transport, sedimentation and resuspension under both quasi steady state and unsteady flows, the knowledge of the fundamental processes governing the erosion of fine grained streambanks is still elementary (Grabowski et al., 2011). Early attempts at cohesive erosion modelling include the use of empirical formulas, known as regime theories, which relate geometric attributes of waterways to allowable discharge to develop stable channels as early as the late 1800s (Kennedy, 1895; Lacey, 1930; Blench, 1952). Although these power relationships have their merits, their application is limited to the regions in which they were developed (Stevens and Nordin, 1987; Chitale, 1996).

According to Mehta and McAnally (2008), the advent of fine grained sediment research in the United States was performed by Hans Albert Einstein (1904 - 1973) and his students at the University of California, Berkeley. The contribution of these efforts can be surveyed in Einstein's work titled 'The Bed-Load Function for Sediment Transporting Open Channel Flows' (Einstein, 1950). Though advances in theoretical fluid mechanics has led to a more mathematically rigorous approach to soil erosion modelling, where the erosive action of water over the sediment surface is quantified in terms of hydraulic shear stress, the lack of understanding of the erosion process means that models have remained largely empirical. Therefore, the challenge of predicting the incidence and rate of cohesive soil erosion continues to be a formidable challenge for researchers

(Grabowski, 2011). Although much work has been done to understand cohesive soil erosion, the interplay of physicochemical forces attendant to cohesive soil erosion resistance, detachment and transport render this problem particularly challenging (Partheniades, 2009). For non-cohesive sediment, the movement of particles is governed by the balance of drag, lift and gravitational forces on the non-cohesive particle. However, for cohesive soils, in addition to hydraulic forces imposed by the eroding fluid, the chemical interaction between the fluid and the clay minerals determine, to a large extent, the response of the clay particles (Winterwerp and van Kesteren, 2004). The properties of cohesive soils which influence their erosion behavior include properties which can be classified as either physical, chemical or biological (Grabowski, 2011; Table 1). While these properties are important in understanding the fundamental behavior of cohesive soils, it is also important to consider the effects of the physical and chemical properties of the eroding fluid on erosion rates. For example, cohesive soils have been shown to erode differently under similar hydraulic shear stresses but different water temperature, salinity or pH. Therefore, for soil and water resource conservation, it is necessary to have a workable erosion model that is simple to use yet powerful enough to capture the response of cohesive soil surfaces to the most important hydraulic and chemical properties of the soil/water system.

Table 5.1 Sediment properties and processes that affect soil erodibility (after Grabowski, 2011)

Classification	Soil Property
Physical	Mean particle size
	Particle size distribution
	Bulk density
	Water content
	Temperature
Geochemical	Clay mineralogy
	Total salinity
	Sodium adsorption ratio
	pH
	Metals
	Organic content
Biological	Sediment disturbance
	Feeding and egestion
	Biogenic structures

In eroding cohesive streambanks, two of the most important fluid properties pertaining to fluvial erosion of bank material are stream hydraulic shear stress and stream temperature. Although other properties such as stream pH and salinity are important, these do not vary as much as hydraulic shear stress and water temperature. In addition to expected seasonal changes in stream discharge and temperature, other phenomena can cause a dramatic shift in stream discharge and temperature. For example, urbanization reduces the amount of infiltrated rainfall and increases runoff to stream networks. Also, summer storm events in an urbanized locality can lead to an increase in stream temperature by almost 10°C (Hester and Bauman, 2013; Nelson and Palmer, 2007). Considering that many hydraulic and hydrologic models can be used to estimate the

variation of hydraulic shear and water temperature over various timescales, an erosion model that accounts for both factors concurrently would be a welcome development. Therefore, the aim of this study is evaluate two common erosion models, the excess shear stress model and the Wilson erosion model, and to modify them to capture the influence of stream temperature on the erosion rate of cohesive soils.

Erosion Models

Excess shear stress model

Currently, there are a handful models used in in-situ and laboratory-based cohesive erosion research. However, the empirical erosion model known as the excess shear stress model is the most widely used (Al-Madhhachi, 2014). This model, in a simplified form, is a linear equation which relates the observed erosion rate to the average boundary shear stress (equation 5.1).

$$E_r = K_d(\tau - \tau_c) \quad (5.1)$$

where E_r is the erosion rate in m/s; K_d is the soil erodibility coefficient ($m^3/N{\cdot}s$); τ is the applied hydraulic boundary shear stress (Pa) and τ_c is the soil critical shear stress (Pa).

This model is typically used with the assumption that the erodibility coefficient and critical shear stress for a given soil are constant. It is further assumed that the erosion rate is linearly related to the applied hydraulic shear once the applied hydraulic shear stress is exceeds the soil critical shear stress. However, this simple form of the excess shear stress equation belies its source from a more complex erosion model presented by Partheniades (1965) who performed erosion studies on cohesive silt, clay and sand mixtures using a rectangular recirculating flume. The Partheniades erosion model was derived as follows:

The time-averaged shear stress at the cohesive bed, $\overline{\tau_b}$, is given by the following relation,

$$\overline{\tau_b} = R_b S_e \gamma_w \tag{5.2}$$

where, R_b is the hydraulic radius; S_e is the slope of the energy grade line; γ_w is the unit weight of water.

According to Einstein and Li (1956), the instantaneous bed shear stress , τ_o, is given by the following relation,

$$\tau_o = \frac{\mu u_i}{\sqrt{\pi}\, v\, t} \tag{5.3}$$

where, μ is the dynamic viscosity, u_i is the instantaneous turbulent velocity, v is the kinematic viscosity, and t is time.

According to Einstein and El-Samni (1949), semi-spherical roughness elements in a turbulent flow field experience uplift forces, L, which are normally distributed and are characterized by a time averaged value, $\bar{L}$, and standard deviation, L/η_o, where η_o is an experimental constant. If the statistical variation of uplift forces is assumed to hold for the bed shear stress, its frequency is then given as:

$$f(\tau_o) = \frac{1}{\sqrt{2\pi}\,\frac{\overline{\tau_o}}{\eta_o}} \exp\left[-\frac{(\overline{\tau_o}-\tau_o)^2}{2\left(\frac{\overline{\tau_o}}{\eta_o}\right)^2}\right] \tag{5.4a}$$

and

$$\tau_o = \overline{\tau_o}\,\eta_0\left(\eta^* + \frac{1}{\eta_o}\right) \tag{5.4b}$$

where, η^* is a random variable with a mean of zero and a standard deviation of 1 and $\overline{\tau_o}/\eta_o$ is the standard deviation of τ_o.

Taking N as the number of of cohesive units subject to hydraulic shear stress, the maximum tensile stress, σ_{max} , and the average interaggregate cohesive force, F_c , can be expressed by the following relations:

$$\sigma_{max} = \frac{K^I \tau_o}{N} \tag{5.5a}$$

and

$$F_c = \frac{K^{II} C_e}{N} \tag{5.5b}$$

where, K^I is a factor that accounts for bending; K^{II} is a proportionality factor; C_e is the average erosive resistance per cohesive unit. Therefore, for erosion to occur, the maximum tensile stress, $\sigma_{max,}$ must exceed the interaggregate cohesive force, F_c. That is:

$$\sigma_{max} \geq F_c \equiv K_e \frac{\tau_o}{C_e} \geq 1 \tag{5.6a}$$

where, K_e is K^I/K^{II}.

The probability of erosion, Pr, per unit time is therefore given as:

$$Pr = Probabilty\left\{K_e \frac{\tau_o}{C_e} \geq 1\right\} \tag{5.7a}$$

$$Pr = Probability\left\{K_e \frac{\tau_o}{C_e}\left[\eta^* + \frac{1}{\eta_o}\right] \geq 1\right\} \tag{5.7b}$$

$$Pr = Probability\left\{\left[\eta^* + \frac{1}{\eta_o}\right] \geq \frac{C_e}{K_e \overline{\tau_o} \eta_o}\right\} \tag{5.7c}$$

To impose a positive instantaneous shear stress condition, the term in the bracket is squared thus:

$$Pr = Probability\left\{\left[\eta^* + \frac{1}{\eta_o}\right]^2 \geq \frac{(C_e)^2}{(K_e \overline{\tau_o} \eta_o)^2}\right\} \tag{5.7d}$$

which has the following definite expression:

$$\Pr = 1 - \frac{1}{\sqrt{2\pi}}\left\{\int_{\frac{-C_e}{K_e\overline{\tau_o}\eta_o}-\frac{1}{\eta_o}}^{\frac{C_e}{K_e\overline{\tau_o}\eta_o}-\frac{1}{\eta_o}} \exp\left(-\frac{\omega^2}{2}\right)\right\} \tag{5.7e}$$

where ω is a dummy variable.

The number of particles available for erosion per unit bed area is $1/A_1 d_a^2$, where A_1 is a surface shape factor and d_a is the average diameter of eroded particles. If an eroding force acts on the bed surface over a time, t^*, then the number of units eroded per t^* will be Pr/t^*. Accounting for the weight of each eroded particle as $A_2 d_a^3 \gamma_s$, where A_2 is a volume shape factor, and γ_s is the average weight of eroding particles, the erosion rate E, in weight per unit bed area per unit time, is therefore given by:

$$E = \text{Number of available particles per unit bed area} \times \text{Number of particles eroded per } t^* \times \text{weight of each particle}$$

That is:

$$E = \frac{A_2 d_a \gamma_s}{A_1 t^*}\left\{1 - \frac{1}{\sqrt{2\pi}}\left(\int_{\frac{-C_e}{K_e\overline{\tau_o}\eta_o}-\frac{1}{\eta_o}}^{\frac{C_e}{K_e\overline{\tau_o}\eta_o}-\frac{1}{\eta_o}} \exp\left(-\frac{\omega^2}{2}\right)\right)\right\} \tag{5.8}$$

This equation (equation 5.8) was applied to conditions where cohesive bed density increased with depth, typical of beds formed from deposition, as well as to conditions where bed density was uniform through the depth of the cohesive soil bed. For the second case, equation 5.8 was simplified and parameterized by Kandiah (1974) and Ariathurai and Arulanandan (1978) by assuming zero erosion at very lower shear stresses and extending the linear part of equation 5.8 to the inception of the erosion process. The highest shear stress at above which erosion occurs was called the critical shear stress and the simplified erosion equation proposed has the following form:

$$E = M\left(\frac{\tau_b - \tau_c}{\tau_c}\right) \qquad \text{for } \tau_b > \tau_c \qquad (5.9)$$

This equation is essentially the same as the common form of the excess shear equation presented in equation 5.1. Although the use of this linear excess shear equation for all types of erosion has been cautioned by Partheniades (2009), since this linear form only represents a portion of the original Partheniades equation, this equation has persisted in different forms since, the most common form being equation 5.1 above.

Wilson erosion model

Another erosion model, known as the Wilson erosion model (Wilson, 1993a, b), has been used in modelling the erosion of cohesive sediment. The Wilson model is a mechanistic model based on the interaction of dislodging and resisting forces on a two-dimensional particle generalized to soil aggregates. Similar to the moment balance approach used in the design of stable channels (Stevens and Simons, 1971; Vanoni, 1977), Wilson derived this erosion model, hereafter called the 'Wilson erosion model' as follows:

Based on the two-dimensional particle representation shown in Figure 5.1, at the point of incipient motion, the clockwise moment is balanced by the anticlockwise moment according to equations 5.10 and 5.11.

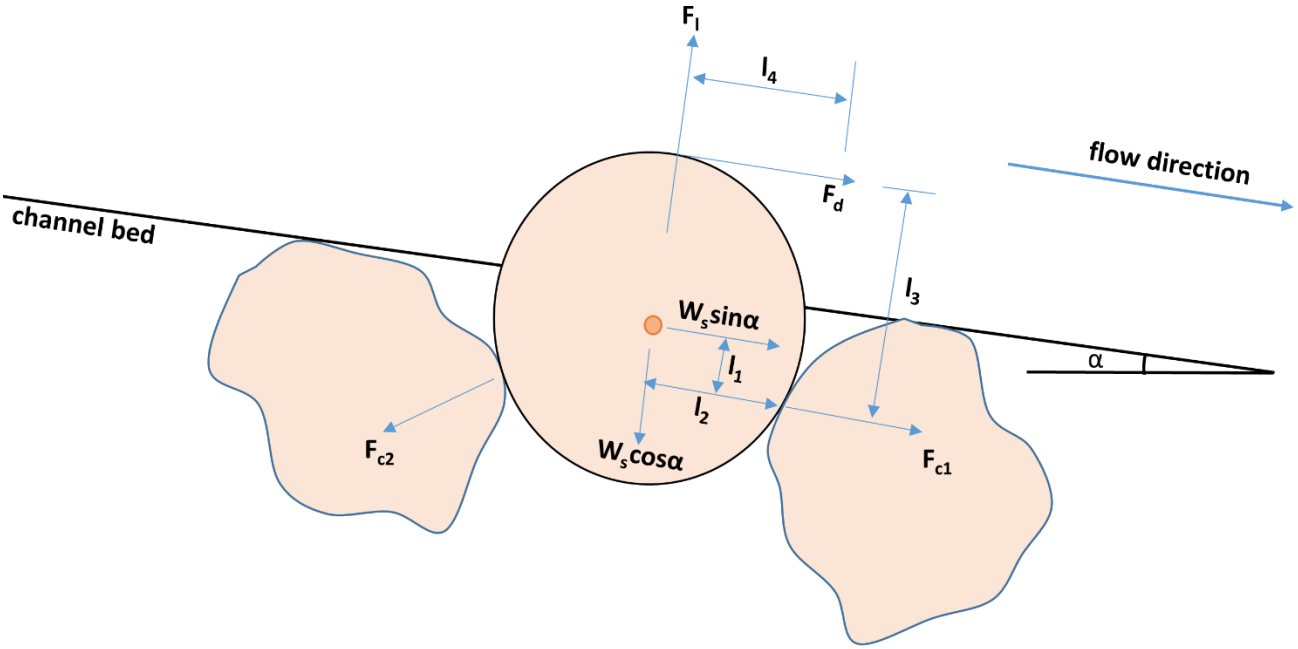

Figure 5.1 Schematic of forces and moment lengths acting on a particle

$$F_d l_3 + F_l l_4 + W_s \sin\alpha = W_s \cos\alpha + M_c \tag{5.10}$$

$$\sum M_c = \sum_{i=1}^{n_c} F_{ci} l_i \tag{5.11}$$

where W_s is the submerged weight of the particle, M_c is the sum of moment and cohesive forces, F_{ci} is the contact force between adjacent particles, and l_i is the corresponding moment length.

By assuming that drag and lift forces are proportional, Wilson proposed, similar to Chepil, 1959, that equation 5.10 can be expressed as:

$$F_d = W_s(k_{ls} + f_c) \tag{5.12a}$$

where k_{ls}, a dimensionless parameter related to the particle size, orientation and bed slope, is given by:

$$k_{ls} = \frac{\cos\alpha(l_2 - l_1 S_o)}{l_3 + l_4 k_l / k_f} \tag{5.12b}$$

where S_o is the bed slope equal to tanα, k_l is the ratio of ratio of drag and lift coefficients, k_f is the ratio of the projected area drag and lift forces; k_l/k_f is equal to F_l/F_d.

Also,

$$f_c = \frac{M_c/(l_3+l_4k_l/k_f)}{W_s} \tag{5.12c}$$

Based on the work of Einstein and El-Samni (1949), where the time averaged bed force was related to the time averaged flow velocity, Wilson defined the time averaged drag force at the bed, $\overline{F_d}$, as:

$$\overline{F_d} = C_D k_f k_a d^2 \frac{\rho u_d^2}{2} \tag{5.13a}$$

where $\bar{F}_d$ is the time averaged drag force, C_D is the drag coefficient, k_a is an area constant for a sphere which is equal to $\pi/4$, u_d is the time averaged flow velocity, d is the particle diameter, and ρ is the flow density.

Wilson further simplified equation 5.13a by relating the time averaged velocity to the average bed shear stress, by way of the log law and shear velocity formulations, to give the following equation:

$$\overline{F_d} = k_d k_a d^2 \bar{\tau} \tag{5.13b}$$

where k_d is a dimensionless drag and velocity parameter, and $\bar{\tau}$ is the average bed shear stress.

Expressing the particle area and volume in terms of the particle diameter, the particle volume, V_p, and projected area, V_a, was defined as:

$$V_p = k_v d^3 \tag{5.14a}$$

$$A_p = k_a d^2 \tag{5.14b}$$

where k_v is the volume constant for a sphere which is equal to $\pi/6$ and k_a was previously defined.

Therefore, the submerged weight of the particle, W_s, is given by:

$$W_s = g(\rho_s - \rho) \tag{5.15}$$

where ρ_s and ρ are the particle and water densities respectively.

At the point of incipient motion (where the average bed shear stress, $\bar{\tau}$, is equal to the critical bed shear stress, τ_c), the drag force (equation 5.13b) is equal to the time averaged drag force (equation 5.12a). Rearranging these equations gives:

$$\frac{\tau_c}{g(\rho_s - \rho)d} = \tau_c^* = \frac{k_r}{k_d}(k_{ls} + f_c) \tag{5.16}$$

where τ_c^* is the dimensionless critical Shields stress, and kr is k_v/k_a, which for a sphere, is 2/3.

Using a probabilistic framework similar to that by Einstein (1950) and Partheniades (1965), Wilson defined the probability of the drag force overcoming the resisting forces of particle weight and cohesion, P, as follows:

$$P = 1 - \int_{-\infty}^{W_S(k_{ls}+f_c)} f(F_d)\, d(F_d) \tag{5.17}$$

where $f(F_d)$ is the exceedance probability of the drag forces being greater than the resisting forces.

The rate of particle detachment, n_{ri}, which is the number of eroded particles divided by the time of the erosion event, was defined as:

$$n_{ri} = \frac{\Delta FF_i P}{k_a d^2 (K_e t_e)} \tag{5.18}$$

Where ΔFF_i is the fraction finer value of detached particles, $k_a d^2$ is the projected area of a single particle, K_e is a parameter accounting for the time for the complete exposure of underlying particles, and t_e is the exchange time of a single particle.

Wilson defined the exchange time, t_e, as:

$$t_e = d\sqrt{\frac{k_{dd}}{gd(k_n\tau^* - \mu_f)}} \qquad \text{when} \quad k_n\tau^* > \mu_f \tag{5.19}$$

where μ_f is the friction coefficient, k_n is a combinative factor accounting for cumulative instantaneous fluid forces as well as particle factors k_d and ka, $\tau^*$is the Shields parameter, and k_{dd} is the detachment distance parameter which, according to Einstein (1950), is equal to 2.

The detachment rate, E_{ri}, in mass per area per time, obtained by multiplying n_{ri} by the density and volume of each particle, is given by:

$$E_{ri} = n_{ri}\rho_s k_v d^3 = \Delta F F_i P \rho_s k_r \frac{d}{k_e t_e} \tag{5.20}$$

To calculate the exceedance probability, P, Wilson suggested using the extreme value type I probability distribution over the normal or the log-normal distributions because the extreme value type I probability distribution is simple to use and approximates the log-normal distribution. Also, the probability of having negative drag forces are small when the log-normal distribution is used.

The exceedance probability of the extreme value type I distribution is given as:

$$P = 1 - \exp[-\exp(-U_e)] \tag{5.21a}$$

where U_e is the upper limit of the distribution and is given by:

$$U_e = \frac{\pi}{e_v\sqrt{6}}\left[\frac{k_r(k_{ls} + f_c)}{k_d\tau^*} - \left(1 - \frac{1.365e_v}{\pi}\right)\right] \tag{5.22b}$$

Where e_v is the coefficient of variation, which is equal to 0.35 (Einstein and El-Samni, 1949).

By combining equations 5.19, 5.20 and 5.21a, Wilson expressed the detachment rate, E_{ri}, for $k_n\tau > \mu_f$, as:

$$E_r = \frac{\Delta FF_i}{k_e}\rho_s k_r \sqrt{\frac{gd(k_n\tau^* - \mu_f)}{k_{dd}}} \times \{1 - \exp[-\exp(-U_e)]\} \qquad (5.23)$$

Wilson lumped most of the model parameters into two parameters, b_0 and b_1, and expressed the erosion rate, E_r, as:

$$E_r = b_o\sqrt{\tau}\left\{1 - \exp\left[-\exp\left(3 - \frac{b_1}{\tau}\right)\right]\right\} \qquad (5.24a)$$

where

$$b_o = \rho_s \frac{k_r}{k_e}\sqrt{\frac{k_n}{k_d(\rho_s - \rho)}} \qquad (5.24b)$$

$$b_1 = \left(\frac{\pi}{e_v\sqrt{6}}\right)\left(\frac{k_r(k_{ls} + f_c)}{k_d}\right) g(\rho_s - \rho)d \qquad (5.24c)$$

It is noted that, like the original Partheniades erosion equation (equation 5.8), the Wilson model cannot be evaluated through direct measurements of most of the model parameters and variables. Therefore, this model is utilized using the two-parameter model (equation 5.24a) by estimating b_0 and b_1 using curve-fitting methods.

Study Objectives

The aim of this study was to compare the linear excess shear stress model and the Wilson model using data from flume experiments. Additionally, these models were modified to simulate temperature effects on erosion rate (presented in the previous chapter). The modified models were parameterized, and their performance in predicting erosion rates from hydraulic shear stress and temperature was compared using statistical indices derived from cross-validation prediction errors.

Methodology

Overview

Data sets from two separate studies, study 1 and study 2, were used in developing and testing an erosion model which captures the effect of both the hydrodynamic and the thermal properties of the flow on the erosion of select cohesive soils. In the first study (Hoomehr et al., 2018), erosion tests were conducted using a recirculating flume. Two different cohesive soils sourced from floodplains within Montgomery County, VA, were remolded and subjected to a range of shear stresses; the erosion rate was measured as the distance eroded per test period. For each soil type, erosion tests were performed at combinations of water pH values of 6 and 8, salinity values of 0 and 5000 mg/L NaCl, and temperatures of 10°C, 20°C and 30°C for a total of 12 water chemistry conditions. The excess shear stress and the Wilson model parameters were estimated using data from this study and the variations of the model parameters with the test conditions were evaluated. Also, the two erosion models were assessed using the leave-one-out-cross-validation (LOOCV) procedure. In the second study (Chapter 4), erosion tests were performed on the same soils as in the first study but under at a single shear stress of about 5 Pa. A different soil preparation protocol was utilized, and the effects of soil and water temperatures on surface erosion were investigated by conducting erosion tests on the soils at 0°C, 15°C and 25°C at a 15°C water condition, and 15°C, 25°C and 40°C at a 25°C water condition.

Using data from the second study, which was performed at a single shear stress, the effects of soil and eroding water temperatures on erosion rate was modelled and this relation was combined with the excess shear stress and the Wilson erosion models. The modified models, which now incorporate both the hydrodynamic forces and temperature of the eroding water, were

parameterized and their predictive powers were compared using the LOOCV procedure. The overview of the study methodology is outlined in Figure 5.2.

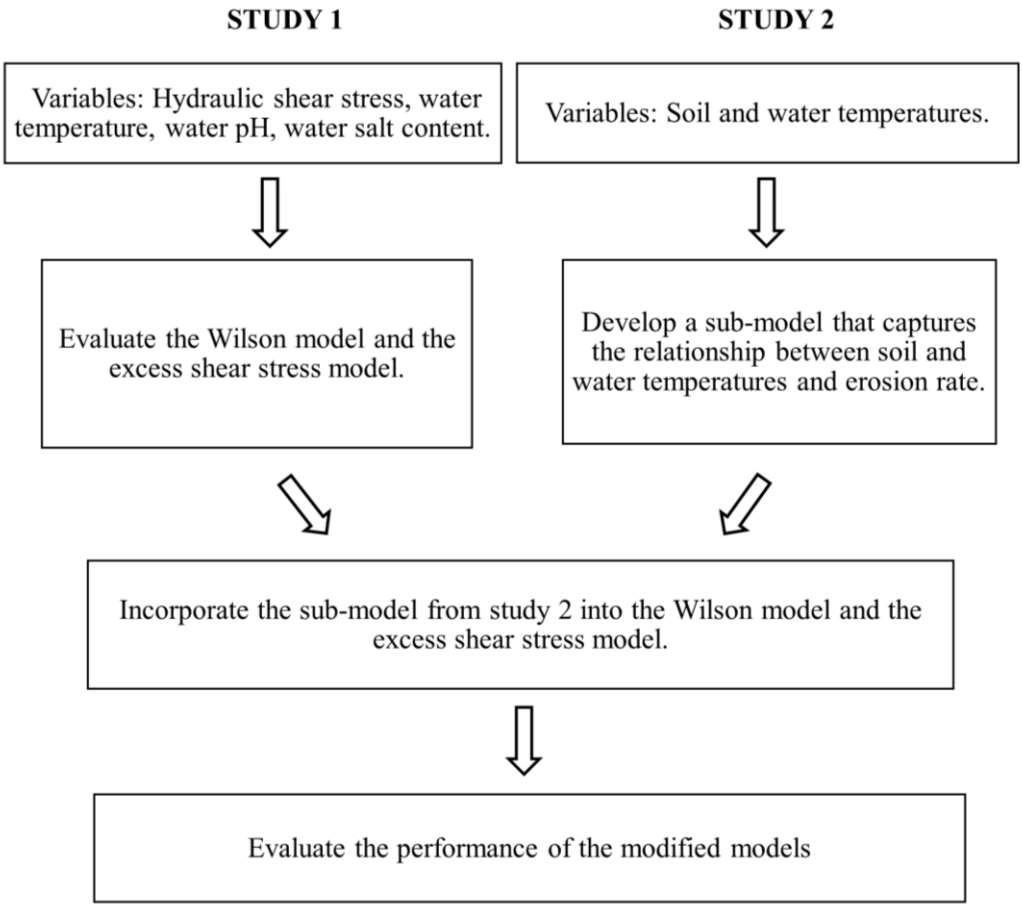

Figure 5.2 Overview of study methodology

Soil mineralogy

The same two soils were used for both study 1 and study 2. The first soil is a vermiculite-dominated natural soil obtained at a depth of 8 to 38 cm from the New River floodplain, at the Virginia Tech Kentland farm at Whitethorne, VA. This soil contains 44% sand, 43% silt and 13% clay with the clay fraction comprising of 35% H-I vermiculite, 10% vermiculite, 10% mica, 15% kaolinite, 13% quartz, 10% chlorite and 6% smectite. The second soil is a montmorillonite-

dominated natural soil obtained from the banks of Stroubles Creek, Blacksburg, VA, at a depth of 45 to 60 cm from the bank top. This soil contains 27% sand, 65% silt and 8% clay with the clay fraction comprising of 35% kaolinite, 25% montmorillonite, 20% illite, 15% H-I vermiculite, 3% chlorite and 2% quartz. For more detailed descriptions of these soils, the reader is referred to Hoomehr et al. (2018) and Akinola et al. (2018).

Soil preparation

Although both studies utilized the same soils, sample preparation protocols differed. For study 1, field soils were air-dried, pulverized and sieved using a 2-mm diameter sieve. Each soil core was prepared at selected moisture contents and bulk densities in a 5-cm by 5-cm cylindrical ring using a 4.64 kg-slide hammer and a specially designed base which held the soil core ring. Prior to testing, the soil core was saturated in deionized water for 12 hours and then placed in a pressure plate at a vacuum pressure of 1/3 bars for three days to bring the core to field capacity. The soil preparation procedures as well as the physical properties of the soil cores as prepared are given in detail in Hoomehr et al. (2018). For study 2, soil cores were prepared in the same core rings as in study 1, but the cores were prepared at optimum moisture content and maximum dry density, as determined by standard proctor compaction tests [ASTM D698 (ASTM 2003)]. Also, a different compaction method was used, as the soils were reconstructed using a manually operated hydraulic press (Dake 10 Ton Floor Press, # 972210). Each soil core was then placed in a water-tight plastic bag and immersed in a temperature-controlled water bath for two hours to bring it to the testing temperature. The physical properties of the soils as prepared are given in Chapter 4.

Flume preparation

An 8-m by 1-m by 0.4-m recirculating flume (Figure 5.3; Engineering Laboratory Design Inc., Lake City, MN) was used for the study 1 and study 2 experiments. A vertical insert was

installed down the center of the flume to create a wall simulating a vertical streambank through which the soil core was introduced into the flow. The flume has a tank capacity of 5000 L, a bed slope range of 0 to 5%, and is equipped with a 373 kW pump. A screw advancer was installed behind the core inlet to move the eroding soil front flush with the vertical wall as erosion progressed to maintain consistent boundary conditions as the core eroded. Erosion was monitored using a Vectrino II acoustic Doppler profiling velocimeter (ADP; Nortek AS, Vangkroken, Norway) mounted in the flume channel perpendicular to the surface of the soil core. The ADP monitored the distance from the probe head to the eroding front and also recorded three dimensional velocity profiles in 1-mm bins at a frequency of 50 Hz. For the first study, in addition to hydraulic shear stress, water chemistry variables included temperature, pH and salt content. The pH of the flume water was adjusted using 0.01 M HCl and KOH, and the salt content was adjusted using sodium chloride deicing rock salt (Scotwood Industries, Inc., CAS #007647-14-5, Overland Park, KS). Water temperature was controlled using aquarium heaters installed in the flume tank (True Temp T-1000, Transworld Aquatic Ent., Inglewood, CA) or with the use of buckets of ice, as appropriate. For the second study, the lower water temperature was achieved by cooling the laboratory space to the test temperature while the higher water temperature was obtained using the aquarium heaters.

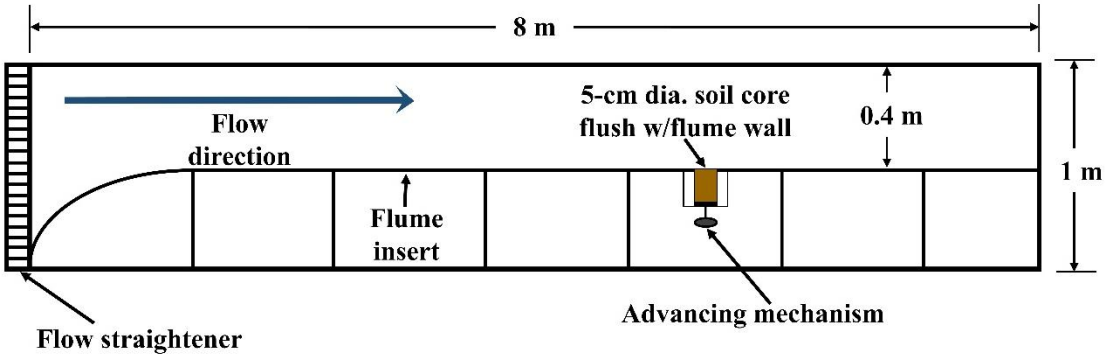

Figure 5.3 Flume schematic; not drawn to scale

Testing process

The testing process in both studies was similar. Utilizing the flume configuration (Figure 5.3), the soil core was introduced into the flow through an orifice in a vertical wall. Unlike many erosion tests where the cohesive material to be tested forms the flume bed, this orientation was chosen to simulate an eroding streambank rather than a streambed. To start the experiment, the soil core was inserted in the flume wall, shaved flush with the wall and covered with a plastic tray before the flume was turned on. Once flow became fully developed, the plastic tray covering the soil surface was removed and the ADV was turned on in succession. The distance of the soil surface to the ADV probe head was monitored on a PC and the soil core was advanced back to its initial position after each millimeter of erosion. Each erosion test was run for 15 minutes and erosion rate was taken as the total distance eroded divided by the test duration. For the first study, after an erosion experiment, the flume was drained, the soil core was advanced a few millimeters, and then shaved flush with the wall to obtain a fresh surface for the next hydraulic shear stress setting. For the second study, a new soil core was used for each test.

Velocity data analyses

For each flume run, turbulence kinetic energy (TKE) was calculated from the three dimensional velocity data recorded by the ADV to characterize the hydrodynamic contribution of flow to erosion rate. TKE can be defined as the mean kinetic energy associated with eddies in turbulent flow. The velocity time series data from the ADV were preprocessed in Matlab by filtering out data points with correlation less than 40% and signal to noise ratio (SNR) less than 10 dB. The TKE pertaining to each erosion run was calculated from velocity data using the following relation:

$$\mathrm{TKE} = 0.5 \times \rho_w \times \left(\overline{(u')^2} + \overline{(v')^2} + \overline{(w')^2}\right) \tag{5.25}$$

where ρ_w is the density of water, and the bracketed terms are the mean of the squared velocity fluctuations associated with the three velocity dimensions. The water density, which changes with temperature, is estimated from the following equation (Jones and Harris, 1992):

$$\rho_w = 999.85308 + (6.32693 \times 10^{-2} \times T) + (8.523829 \times 10^{-3} \times T^2) + (6.943248 \times 10^{-5} \times T^3) + (3.821216 \times 10^{-7} \times T^4) \quad (5.26)$$

where T (˚C) is the mean water temperature.

The wall shear stress was then calculated from the TKE using the following relation (Soulsby, 1983):

$$\tau = 0.19 \times TKE \quad (5.27)$$

Model evaluation and comparison

Evaluating the parameters of the excess shear stress equation and the Wilson erosion model require performing erosion tests at multiple hydraulic shear stresses, therefore data from study 1, which was conducted at multiple hydraulic shear stresses, were used parameterize these models. The linear excess shear stress model parameters, k_d and τ_c, and the nonlinear Wilson model parameters b_0 and $b_1$were estimated for each experimental condition using linear and nonlinear curve fitting procedures in Matlab. Both of these curve fitting methods utilized a least-squares approach, and appropriate constraints were placed on the solution space to ensure that nonsense values, such as negative parameter estimates, were unobtainable. The performance of these models was estimated using the leave-one-out cross validation (LOOCV). Although other cross-validation

techniques exist, the LOOCV, also known as delete-one-cross-validation or ordinary-cross-validation is an exhaustive procedure in which a data point is held back from model parametrization and the error between the model's prediction and the held back data gives a measure of the model's generalizability. The LOOCV could be computationally expensive, since the model is fit as many times as there are data points, but it is well suited to this study since the data sets are not large. Considering an erosion data set for which the excess shear stress and the Wilson model parameters are to be estimated, the LOOCV procedure was as follows:

For every data point i = 1,…, n:

1) Estimate model using every data point except i,
2) Calculate test error on i
3) Average the cross-validation error to get the CVE (equ 5.14):

$$\mathrm{CVE} = \frac{\sum_{i=1}^{n} \frac{\sqrt{(y_i - \bar{y}_i)^2}}{n}}{\sum_{i=1}^{n} \frac{y_i}{n}} \equiv \frac{\sum_{i=1}^{n} \sqrt{(y_i - \bar{y}_i)^2}}{\sum_{i=1}^{n} y_i} \tag{5.28}$$

where y_i is the erosion rate at point i, and $\bar{y}_i$ is the estimated erosion rate at point i using the model estimated with all other data points except data at i.

Based on previous work where the influence of soil and water temperatures on erosion rate were discussed (see chapter 5), the model derived from that study was incorporated into the excess shear stress model (eqn. 1 and the Wilson model (eqn. 10a) as follows:

$$E = (A_1(\Delta T) + A_2) + K_d(\tau - \tau_c) \tag{5.29}$$

$$E = (C_1(\Delta T) + C_2) + b_o\sqrt{\tau}\left\{1 - \exp\left[-\exp\left(3 - \frac{b_1}{\tau}\right)\right]\right\} \quad (5.30)$$

These models were compared using the LOOCV procedure as before. Additionally, the percent deviation of the erosion predictions (using the leave-one-out procedure) from the observed erosion rate was computed using the normalized objective function, NOF, (Pennell et al., 1990; Hession et. al. 1994). The NOF is the ratio of the root mean squared error, RMSE, to the mean of the experimental data, where the RMSE is the average error of the predicted values using the leave-one-out procedure and the observed experimental values, for each soil type, pH and salinity condition. A NOF value of 0.1 and 0.9 means that the cross-validation predictions deviated 10% and 90%, respectively, from the experimental data (Fox et al., 2006; Al-Madhhachi et al., 2013). The cross-validation NOF is calculated as follows:

$$NOF = \frac{\sqrt{\sum_{i=1}^{n} \frac{(y_i - \bar{y}_i)^2}{n}}}{\sum_{i=1}^{n} \frac{y_i}{n}} \quad (5.31)$$

Result and Discussion

Overall data

First, using data from study 1, the excess shear stress and the Wilson erosion model parameters were estimated using linear and nonlinear least squares regression in Matlab; these estimates are presented in Tables 5.2 and 5.3 for the fat clay and the lean clay respectively. The plots of these data are presented in Figures 5.4 and 5.5. The estimated model parameters were also

plotted against the experimental variables of water temperature, salt content and pH to visually assess changes in the models' parameters with these variables. However, these plots did not show any generalizable relationship between water temperature, salt content, and pH and the parameters of the excess shear stress and the Wilson erosion models, and are therefore not presented. From the plots of the study data (Figures 5.4 and 5.5), the sparseness and degree of variation of the experimental data can be observed, and although these may not be a favorable for modelling purposes, the data is representative of cohesive soil erosion data, and is therefore excellent in evaluating the two erosion models (the excess shear stress model and the Wilson model). The predictive capabilities of these models were judged using the LOOCV procedure described above and the results of this analysis are presented in Tables 5.2 and 5.3.

Table 5.2 Model comparisons – Fat clay

[a]Temp_pH_S condition	n	CVE ExSh[b]	CVE Wil[c]	Parameter estimates - Excess shear stress model			Parameter estimates - Wilson model		
				k_d (mm/hr-Pa)	τ_c (Pa)	RMSE (mm/hr)	b_o (mm/hr-$Pa^{0.5}$)	b_1 (Pa)	RMSE (mm/hr)
10_6_0	5	0.48	5.52e6	42.21	0.15	3.48	71.82	1.51	1.86
20_6_0	6	0.37	0.42	428.10	0.04	23.66	202.80	0.40	26.42
30_6_0	2	Insufficient data		----	----	----	----	----	----
10_6_5000	3	1.75	0.26	140.80	0	15.80	117.50	0.38	3.75
20_6_5000	4	0.56	0.66	858.80	0.10	27.92	325.70	0.62	21.05
30_6_5000	4	1.23	0.98	467.70	0.01	70.15	220.80	0.31	65.88
10_8_0	12	0.74	0.32	19.26	0.37	21.10	83.85	14.29	8.92
20_8_0	12	0.58	0.86	12.41	0.06	19.05	25.03	1.33	20.53
30_8_0	9	0.45	0.25	21.85	0	13.78	35.30	0	7.80
10_8_5000	9	0.44	0.49	39.14	0	34.28	64.47	0.35	27.60
20_8_5000	6	0.16	0.15	748.80	0.08	11.68	271.50	0.48	11.18
30_8_5000	3	0.05	0.04	1570.00	0.04	1.28	500.30	0.32	1.44

[a] Temp_pH_S condition: Water temperature (°C), pH and salt content (mg/L)
[b] CVE_ExSh: Cross validation error for the excess shear stress equation
[c] CVE_Wil: Cross validation error for the Wilson erosion model

Table 5.3 Model comparisons – Lean clay

[a]Temp_pH_S condition	n	CVE_ExSh[b]	CVE_Wil[c]	Parameter estimates - Excess shear stress model			Parameter estimates - Wilson model		
				k_d (mm/hr-Pa)	τ_c (Pa)	RMSE (mm/hr)	b_o (mm/hr-$Pa^{0.5}$)	b_1 (Pa)	RMSE (mm/hr)
10_6_0	9	0.32	0.44	5.56	0	6.98	16.34	0.66	6.86
20_6_0	6	0.46	0.38	363.80	0	27.15	185.20	0.37	22.59
30_6_0	5	0.39	0.20	401.30	0	30.46	184.93	0	19.03
10_6_5000	1	Insufficient data		----	----	----	----	----	----
20_6_5000	6	1.80	0.99	9.33	0	32.46	29.04	0.31	25.01
30_6_5000	5	0.30	0.23	960.10	0.09	12.74	406.73	0.64	9.08
10_8_0	8	1.42	1.43	6.34	0	14.16	9.39	0	14.28
20_8_0	8	0.41	0.35	17.08	0	12.14	28.82	0	10.55
30_8_0	9	0.45	0.31	27.61	0	17.82	43.17	0.23	13.07
10_8_5000	8	0.54	0.60	12.57	0.02	13.25	23.41	0.56	16.42
20_8_5000	6	4.52	1.01	30.92	0	36.72	56.04	0.25	28.11
30_8_5000	6	0.33	0.29	693.60	0.08	20.32	217.53	0.44	17.19

[a] Temp_pH_S condition: Water temperature (°C), pH and salt content (mg/L)
[b] CVE_ExSh: Cross validation error for the excess shear stress equation
[c] CVE_Wil: Cross validation error for the Wilson erosion model

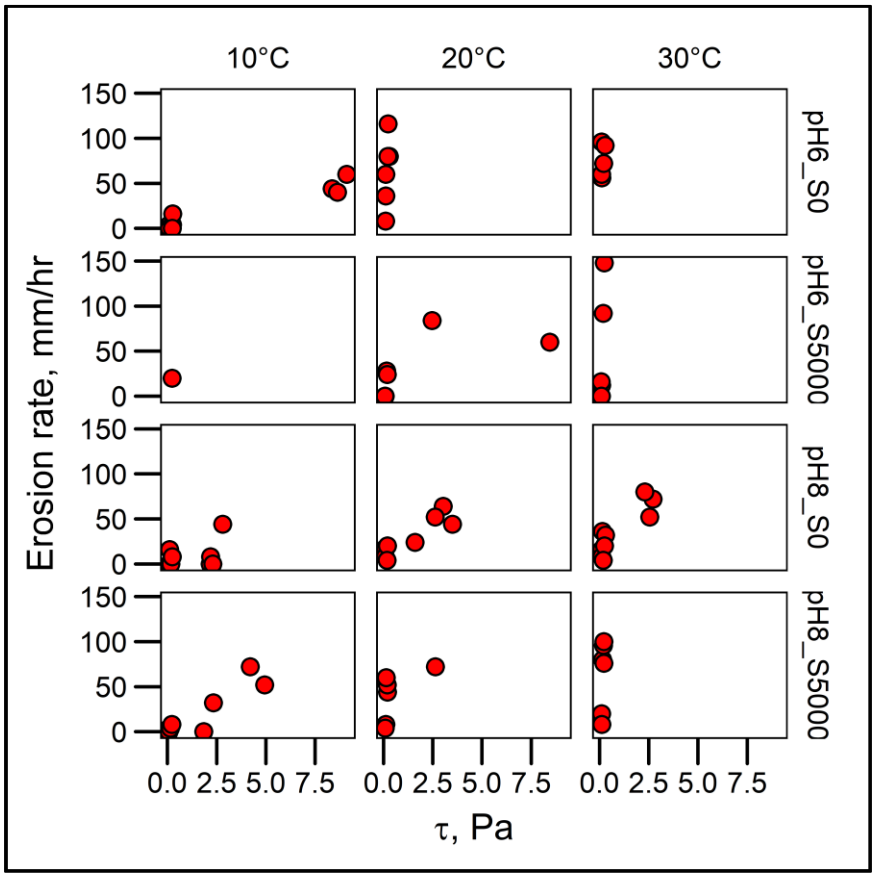

Figure 5.4 Erosion rate vs hydraulic shear stress at all eroding water conditions for the lean clay

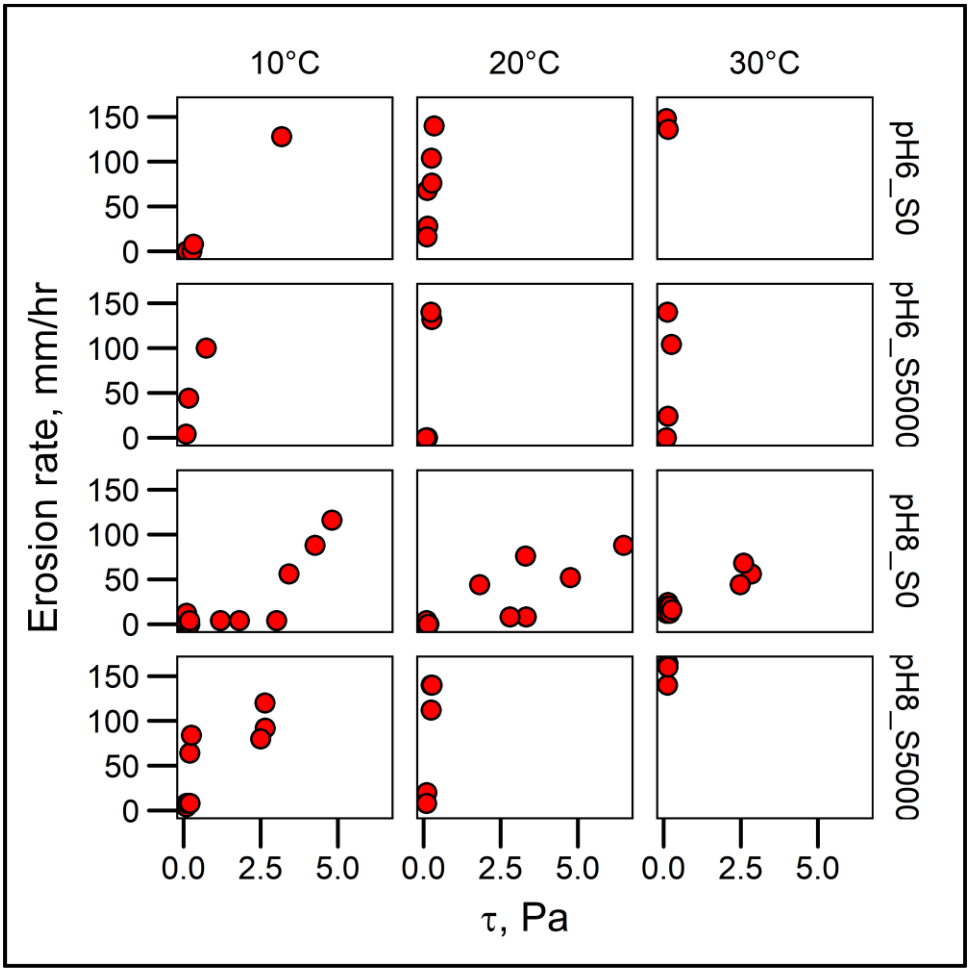

Figure 5.5 Erosion rate vs hydraulic shear stress at all eroding water conditions for the fat clay

The preliminary assessment of both models (Tables 5.2 and 5.3) shows that, overall, the Wilson model performed slightly better than the excess shear stress model, as indicated by the lower CVE for 14 of 24 experimental conditions and soil combinations. For the vermiculite-dominated soil, insufficient data at a water temperature of 10°C, pH of 6 and salinity of 5000 mg/L prevented the assessment of the models at this experimental condition. At the other 11 experimental conditions, the Wilson model performed better than the excess shear stress model eight times. Similarly, for the montmorillonite-dominated natural soil, insufficient data at a water temperature of 30°C, pH of 6 and salinity of 0 mg/L prevented the assessment of the models at this

experimental condition. At the other 11 experimental conditions, the Wilson model and the excess shear stress model performed about the same.

Modified excess shear stress and Wilson models

The relationship between soil and eroding water temperatures and erosion rate was previously investigated and presented in detail (Chapter 4). Although sample preparation protocols between study 1 (erosion tests) and study 2 (temperature tests) were different, the same natural soils were used for both studies. For the vermiculite-dominated lean clay and the montmorillonite-dominated fat clay, Study 2 showed that erosion rate was positively correlated to the difference between water temperature (T_w) and soil temperature (T_s), ($\Delta T = T_w - T_s$, $^{\circ}C$) (Figure 5.6).

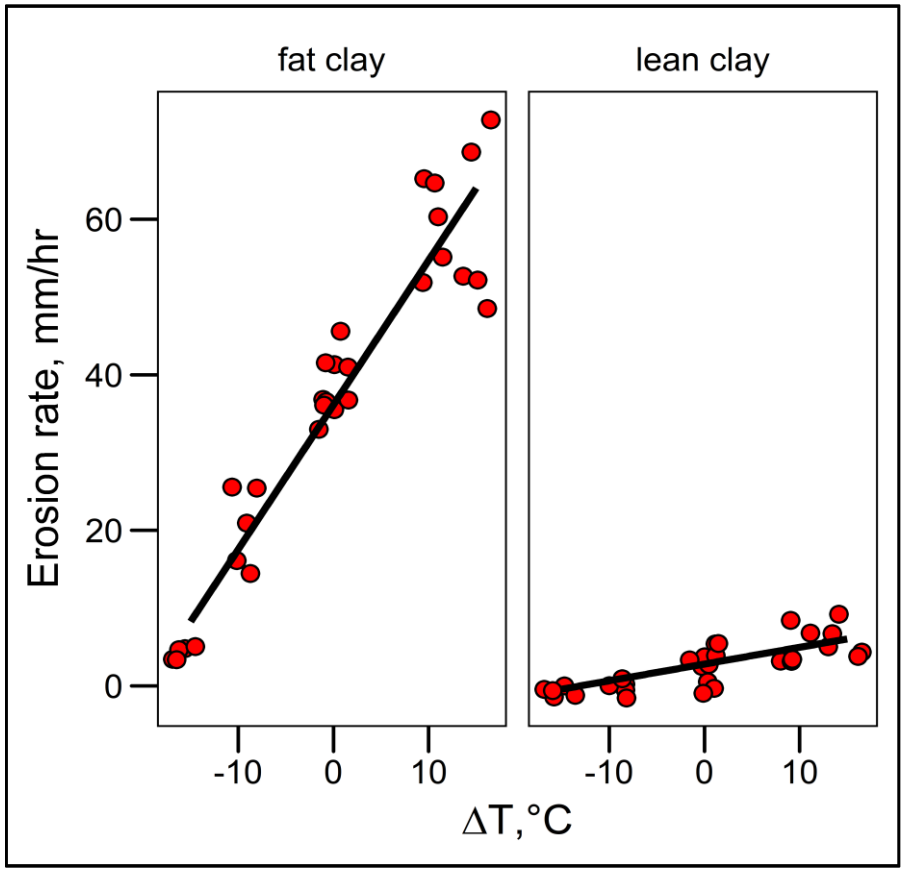

Figure 5.6 Erosion rate vs ΔT (from study 2)

Based on this result, a linear relation between erosion rate and the difference between water and soil temperatures was proposed and incorporated in the excess shear stress model and the Wilson model (equations 5.29 and 5.30). The considerable variability of the erosion data (see Appendix) in an indicator of the type of variability typical of cohesive erosion studies, and underscores the difficulty that has plagued cohesive erosion research. And, considering that these data were collected under highly controlled conditions using remolded soils, the variation exhibited in-situ would be much greater.

Model evaluation

The original and the modified Wilson and excess shear stress models were assessed using the LOOCV and the NOF procedures presented earlier, and the LOOCV statistic and the percent deviation they represent (the NOF), for both original and modified forms of the excess shear equation and the Wilson model are presented in Table 5.4. From this table, it is clear that the modification of both the excess shear stress equation and the Wilson erosion model to incorporate soil and water temperatures resulted in much better predictive models. For almost all experimental conditions, the LOOCV and the NOF were much lower for the modified erosion models compared to the original models, and the few times the modified models did not lead to better predictions were at experimental conditions with the fewest data points. For original erosion models, the deviations of the models' predictions from the experimental data ranged from 80% to 334% and 79% to 156% for the excess shear stress model and the Wilson model respectively. Conversely, the deviations of the modified excess shear stress model predictions from the experimental data ranged from 55% to 227% while the deviations of the modified Wilson erosion model predictions from the experimental data ranged from 51% to 150%. These values support the superiority of the

modified erosion models and indicate that, in practice, the modified erosion models are preferable to the original equations.

Comparisons between the modified Wilson erosion model and the modified excess shear stress model showed that the Wilson erosion model performed better than the excess shear stress erosion model six out of eight times for both soil types altogether. The two times the excess shear stress model performed better were the experiments at a pH of 8 and salinity of 0 mg/L, which had more data points. The reason for the superiority of the Wilson erosion model relative to the excess shear stress model may be inferred from the structure of the models. As a linear model, the excess shear stress equation has been widely accepted since this model is easy to understand and implement, and this is probably why this model continues to persist in practice. The nonlinear Wilson erosion model is less intuitive, more complex, and more difficult to parameterize compared to the excess shear stress model, and is therefore not used in many erosion studies. Overall, complex nonlinear data patterns in erosion data will be better captured with a nonlinear model such as the Wilson erosion model while data patterns which appear linear will be better represented by the linear excess shear stress model. The question remains, therefore, of whether the cohesive soil erosion process, that is the relationship between erosion rate and hydraulic shear stress is linear or not. Based on the result of this study, the relationship between erosion rates and hydraulic shear stress (or turbulent kinetic energy) is typically nonlinear. Nevertheless, more studies are needed to confirm the assumptions particular to the excess shear stress erosion model and the Wilson erosion model, and to confirm the validity of modifying both equations to capture temperature effects on erosion rates.

Table 5.4 The CVE and NOF of the original and modified excess shear stress and Wilson erosion models

Soil Type	pH	Salinity (mg/L)	N	[a]Mean Er (mm/hr)	Modified models (with ΔT factor)				Original models (without ΔT factor)			
					[b]CVE ExSh	[c]CVE Wilson	[d]NOF ExSh	[e]NOF Wilson	[b]CVE ExSh	[d]CVE Wilson	[c]NOF ExSh	[e]NOF Wilson
Lean clay	6	0	20	46.20	0.43	0.40	0.55	0.52	0.87	0.88	1.18	1.10
Lean clay	6	5000	12	40.33	1.41	1.14	1.97	1.50	1.45	0.93	2.59	1.56
Lean clay	8	0	25	25.18	0.54	0.55	0.62	0.64	0.64	0.59	0.83	0.79
Lean clay	8	5000	20	39.60	0.55	0.54	0.69	0.66	0.83	0.76	1.15	1.01
Fat clay	6	0	13	65.54	0.90	0.45	2.27	0.65	1.67	0.87	3.34	1.03
Fat clay	6	5000	11	62.55	0.87	0.83	0.96	0.93	1.14	0.73	1.93	0.93
Fat clay	8	0	33	25.45	0.54	0.64	0.79	0.91	0.59	0.74	0.80	0.96
Fat clay	8	5000	18	75.56	0.49	0.44	0.58	0.51	0.78	0.77	1.09	0.93

[a] Mean Er – Mean erosion rate
[b] CVE ExSh – Leave-one-out cross validation error for the excess shear stress model
[c] CVE Wilson – Leave-one-out cross validation error for the Wilson erosion model
[d] NOF ExSh – Normalized objective function for the excess shear stress model
[e] NOF Wilson – Normalized objective function for the Wilson erosion model

Table 5.5 Estimated model parameters for equations 5.29 and 5.30

Soil type	pH	Salinity (mg/L)	Modified Excess shear stress model					Modified Wilson model				
			A1 (mm/hr-^{0}C)	A2 (mm/hr)	k_d (mm/hr-Pa)	t_c (Pa)	RMSE	C1 (mm/hr-^{0}C)	C2 (mm/hr)	b_0 (mm/hr-Pa$^{0.5}$)	b_1 (Pa)	RMSE (mm/hr)
Lean clay	6	0	3.66	58.09	4.41	0	26.10	3.73	53.55	16.07	0.50	24.80
Lean clay	6	5000	2.30	33.72	5.66	0	50.10	2.75	23.52	24.56	0.46	45.90
Lean clay	8	0	1.50	32.97	13.31	1.50	14.80	1.50	4.67	26.48	0.01	15.30
Lean clay	8	5000	3.14	40.03	13.28	0	26.50	3.09	29.85	31.79	0.41	24.90
Fat clay	6	0	7.23	121.2	44.78	0.80	32.10	7.48	51.97	101.4	0.02	29.20
Fat clay	6	5000	2.49	27.47	192.60	0	60.20	0.99	39.20	54.17	0.43	62.40
Fat clay	8	0	0.70	5.36	14.60	0	19.30	0.73	0	30.16	0.22	20.82
Fat clay	8	5000	6.14	100.4	33.37	0.15	44.89	5.96	72.13	72.88	0.40	38.36

Conclusions

In this study, the excess shear stress and the Wilson erosion models were presented and modified to capture, in addition to hydrodynamic forces, soil and water temperature effects on the erosion rates of two natural cohesive soils. The predictive powers of the original and modified models were assessed using the leave-one-out-cross-validation procedure and comparisons were made between these models. The results show that, generally, the Wilson erosion model produced a better predictive fit to the experimental data compared to the excess shear stress erosion model. Additionally, the modified models, which account for soil and water temperatures, consistently gave better predictions compared to the original models. Overall, the Wilson erosion model in its original and modified form, is a model worth more investigation, and is a viable alternative to the linear excess shear stress erosion model. Furthermore, even if the linear excess shear stress model is preferred over the Wilson model for reasons such as simplicity and familiarity, it is better to use the modified form of the excess shear stress model which integrates temperature effects on erosion rate.

References

Akinola, A. I., Wynn-Thompson, T., Olgun, C. G., Cuceoglu, F., and Mostaghimi, S. (2018). "Influence of sample holding time on the fluvial erosion of remolded cohesive soils." *J. Hydraul. Eng.*144(8),

Al-Madhhachi, A. T., Fox, G. A., Hanson, G. J., Tyagi, A. K., and Bulut, R. (2014). "Mechanistic detachment rate model to predict soil erodibility due to fluvial and seepage forces." *J. Hydraul. Eng.,* 10.1061/(ASCE)HY.1943-7900.0000836, 04014010.

Al-Madhhachi, A. T., Hanson, G. J., Fox, G. A., Tyagi, A. K., and Bulut, R. (2013). "Deriving parameters of a fundamental detachment model for cohesive soils from flume and Jet Erosion Tests." *Trans. ASABE,* 56(2), 489–504.

Ariathurai, R., Arulanandan, K. (1978). "Erosion rates of cohesive soils*." J. Hydr. Div.,* ASCE, 104(2), 279–283.

ASTM. (2003). *Standard test methods for laboratory compaction characteristics of soil using standard effort (*12400 *ft-lbf=ft*^{3} *(*600 *kN-m/m*^{3}*)).* ASTM D698. West Conshohocken, PA: ASTM

Blench, T. (1952). "Regime theory for self-formed sediment-bearing channels." *Trans. ASCE*, 117, 383–400.

Chepil, W. S. (1959). "Equilibrim of soil grains at threshold of movement by wind." *Soil Sci. Soc. Am. Proc.*, 23(6), 422-428.

Chitale, S. V. (1996). "Coordination of empirical and rational alluvial canal formulas." *J. Hydraul Eng*., 10.1061/(ASCE)0733-9429(1996)122:6(357).

Einstein, H. A. (1950). "The bed-load function for sediment transportation in open channel flows." *Technical Bulletin No. 1026,* U.S. Department of Agriculture, Washington, D.C

Einstein, H. A., and El-Samni, E. A. (1949). "Hydrodynamic forces on a rough wall." *Rev. Mod. Phys.*, 21(3), 520–524.10.1103/RevModPhys.21.520

Einstein, H. A., and Li, H. (1956). "The viscous sublayer along a smooth boundary." *J. Engrg. Mech. Div.*, ASCE, 82(2).

Fox, G. A., Sabbagh, G. J. Chen, W., and Russell, M. (2006). "Uncalibrated modeling of conservative tracer and pesticide leaching to groundwater: Comparison of potential Tier II exposure assessment models." *Pest Mgmt. Sci*., 62(6): 537-550.

Grabowski, R. C., Droppo, I. G., and Wharton, G. (2011). "Erodibility of cohesive sediment: The importance of sediment properties." *Earth-Sci. Rev.*, 105(3), 101-120.

Hession, W. C., Shanholtz, V. O., Mostaghimi, S., and Dillaha, T. A. (1994). "Uncalibrated performance of the finite element storm hydrograph model." *Trans. ASAE.,* 37(3): 777-783.

Hester, E. T., and Bauman, K.S. (2013). "Stream and retention pond thermal response to heated summer runoff from urban impervious surfaces." *J. Am. Water Resour. As.,* 49(2), 328–342.

Hoomehr, S., Akinola, A. I., Wynn-Thompson, T., Garnand, W., Eick, M. J. (2018). "Water Temperature, pH, and Road Salt Impacts on the Fluvial Erosion of Cohesive Streambanks." *Water,* 10(3):302.

Jones, F. E., and Harris, G. L. (1992). "ITS-90 density of water formulation for volumetric standards calibration." *J. Res. Natl. Bur. Stand.*, 97 (3), 335–340.

Kandiah, A. (1974). "Fundamental aspects of surface erosion of cohesive soils." PhD thesis, University of California, Davis, Calif.

Kennedy, R. G. (1895). "The prevention of silting in irrigation canals." *Proc., Inst. of Civ. Engrs.*, London, England, Vol. CXIX.

Lacey, G. (1930). "Stable channels in alluvium." *Proc., Inst. of Civ. Engrs*, 229, 259–292.

Mehta, A. J., and McAnally, W. H. (2008). "Fine-grained sediment transport." *Sedimentation engineering: Processes, measurements, modeling and practice, ASCE manual of practice 110,* M. H. Garcia, ed., ASCE, Reston, Va., Chap. 4, 253–306.

Nelson, K. C., and Palmer, M. A. (2007). "Stream temperature surges under urbanization and climate change: Data, models, and responses." *J. Am. Water Resour. As.*, 43(2):440-452.

Partheniades, E. (1965). "Erosion and Deposition of Cohesive Soils." *J. Hydr. Div.*, ASCE, Vol. 91, 105–139.

Partheniades, E. (2009). *Cohesive Sediments in Open Channels*, Butterworth-Heinemann, Burlington, MA.

Pimentel, D., Harvey, C., Resosudarmo, P., Sinclair, K., Kurz, D., McNair, M., Crist, S., Shpritz, L., Fitton, L., Saffouri, R., and Blair, R. (1995). "Environmental and economic costs of soil erosion and conservation benefits." *Science*, 267(5201), 1117–23.

Pennell, K. D., Hornsby, A. G., Jessup, R. E., and Rao, P. S. C. (1990). "Evaluation of five simulation models for predicting aldicarb and bromide behavior under field conditions." *Water Resour. Res*. 26(11): 2679-2693.

Soulsby, R. L. (1983). "The bottom boundary layer of shelf seas". *In Physical oceanography of coastal and shelf seas,* Johns, B., ed., Elsevier, Amsterdam. 189–266.

Stevens, M. A., and Nordin, C. F.(1987). "Critique of the regime theory for alluvial channels."*J. Hydraul. Eng.* 113(11): 1359–1380. 10.1061/(ASCE)0733-9429(1987)113:11(1359)

Stevens, M. A., and Simon, D. B. (1971). “Stability analysis for coarse granular material on slopes. In *River Mechanics*, ed. Shen, Fort Collins, CO: Colorado State University.

Telles, T. S., Guimarães, M. d. F., and Dechen, S. C. F. (2011). “The costs of soil erosion.” *R. Bras. Ci. Solo*, 35(2), 287–298.

Vanoni, V. A. (1977). *Sedimentation Engineering*. ASCE Manuals and Reports on Engineering Practice No. 54. ASCE, New York.

Wilson, B. N. (1993a). “Development of a fundamental based detachment model.” *T. ASAE*, 36(4), 1105–1114.

Wilson, B. N. (1993b). “Evaluation of a fundamental based detachment model.” *T. ASAE*, 36(4), 1115–1122.

Winterwerp, J. C., and van Kesteren, W. G. M. (2004). *Introduction to the physics of cohesive s ediment in the marine environment*, Elsevier, Amsterdam, The Netherlands.

CHAPTER 6

CONCLUSIONS AND FUTURE WORK

In the studies presented, a number of issues related to cohesive soil experiments and models were addressed. In field of cohesive erosion research, progress has not been made as quickly as necessary to address the current problems associated with unfettered cohesive soil erosion and sedimentation, due to the high variability in test results and a general lack of useful prediction methods. Much of this likely arises from the lack of a standard testing protocol coupled with the complexity of the processes of cohesive soil erosion resistance. Results of this study showed that erosion resistance increased exponentially with time since sample wetting (holding time), signifying the importance of maintaining a consistent sample holding time in cohesive erosion experiments. To this end, there is a significant need for a standardized testing procedure so that results from multiple studies can be comparable.

Also, the importance of soil and water temperature on the erosion of cohesive soils was investigated. Although not fully explored in previous research, increasing water temperature was known to result in an increase in cohesive soil erosion rate. This study showed that soil and water temperatures, not just water temperature, were the thermal factors affecting cohesive soil erosion rate, and indicated that streambank degradation commonly observed in urbanized watersheds is partly a result of decreased streambank erosion resistance as a result of increased streambank entropy through heat energy added to streambanks from streamflows. Therefore, it may be necessary to utilized BMPs which control stream temperatures in addition to peak discharge to curtail urban stream degradation.

Despite an improved understanding of erosion processes, predictions of the timing and rate of cohesive soil erosion remain rudimentary. Comparison of two available models showed that the Wilson erosion model performed better than the excess shear stress model, with the Wilson erosion model predictions deviating 79-156% from experimental data compared to the excess shear stress model prediction deviations of 80-334% from experimental data. Incorporating temperature effects improved these models, with the modified Wilson erosion model predictions deviating 51-150% from experimental data, and the modified excess shear stress model predictions deviating 58-227% from experimental data. However, these errors are still significant, indicating ongoing need for an improved understanding of erosion resistance and better models.

Research should continue to investigate the mechanics of cohesive soil erosion process as much is still unknown about this process. Changes in soil surface clay orientation with time, soil temperature, water temperature, pH and salt content, should be investigated to further understand how erosion resistance changes with these variables. Also, experiments should be performed at a range of soil and water temperatures beyond those presented in this study to validate the results at these temperatures. Additionally, in-situ tests to determine the relationship between event-based and seasonal changes in streambank erosion due to stream and streambank temperature changes should be performed. Overall, watershed management should consider the use of storm water BMPs designed to reduce stream temperatures, in addition to runoff volumes, to address streambank erosion problems frequently observed in urbanizing watersheds.

APPENDICES

Appendix A: Experimental Data-Chapter 3

Table A.1 Erosion data for fat clay (holding time study)

Holding time (hr)	Erosion rate (mm/hr)	Shear velocity (m/s)	Erosion rate (m/s)	Nondimensional erosion rate
0	8	0.060364	2.22222E-06	3.68137E-05
0	0	0.06116	0	0
0	4	0.064288	1.11111E-06	1.72833E-05
0	4	0.066708	1.11111E-06	1.66563E-05
0	4	0.063916	1.11111E-06	1.73839E-05
0	0	0.066116	0	0
0	8	0.069276	2.22222E-06	3.20778E-05
0	16	0.068092	4.44444E-06	6.52712E-05
0	0	0.064708	0	0
0	8	0.063916	2.22222E-06	3.47679E-05
6	12	0.061884	3.33333E-06	5.38642E-05
6	6	0.061052	1.66667E-06	2.72991E-05
6	8	0.061496	2.22222E-06	3.6136E-05
6	8	0.06078	2.22222E-06	3.65617E-05
6	20	0.06194	5.55556E-06	8.96925E-05
6	20	0.068404	5.55556E-06	8.12168E-05
6	20	0.0645	5.55556E-06	8.61326E-05
6	12	0.055328	3.33333E-06	6.02468E-05
6	0	0.060452	0	0
6	0	0.065588	0	0
24	0	0.072208	0	0
24	0	0.072208	0	0
24	0	0.070444	0	0
24	0	0.071004	0	0
24	0	0.070628	0	0
24	0	0.074796	0	0
24	0	0.072348	0	0
24	0	0.070916	0	0
24	4	0.078376	1.11111E-06	1.41767E-05
24	0	0.067208	0	0
48	0	0.06404	0	0

Holding time (hr)	Erosion rate (mm/hr)	Shear velocity (m/s)	Erosion rate (m/s)	Nondimensional erosion rate
48	0	0.065844	0	0
48	4	0.081564	1.11111E-06	1.36226E-05
48	4	0.080432	1.11111E-06	1.38143E-05
48	0	0.066848	0	0
48	0	0.068272	0	0
48	4	0.067284	1.11111E-06	1.65137E-05
48	0	0.06174	0	0
48	4	0.054832	1.11111E-06	2.02639E-05
48	0	0.073112	0	0
72	0	0.054196	0	0
72	0	0.060592	0	0
72	0	0.075536	0	0
72	4	0.064728	1.11111E-06	1.71658E-05
72	0	0.050596	0	0
72	0	0.051328	0	0
72	0	0.068572	0	0
72	0	0.06892	0	0
72	4	0.06732	1.11111E-06	1.65049E-05
72	0	0.06638	0	0

Table A.2 Erosion data for lean clay (holding time study)

Holding time (hr)	Erosion rate (mm/hr)	Shear velocity (m/s)	Erosion rate (m/s)	Nondimensional erosion rate
0	44	0.0693	1.22222E-05	0.000176367
0	40	0.070484	1.11111E-05	0.00015764
0	48	0.064968	1.33333E-05	0.000205229
0	32	0.066648	8.88889E-06	0.000133371
0	88	0.05776	2.44444E-05	0.000423207
0	48	0.056644	1.33333E-05	0.000235388
0	48	0.054156	1.33333E-05	0.000246202
0	60	0.072244	1.66667E-05	0.0002307
0	48	0.07008	1.33333E-05	0.000190259
0	40	0.065732	1.11111E-05	0.000169037
6	32	0.067944	8.88889E-06	0.000130827
6	36	0.063904	0.00001	0.000156485
6	36	0.064736	0.00001	0.000154474
6	24	0.065328	6.66667E-06	0.000102049
6	36	0.065336	0.00001	0.000153055

Holding time (hr)	Erosion rate (mm/hr)	Shear velocity (m/s)	Erosion rate (m/s)	Nondimensional erosion rate
6	32	0.062436	8.88889E-06	0.000142368
6	28	0.059036	7.77778E-06	0.000131746
6	32	0.061924	8.88889E-06	0.000143545
6	28	0.057524	7.77778E-06	0.000135209
6	34	0.054396	9.44444E-06	0.000173624
24	16	0.069672	4.44444E-06	6.3791E-05
24	16	0.065224	4.44444E-06	6.81412E-05
24	20	0.064852	5.55556E-06	8.56651E-05
24	24	0.064312	6.66667E-06	0.000103661
24	8	0.061368	2.22222E-06	3.62114E-05
24	20	0.056856	5.55556E-06	9.77127E-05
24	14	0.058088	3.88889E-06	6.69482E-05
24	12	0.05654	3.33333E-06	5.89553E-05
24	12	0.058472	3.33333E-06	5.70073E-05
24	8	0.062332	2.22222E-06	3.56514E-05
48	10	0.064948	2.77778E-06	4.27693E-05
48	8	0.066212	2.22222E-06	3.35622E-05
48	10	0.067596	2.77778E-06	4.10938E-05
48	8	0.065412	2.22222E-06	3.39727E-05
48	4	0.066196	1.11111E-06	1.67852E-05
48	0	0.067456	0	0
48	8	0.067844	2.22222E-06	3.27549E-05
48	4	0.060228	1.11111E-06	1.84484E-05
48	8	0.057712	2.22222E-06	3.85054E-05
48	0	0.062248	0	0
72	4	0.091044	1.11111E-06	1.22041E-05
72	4	0.093848	1.11111E-06	1.18395E-05
72	8	0.094192	2.22222E-06	2.35925E-05
72	8	0.09172	2.22222E-06	2.42283E-05
72	0	0.0937	0	0
72	0	0.09522	0	0
72	0	0.095628	0	0
72	0	0.085376	0	0
72	0	0.081932	0	0
72	0	0.08964	0	0

Table A.3 Erosion data for silty sand (holding time study)

Holding time (hr)	Erosion rate (mm/hr)	Shear velocity (m/s)	Erosion rate (m/s)	Nondimensional erosion rate
0	168	0.068768	4.66667E-05	0.00067861
0	126	0.066672	0.000035	0.000524958
0	144	0.066244	0.00004	0.000603828
0	150	0.064924	4.16667E-05	0.000641776
0	120	0.058368	3.33333E-05	0.000571089
0	144	0.059712	0.00004	0.000669882
0	168	0.057168	4.66667E-05	0.000816307
0	150	0.057808	4.16667E-05	0.000720777
0	150	0.057808	4.16667E-05	0.000720777
0	150	0.062808	4.16667E-05	0.000663397
6	114	0.063852	3.16667E-05	0.000495939
6	108	0.072984	0.00003	0.000411049
6	102	0.0719	2.83333E-05	0.000394066
6	96	0.068436	2.66667E-05	0.000389658
6	90	0.060784	0.000025	0.000411292
6	102	0.069436	2.83333E-05	0.00040805
6	102	0.069132	2.83333E-05	0.000409844
6	96	0.065392	2.66667E-05	0.000407797
6	105	0.065428	2.91667E-05	0.000445783
6	168	0.0572	4.66667E-05	0.000815851
24	48	0.070336	1.33333E-05	0.000189566
24	36	0.067396	0.00001	0.000148377
24	42	0.072508	1.16667E-05	0.000160902
24	48	0.07028	1.33333E-05	0.000189717
24	54	0.068968	0.000015	0.000217492
24	54	0.06892	0.000015	0.000217644
24	42	0.068236	1.16667E-05	0.000170975
24	42	0.067992	1.16667E-05	0.000171589
24	78	0.071548	2.16667E-05	0.000302827
24	90	0.069348	0.000025	0.000360501
48	36	0.068472	0.00001	0.000146045
48	33	0.067236	9.16667E-06	0.000136336
48	42	0.071508	1.16667E-05	0.000163152
48	60	0.064792	1.66667E-05	0.000257233

Holding time (hr)	Erosion rate (mm/hr)	Shear velocity (m/s)	Erosion rate (m/s)	Nondimensional erosion rate
48	48	0.063092	1.33333E-05	0.000211332
48	72	0.061428	0.00002	0.000325584
48	60	0.063468	1.66667E-05	0.0002626
48	6	0.06226	1.66667E-06	2.67695E-05
48	90	0.053004	0.000025	0.000471663
48	90	0.064596	0.000025	0.000387021
72	24	0.078068	6.66667E-06	8.53956E-05
72	12	0.072792	3.33333E-06	4.57926E-05
72	18	0.073296	0.000005	6.82165E-05
72	24	0.078128	6.66667E-06	8.53301E-05
72	24	0.067184	6.66667E-06	9.923E-05
72	12	0.071164	3.33333E-06	4.68402E-05
72	24	0.067	6.66667E-06	9.95025E-05
72	12	0.072496	3.33333E-06	4.59795E-05
72	30	0.067788	8.33333E-06	0.000122932
72	24	0.065688	6.66667E-06	0.00010149
96	6	0.068576	1.66667E-06	2.43039E-05
96	12	0.073088	3.33333E-06	4.56071E-05
96	12	0.071996	3.33333E-06	4.62989E-05
96	6	0.069572	1.66667E-06	2.3956E-05
96	12	0.068192	3.33333E-06	4.88816E-05
96	12	0.064668	3.33333E-06	5.15453E-05
96	3	0.069676	8.33333E-07	1.19601E-05
96	12	0.068908	3.33333E-06	4.83737E-05
96	15	0.060812	4.16667E-06	6.85172E-05
96	12	0.068356	3.33333E-06	4.87643E-05
120	0	0.069476	0	0
120	0	0.069336	0	0
120	0	0.066996	0	0
120	0	0.068084	0	0
120	0	0.068072	0	0
120	0	0.067012	0	0
120	0	0.071752	0	0
120	0	0.072612	0	0
120	0	0.069584	0	0

Holding time (hr)	Erosion rate (mm/hr)	Shear velocity (m/s)	Erosion rate (m/s)	Nondimensional erosion rate
120	0	0.071496	0	0

Appendix B: Experimental Data-Chapter 4

Table B.1 Erosion data for fat clay (temperature study)

Erosion rate (mm/hr)	Soil temp. (^{0}C)	Water temp. (^{0}C)	Nondimensional erosion rate
0	40	25	0
0	40	25	0
0	40	25	0
0	40	25	0
0	40	25	0
4	25	25	0.000017
0	25	25	0
4	25	25	0.000017
0	25	25	0
4	25	25	0.000016
8	15	25	0.000037
4	15	25	0.000016
4	15	25	0.000017
8	15	25	0.000038
4	15	25	0.000017
0	25	15	0
0	25	15	0
0	25	15	0
0	25	15	0
0	25	15	0
4	15	15	0.000018
0	15	15	0
4	15	15	0.000018
4	15	15	0.00002
4	15	15	0.000018
4	0	15	0.000015
4	0	15	0.000018
8	0	15	0.000037
4	0	15	0.00002
8	0	15	0.000034

Table B.2 Erosion data for lean clay (temperature study)

Erosion rate (mm/hr)	Soil temp. (^{0}C)	Water temp. (^{0}C)	Nondimensional erosion rate
4	40	25	1.70E-05
4	40	25	1.70E-05
4	40	25	1.70E-05
4	40	25	1.60E-05
4	40	25	1.60E-05
36	25	25	0.00014
36	25	25	0.00014
32	25	25	0.00012
40	25	25	0.00017
40	25	25	0.00017
52	15	25	0.00022
56	15	25	0.00023
60	15	25	0.00026
64	15	25	0.00028
64	15	25	0.00027
24	25	15	0.00012
16	25	15	7.90E-05
20	25	15	0.0001
16	25	15	7.70E-05
24	25	15	0.00011
44	15	15	0.0002
36	15	15	0.00017
40	15	15	0.00016
36	15	15	0.00017
36	15	15	0.00016
72	0	15	0.0003
52	0	15	0.00024
48	0	15	0.00021
68	0	15	0.00032
52	0	15	0.00025

Table B.3 Erosion data for silty sand (temperature study)

Erosion rate (mm/hr)	Soil temp. (^{0}C)	Water temp. (^{0}C)	Nondimensional erosion rate
12	40	25	4.90E-05
8	40	25	3.20E-05
12	40	25	4.70E-05
12	40	25	0.00005
16	40	25	6.70E-05
72	25	25	0.00024
76	25	25	0.00027
84	25	25	0.00031
76	25	25	0.00027
80	25	25	0.00031
96	15	25	0.00038
100	15	25	0.00043
100	15	25	0.0004
96	15	25	0.00038
96	15	25	0.00038
60	25	15	0.00025
56	25	15	0.00023
64	25	15	0.00025
64	25	15	0.00026
64	25	15	0.00026
72	15	15	0.00028
68	15	15	0.00028
72	15	15	0.00028
76	15	15	0.00033
76	15	15	0.00032
84	0	15	0.00034
88	0	15	0.00039
100	0	15	0.00042
88	0	15	0.00036
100	0	15	0.00043

Appendix C: Experimental Data-Chapter 5

Table C.1 Erosion data for fat clay (modelling)

Water temperature (^{0}C)	Water pH	Salt content (mg/L)	TKE (kg/m-s^2)	Shear Stress (Pa)	Erosion rate (mm/hr)
10	6	0	0.4696	0.0892	0
10	6	0	0.6027	0.1145	0
10	6	0	1.4314	0.272	0
10	6	0	1.6718	0.3176	8
10	6	0	16.7211	3.177	128
10	6	5	0.4458	0.0847	4
10	6	5	0.8763	0.1665	44
10	6	5	3.8766	0.7365	100
10	8	0	0.5145	0.0978	0
10	8	0	0.5118	0.0972	0
10	8	0	0.5293	0.1006	12
10	8	0	1.0314	0.196	0
10	8	0	1.0568	0.2008	0
10	8	0	1.0378	0.1972	4
10	8	0	9.5265	1.81	4
10	8	0	15.8818	3.0175	4
10	8	0	6.305	1.198	4
10	8	0	22.4172	4.2593	88
10	8	0	25.2938	4.8058	116
10	8	0	17.9988	3.4198	56
10	8	5	0.505	0.0959	8
10	8	5	0.4739	0.09	4
10	8	5	0.6207	0.1179	8
10	8	5	1.1031	0.2096	8
10	8	5	1.068	0.2029	64
10	8	5	1.3236	0.2515	84
10	8	5	13.887	2.6385	120
10	8	5	13.9138	2.6436	92
10	8	5	13.1618	2.5007	80
20	6	0	0.628	0.1193	68
20	6	0	0.6862	0.1304	28
20	6	0	0.5946	0.113	16
20	6	0	1.4111	0.2681	76
20	6	0	1.801	0.3422	140
20	6	0	1.3301	0.2527	104
20	6	5	0.6716	0.1276	0

Water temperature (^{0}C)	Water pH	Salt content (mg/L)	TKE (kg/m-s^2)	Shear Stress (Pa)	Erosion rate (mm/hr)
20	6	5	0.4339	0.0824	0
20	6	5	1.4127	0.2684	132
20	6	5	1.2329	0.2342	140
20	8	0	0.5198	0.0988	0
20	8	0	0.4407	0.0837	0
20	8	0	0.4913	0.0934	4
20	8	0	0.8642	0.1642	0
20	8	0	0.9185	0.1745	0
20	8	0	0.7927	0.1506	0
20	8	0	9.5596	1.8163	44
20	8	0	17.501	3.3252	8
20	8	0	14.7503	2.8025	8
20	8	0	25.0327	4.7562	52
20	8	0	34.1227	6.4833	88
20	8	0	17.3995	3.3059	76
20	8	5	0.4937	0.0938	8
20	8	5	0.5303	0.1008	20
20	8	5	0.5243	0.0996	8
20	8	5	1.2891	0.2449	140
20	8	5	1.3036	0.2477	112
20	8	5	1.4413	0.2738	140
30	6	0	0.4557	0.0866	148
30	6	0	0.7595	0.1443	136
30	6	5	0.7246	0.1377	24
30	6	5	0.4548	0.0864	0
30	6	5	1.3132	0.2495	104
30	6	5	0.6709	0.1275	140
30	8	0	0.5103	0.097	12
30	8	0	0.7349	0.1396	24
30	8	0	0.6228	0.1183	20
30	8	0	1.0535	0.2002	20
30	8	0	1.0323	0.1961	12
30	8	0	1.3938	0.2648	16
30	8	0	14.9845	2.8471	56
30	8	0	13.6325	2.5902	68
30	8	0	13.0363	2.4769	44
30	8	5	0.6612	0.1256	140
30	8	5	0.7387	0.1404	164
30	8	5	0.7316	0.139	160

Table C.2 Erosion data for lean clay (modelling)

Water temperature (^{0}C)	Water pH	Salt content (mg/L)	TKE (kg/m-s^2)	Shear Stress (Pa)	Erosion rate (mm/hr)
10	6	0	0.4855	0.0922	0
10	6	0	0.5182	0.0985	4
10	6	0	0.5472	0.104	0
10	6	0	1.3321	0.2531	4
10	6	0	1.3973	0.2655	16
10	6	0	1.2867	0.2445	0
10	6	0	44.0031	8.3606	44
10	6	0	45.4166	8.6292	40
10	6	0	47.9166	9.1041	60
10	6	5000	1.2394	0.2355	20
10	8	0	0.4932	0.0937	0
10	8	0	0.614	0.1167	16
10	8	0	0.9285	0.1764	0
10	8	0	1.3027	0.2475	8
10	8	0	11.4285	2.1714	0
10	8	0	11.5409	2.1928	8
10	8	0	12.1446	2.3075	0
10	8	0	14.7431	2.8012	44
10	8	5000	0.4739	0.09	4
10	8	5000	0.4116	0.0782	0
10	8	5000	0.8218	0.1562	4
10	8	5000	1.1664	0.2216	8
10	8	5000	9.72	1.8468	0
10	8	5000	12.281	2.3334	32
10	8	5000	25.964	4.9332	52
10	8	5000	22.1224	4.2033	72
20	6	0	0.5616	0.1067	8
20	6	0	0.6422	0.122	60
20	6	0	0.6211	0.118	36
20	6	0	1.5807	0.3003	80
20	6	0	1.1669	0.2217	80
20	6	0	1.2375	0.2351	116
20	6	5000	0.4463	0.0848	0
20	6	5000	0.4365	0.0829	0
20	6	5000	0.8713	0.1655	28
20	6	5000	1.0183	0.1935	24
20	6	5000	12.9763	2.4655	84
20	6	5000	44.4652	8.4484	60

Water temperature (^{0}C)	Water pH	Salt content (mg/L)	TKE (kg/m-s^2)	Shear Stress (Pa)	Erosion rate (mm/hr)
20	8	0	0.5152	0.0979	17.6
20	8	0	0.5259	0.0999	8
20	8	0	1.0539	0.2002	20
20	8	0	0.9585	0.1821	4
20	8	0	18.4578	3.507	44
20	8	0	8.4471	1.6049	24
20	8	0	15.9661	3.0336	64
20	8	0	13.8435	2.6303	52
20	8	5000	0.628	0.1193	8
20	8	5000	0.4431	0.0842	4
20	8	5000	1.0814	0.2055	44
20	8	5000	0.9931	0.1887	52
20	8	5000	0.7608	0.1446	60
20	8	5000	13.878	2.6368	72
30	6	0	0.6172	0.1173	56
30	6	0	0.5794	0.1101	96
30	6	0	0.5493	0.1044	60
30	6	0	1.4971	0.2844	92
30	6	0	1.0927	0.2076	72
30	6	5000	0.5699	0.1083	12
30	6	5000	0.4798	0.0912	16
30	6	5000	0.5337	0.1014	0
30	6	5000	1.0277	0.1953	92
30	6	5000	1.2518	0.2378	148
30	8	0	0.6266	0.1191	16
30	8	0	0.7876	0.1496	36
30	8	0	0.596	0.1132	8
30	8	0	1.6023	0.3044	32
30	8	0	1.3458	0.2557	20
30	8	0	0.9846	0.1871	4
30	8	0	13.4026	2.5465	52
30	8	0	14.3041	2.7178	72
30	8	0	12.1143	2.3017	80
30	8	5000	0.5795	0.1101	20
30	8	5000	0.6033	0.1146	8
30	8	5000	0.8434	0.1602	80
30	8	5000	1.0465	0.1988	96
30	8	5000	1.1417	0.2169	100
30	8	5000	1.1823	0.2246	76

Appendix D: Matlab code for shear stress estimation from LOW

```
% LOW - law of the wall

% code for data inspection

% Load Data File
a=10; %Number of flume replicates

% MeanBottom = ones(1,a);

n = ones(1,a);
m = ones(1,a);

% load data files e.g if file name are V72_1 to V72_10,
% 10 vectrino files

for i = 1:10;
    run = load(['V72_',num2str(i),'.mat']);

% Get Average bottom distance and number of data doints
Bottom = run.Data.BottomCheck_BottomDistance;
MeanBottom(i) = mean(Bottom);
[n(i),m(i)] =  size(run.Data.Profiles_VelX);
end
fprintf('MeanBottom in mm')
format bank
1000*[MeanBottom]'
format shortg
fprintf('Number of Data points')
[m]'

clear all


%% Load and Filter Data

% Modified from Parks (2012)

clear
clear all
clc

% Load Data File
a=10; %Number of flume replicates
SNRAA = zeros(1,10);
Tavg = zeros(10,27);
VXavg = zeros(10,27);
for i = 1:10;
    run = load(['V72_',num2str(i),'.mat']); %
%Set filtration criteria

cor=40;
snr=10;
remove=0.15;
```

```
% Data filtration
% Load in vectors to be used for data filtration: SNR and Correlation for
% each APD Beam

SNR1=run.Data.Profiles_SNRBeam1;
SNR2=run.Data.Profiles_SNRBeam2;
SNR3=run.Data.Profiles_SNRBeam3;
SNR4=run.Data.Profiles_SNRBeam4;
COR1=run.Data.Profiles_CorBeam1;
COR2=run.Data.Profiles_CorBeam2;
COR3=run.Data.Profiles_CorBeam3;
COR4=run.Data.Profiles_CorBeam4;

%Set up vectors for binary filtration
[m,n]=size(SNR1);
SNR1F=[m,n];
SNR2F=[m,n];
SNR3F=[m,n];
SNR4F=[m,n];
SNRAA(i)=[n]';
COR1F=[m,n];
COR2F=[m,n];
COR3F=[m,n];
COR4F=[m,n];

%Filter SNR and Correlation based on criteria: if data point is ok vector
% position is saved as 1, if data point is poor, point is replaced by NaN
for ii=1:n
    for jj=1:m
        if SNR1(jj,ii)<snr
            SNR1F(jj,ii)=NaN;
        else
            SNR1F(jj,ii)=1;
        end
        if SNR2(jj,ii)<snr
            SNR2F(jj,ii)=NaN;
        else
            SNR2F(jj,ii)=1;
        end
        if SNR3(jj,ii)<snr
            SNR3F(jj,ii)=NaN;
        else
            SNR3F(jj,ii)=1;
        end
        if SNR4(jj,ii)<snr
            SNR4F(jj,ii)=NaN;
        else
            SNR4F(jj,ii)=1;
        end
        if COR1(jj,ii)<cor
            COR1F(jj,ii)=NaN;
        else
            COR1F(jj,ii)=1;
        end
        if COR2(jj,ii)<cor
            COR2F(jj,ii)=NaN;
```

```
        else
            COR2F(jj,ii)=1;
        end
        if COR3(jj,ii)<cor
            COR3F(jj,ii)=NaN;
        else
            COR3F(jj,ii)=1;
        end
        if COR4(jj,ii)<cor
            COR4F(jj,ii)=NaN;
        else
            COR4F(jj,ii)=1;
        end
    end
end

% Read in velocity vectors
VX=run.Data.Profiles_VelX; %Stream-wise

%Filters out bad values based on SNR and Correlation
VXF=VX.*SNR1F.*SNR2F.*SNR3F.*SNR4F.*COR1F.*COR2F.*COR4F.*COR4F;

%Remove Bin of data if more that 15% has been filtered out
BAD=m*remove;
for ii=1:n
    TF=isnan(VXF(:,ii));
    TFsum=sum(TF);
    if TFsum>BAD
        VXF(:,ii)=NaN;
    end
end

%Average data in each bin
for ii=1:n
    VXavg(i,ii)=nanmean(VXF(:,ii));

end

%Get average temperature data
Temp=run.Data.Profiles_Temperature;
Tavg(i)=mean(Temp);
clear run; %clear previous file and variable
clear SNR1 SNR2 SNR3 SNR4 COR1 COR2 COR3 COR4 VXF VYF VZ1F VZ2F VX VY VZ1 VZ2
clear SNR1F SNR2F SNR3F SNR4F COR1F COR2F COR3F COR4F ii jj TF TFsum BAD Temp
end
Datapoints = SNRAA';
clear SNRAA

tao = zeros(1,10);
VXX =(fliplr(VXavg));


VX = VXX(:,(9:35));
%   VX = VXX;

x = log(1:1:27);
for i = 1:10;
```

```
% for i = 2;
no_of_datapoints = length(VX(i,:))

figure
plot(x,VX(i,:),'*')
% plot(x(15:27),VX(i,(15:27)),'*')
i
sp = input('inspect plot and input start point,sp:  ');
ep = input('inspect plot and input end point,ep:  ');

% note, sp and ep correspond to the start and end of the
% log-law region obtained by inspecting the plot

[r(i),m(i),c(i)] = regression(x(sp:ep),VX(i,(sp:ep)));
y = m(i).*x + c(i);
tao(i) = (m(i)*0.4)^2*1000
hold on
plot(x,y)
title(num2str(i))
legend(['slope=',num2str(m(i))])
end

[tao]'

% Save data into a struct
% save('Mont0.mat');


% Tanaka equation to calculate density based on water temperature

% a1 = -3.983035; a2 = 301.797; a3 = 522528.9; a4 = 69.34881; a5 =
0.999974950;
% rho = a5*(1 -((t+a1^2)*(t+a2))/(a3*(t+a4)))*1000
```

Appendix E: Matlab code for shear stress estimation from TKE

```
% Modified from Parks (2012)

% Set filtration criteria
% SNRAA = zeros(1,10);
% Tavg = zeros(10,27);
% VXavg = zeros(10,27);

cor=40;
snr=10;
remove=0.15;

% Data filtration
% Load in vectors to be used for data filtration: SNR and Correlation for
% each APD Beam

SNR1=Data.Profiles_SNRBeam1;
SNR2=Data.Profiles_SNRBeam2;
SNR3=Data.Profiles_SNRBeam3;
SNR4=Data.Profiles_SNRBeam4;
COR1=Data.Profiles_CorBeam1;
COR2=Data.Profiles_CorBeam2;
COR3=Data.Profiles_CorBeam3;
COR4=Data.Profiles_CorBeam4;

%Set up vectors for binary filtration
[m,n]=size(SNR1);

SNR1F=[m,n];
SNR2F=[m,n];
SNR3F=[m,n];
SNR4F=[m,n];
SNRAA=[n]';
COR1F=[m,n];
COR2F=[m,n];
COR3F=[m,n];
COR4F=[m,n];

%Filter SNR and Correlation based on criteria: if data point is ok vector
% position is saved as 1, if data point is poor, point is replaced by NaN
for ii=1:n
    for jj=1:m
        if SNR1(jj,ii)<snr
            SNR1F(jj,ii)=NaN;
        else
            SNR1F(jj,ii)=1;
        end
        if SNR2(jj,ii)<snr
            SNR2F(jj,ii)=NaN;
        else
            SNR2F(jj,ii)=1;
        end
        if SNR3(jj,ii)<snr
            SNR3F(jj,ii)=NaN;
```

```
        else
            SNR3F(jj,ii)=1;
        end
        if SNR4(jj,ii)<snr
            SNR4F(jj,ii)=NaN;
        else
            SNR4F(jj,ii)=1;
        end
        if COR1(jj,ii)<cor
            COR1F(jj,ii)=NaN;
        else
            COR1F(jj,ii)=1;
        end
        if COR2(jj,ii)<cor
            COR2F(jj,ii)=NaN;
        else
            COR2F(jj,ii)=1;
        end
        if COR3(jj,ii)<cor
            COR3F(jj,ii)=NaN;
        else
            COR3F(jj,ii)=1;
        end
        if COR4(jj,ii)<cor
            COR4F(jj,ii)=NaN;
        else
            COR4F(jj,ii)=1;
        end
    end
end

% Read in velocity vectors

VX=Data.Profiles_VelX; %Stream-wise
VY=Data.Profiles_VelY; %Up the wall
VZ1=Data.Profiles_VelZ1; %Into stream, perpendicular to wall 1
VZ2=Data.Profiles_VelZ2; %Into stream, perpendicular to wall 2

% Filters out bad values based on SNR and Correlation

VXF=VX.*SNR1F.*SNR2F.*SNR3F.*SNR4F.*COR1F.*COR2F.*COR4F.*COR4F;
VYF=VY.*SNR1F.*SNR2F.*SNR3F.*SNR4F.*COR1F.*COR2F.*COR4F.*COR4F;
VZ1F=VZ1.*SNR1F.*SNR2F.*SNR3F.*SNR4F.*COR1F.*COR2F.*COR4F.*COR4F;
VZ2F=VZ2.*SNR1F.*SNR2F.*SNR3F.*SNR4F.*COR1F.*COR2F.*COR4F.*COR4F;

%Remove Bin of data if more that 15% has been filtered out

BAD=m*remove;
for ii=1:n
    TF=isnan(VXF(:,ii));
    TFsum=sum(TF);
    if TFsum>BAD
       VXF(:,ii)=NaN;
       VYF(:,ii)=NaN;
       VZ1F(:,ii)=NaN;
       VZ2F(:,ii)=NaN;
    end
```

```
end

%Average data in each bin
for ii=1:n
    VXavg(ii)=nanmean(VXF(:,ii));
    VYavg(ii)=nanmean(VYF(:,ii));
    VZ1avg(ii)=nanmean(VZ1F(:,ii));
    VZ2avg(ii)=nanmean(VZ2F(:,ii));
    VZavg(ii)=(VZ2avg(:,ii)+VZ1avg(:,ii))/2;

 x_prime(:,ii) = VXF(:,ii) - VXavg(ii);
 y_prime(:,ii) = VYF(:,ii) - VYavg(ii);
 z_prime(:,ii) = VZ1F(:,ii) - VZ1avg(ii);

 %Get average temperature data

tempr=Data.Profiles_Temperature;
temp = mean2(tempr);

%density = 1000, or from equation below

density = 999.85308 + 6.32693*10^-2*temp - 8.523829*10^-3*temp^2 + ...
     6.943248*10^-5*temp^3 -3.821216*10^-7*temp^4;


TKEE(:,ii) = 0.5*density*(x_prime(:,ii).^2 + y_prime(:,ii).^2 +
z_prime(:,ii).^2);

 end

%  tau_final = nanmean(tau_m)
 TKE = nanmean(nanmean(TKEE))
 tau_final = 0.19*TKE
```

Appendix F: Matlab code for cross validation

```
% Program to perform a leave-one-out cross validation on the excess shear
% stress model and the Wilson model. This program fits both models to data
% using N-1 data points and predicts the left out data point. The
% difference between the left out point and the actual data is squared and
% normalized with the sum of all y data.

% x is the shear stress
% y is the erosion rate


% initialize arrays for faster processing
%  x(shear stress) and y(erosion rate) already loaded into the workspace

N = length(x);
predicted1 = zeros(1,N);
predicted2 = zeros(1,N);

% using a loop, step throught the data by holding one response data back,
% fitting both models to the data ,and predicting the held back data.

for  i = 1:N

XX = x(setdiff(1:N,i));
YY = y(setdiff(1:N,i));

X = x(i);

% kd*(x-tc)    excess shear stress model
% bo*sqrt(x)*(1-exp(-exp(3-(b1/x))))  wilson model

% set model types and constraints on the models' parameters since
% parameters cannot be negative.

ft1 = fittype('kd*(XX-tc)','independent','XX','dependent','YY');
ft2 = fittype('bo*sqrt(XX)*(1-exp(-exp(3-(b1/XX))))','independent','XX',...
    'dependent','YY');

% change ft1 and ft2 above to perform on the the modified excess shear
% and Wilson erosion models

opts = fitoptions('Method','NonlinearLeastSquares');
opts.Display = 'Off';
opts.Lower = [0 0];
opts.StartPoint = [0 0];

% verify that global solutions are obtained by changing options, constraining
% search region and inspecting results

% fit the models
mdl1 = fit(XX,YY,ft1,opts);    % excess shear stress
```

```
mdl2 = fit(XX,YY,ft2,opts);    % wilson

% predict the heldback erosion rate using both models

predicted1(i) = feval(mdl1,X);
predicted2(i) = feval(mdl2,X);

end

% calculate leave-one-out prediction indices


CVE_Ex = sum(sqrt((y'-predicted1).^2)))/sum(y)
CVE_Wil = sum(sqrt((y'-predicted2).^2)))/sum(y)
NOF_Ex = (sqrt(sum((y'-predicted1).^2)/N))/mean(y)
NOF_Wil = (sqrt(sum((y'-predicted1).^2)/N))/mean(y)
```